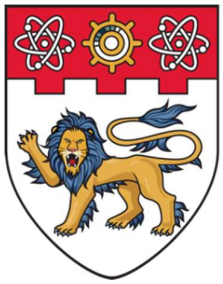

NANYANG TECHNOLOGICAL UNIVERSITY
SINGAPORE

Catalytic hydroboration of carbonyl compounds and pyridine derivatives with the NHC-parent silyliumylidene cation

LEE JIAWEN

SCHOOL OF PHYSICAL AND MATHEMATICAL SCIENCES

2019

Catalytic hydroboration of carbonyl compounds and pyridine derivatives with the NHC-parent silyliumylidene cation

LEE JIAWEN

SCHOOL OF PHYSICAL AND MATHEMATICAL SCIENCES

A thesis submitted to the Nanyang Technological University in partial fulfilment of the requirement for the degree of Master of Science

2019

Statement of Originality

I hereby certify that the work embodied in this thesis is the result of original research done by me except otherwise stated in this thesis. The thesis work has not been submitted for a degree or professional qualification to any other university or institution. I declare that this thesis is written by myself and is free of plagiarism and is of sufficient grammatical clarity to be examined. I confirm that the investigations were conducted in accord with the ethics policies and integrity standards of Nanyang Technological University and that the research data are presented honestly without prejudice.

14th August 2019

Date

Lee Jiawen

Supervisor Declaration Statement

I have reviewed the content and presentation style of this thesis and declare it of sufficient grammatical clarity to be examined. To the best of my knowledge, the thesis is free of plagiarism and the research writing are those of the candidate's except as acknowledged in the Author Attribution Statement. I confirm that the investigations were conducted in accord with the ethics policies and integrity standards of Nanyang Technological University and that the research data are presented honestly without prejudice.

14th August 2019

Date

Dr So Cheuk-Wai

Authorship Attribution Statement

Please select one of the following; *delete as appropriate:

*(B) This thesis contains material from 1 paper published in the following peer-reviewed journal conferences in which I am listed as an author.

Part of the thesis is published as B.-X. Leong; J. Lee; Dr. Y. Li; M.-C. Yang; C.-K. Siu; M.-D. Su; Dr. C.-W. So. A Versatile NHC-Parent Silyliumylidene Cation for Catalytic Chemo- and Regioselective Hydroboration, *J. Am. Chem. Soc.* **2019**, *141*, 17629-17636.

The contributions of the co-authors are as follows:

- Dr C.-W. So was the corresponding author of the manuscript and proposed the project in the manuscript.
- Dr Y. Li initiated the feasibility of substrate scopes in the catalysis.
- I performed the catalytic hydroboration of carbonyl compounds and pyridines.
- B.-X. Leong executed the hydroboration of CO_2, mechanistic studies, the synthesis of the NHC-parent silyliumylidene cation and shortening of reaction time.
- Prof. M.-D. Su and Prof. C.-K. Siu performed the DFT calculations for the reaction mechanism and the possible intermediates.

14th August 2019

Date

Lee Jiawen

Abstract

This thesis describes the catalytic hydroboration of carbonyl compounds and pyridine derivatives mediated by an N-heterocyclic carbene-parent silyliumylidene cation to give the corresponding borate esters and N-boryl-1,4-dihydropyridine products in good yield, respectively. The catalysis also shows chemo- and regioselectivity. The mechanism was proposed and investigated by DFT calculations.

Acknowledgements

I would like to thank Dr Cheuk-Wai So for giving me this opportunity to study and learn from him. Thank you for your patience, guidance and support throughout my time with you, as well as all your random jokes and illuminating discussions.

I would also like to thank the Graduate Studies and Research Office staff, Ms Chan Ion Cheng, Prudence and Ms Lee Yean Chin, as well as the NMR support staff, Ms Goh Ee Ling and Mr Keith Leung, for all the help provided for me during my course of studies and research.

I would also like to extend my gratitude towards my fellow group members, Luthfi, Cher-Chiek, Bi-Xiang, Fan Jun, Melissa, Meldon, Qing Xin, Fiona and other colleagues and friends of CBC for their companionship, encouragement and help throughout the my stay here in Dr So's lab.

The contents of this thesis and the corresponding paper would not have been completed without the idea and guidance of Dr Cheuk-Wai So, the groundwork done by Dr Yan Li on investigating the substrate scope for catalysis, the synthesis of the catalyst and its catalytic hydroboration of CO_2 accomplished by Ms Bi-Xiang Leong. The DFT calculations were also done by Professor Ming-De Su of National Chiayi University in Taiwan.

Table of Contents

List of Figures

List of Tables

Introduction

N-heterocyclic carbenes

Carbenes are known to be highly reactive and neutral compounds. This is due to the incomplete octet configuration on the central divalent carbon of the compound. As such, the first carbenes were in the form of transition metal-carbene complexes such as those by Fischer,[1] Schrock, Wanzlick[2] and Öfele.[3, 4] The isolation and characterisation of a free carbene was challenged until 1991 when Arduengo isolated the first stable crystalline adamantyl N-heterocyclic carbene (NHC).[5]

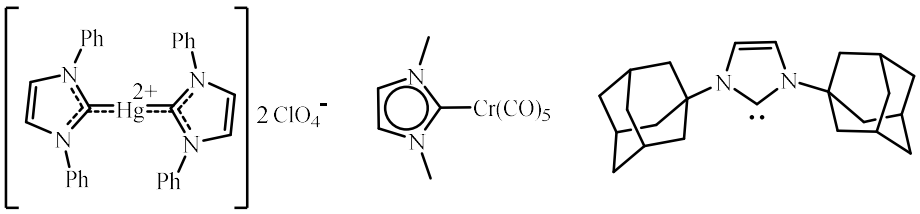

Wanzlick (1968) | Öfele (1968) | Arduengo (1991)

Figure 1: First NHC-transition metal complexes reported by Wanzlick and Öfele. First stable crystalline NHC isolated and reported by Arduengo

Subsequent synthesis and studies on NHC-transition metals complexes and catalysts have shown that NHCs are electron rich and highly nucleophilic, giving rise to its strong σ-donating properties. This property increases the NHC-transition metal bond strength, resulting in more stable NHC transition metal complexes, preventing their\ decomposition. [6-13] It is also found that the strong σ-donating properties of NHCs have a stabilising effect on highly reactive complexes and facilitating the catalytic activity of NHC-transition metal catalysts, which will be discussed in the later sections.

N-heterocyclic carbenes in transition metal catalysts

The first work on NHC-transition metal catalysts was done by Hermann et al. using a palladium (0) complex in Heck olefin cross coupling reactions, where the acetate or phosphine ligand in the Heck reaction catalyst was replaced by a 1,3-dimethylimidazol-2-ylidene. The change in the spectator ligand led to the increase in turnover frequency to above 15 000 without the deposition of catalytically inactive palladium.[14-16] With the discovery that NHCs can stabilise transition metal to prevent catalyst decomposition and can increase catalytic activity,[6, 13, 17, 18] many other NHC-transition metal catalysts were developed.

One prominent example of a NHC-transition metal catalyst would be the second-generation Grubbs catalyst for olefin metathesis where a tricyclohexylphosphine ligand of the first-generation Grubbs catalyst is replaced by a 1,3-bis(2,4,6-trimethylphenyl) imidazolin-2-ylidene. Grubbs reported a large increase in reactivity of the carbene catalyst for ring closing metathesis reactions at slightly increased temperatures compared to the first-generation phosphine catalyst.[19-21]

NHCs were also found to be capable of replacing olefinic and pyridine ligands, as demonstrated by Markó et al. and Fort et al. respectively. Markó et al. replaced the bridging 1,1,3,3-tetramethyl-1,3-divinyl disiloxane ligand on the Karstedt's catalyst with either a phosphine or NHC ligand and the catalytic hydrosilylation was examined. While the NHC-platinum catalyst has a slightly lower catalytic activity than the phosphine-platinum catalyst, it was observed that there was no decomposition of the NHC-platinum catalyst, demonstrating the ability of NHC in stabilising transition metal complex.[22] On the other hand, Fort et al. replaced the 2,2'-bipyridine ligand on the nickel(0) center with a 1,3-bis(2,4,6-trimethylphenyl)imidazol-2-ylidene, leading to increase the activity of the catalyst in the reduction of fluoroarenes and hence improve the yield of the products.[23,24] The increase in catalytic activity was also observed

for other NHC-nickel(0) catalysts in cross coupling reactions involving aryl halides by Fort et al..[25-27]

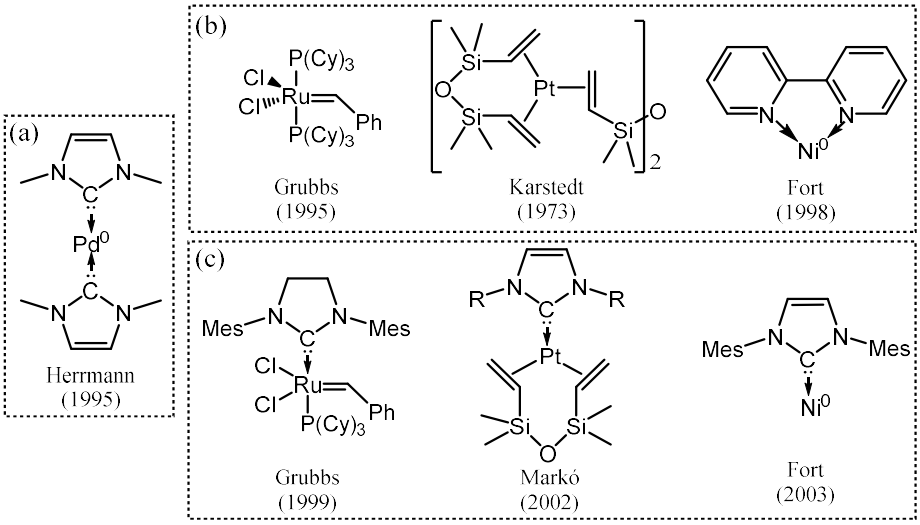

Figure 2: Selection of NHC-transition metal catalysts, (a) first reported catalyst with NHC as ligands, (b) predecessor catalyst, (c) Catalyst with a ligand replaced by a N-heterocyclic carbene.

With the success of NHCs in stabilising transition metal complexes in catalysts, it was proposed that NHCs could also be useful in stabilising heavier main group element compounds, which have properties similar to those of transition metals.[28]

N-heterocyclic carbenes in main-group element catalysts

Main-group compound showing transition-metal-like electronic property was first examined by Lappert et al. in 1965, who isolated a stable and dimeric tin(II) complex $[(SiMe_3)_2CH]_2SnSn[CH(SiMe_3)_2]_2$ with multiple bonding between the two tin atoms as shown in the X-ray crystallographic structure. In solution, however, this main-group complex dissociated into the monomeric form consisting of a lone pair of electrons on the tin center, as well as a vacant p-orbital, making the tin center resemble transition metal filled and empty d-orbitals.[29] Subsequent analysis of its crystal structure showed that the sum of angles around the Sn center is 342°, which is neither expected for sp^2 hybridisation at 360° or sp^3 hybridisation

at 327°.[4, 30] Further studies by other groups attributed this observation to second order Jahn-Teller effect, arising from the mixing of a symmetry allowed, intramolecular mixing of a bonding orbital and an unoccupied anti-bonding orbital.[31] This geometrical disorder to the trans bent structure was observed to increase down the group, with increasing degree of non-bonding electron localisation at the heavier element while having an electron deficient and unsaturated character from an incomplete electron sharing in the main group element-main group element multiple bond. As such, both donor and acceptor sites are created in the molecule, giving it properties similar to a transition metal catalyst.[28, 31-37]

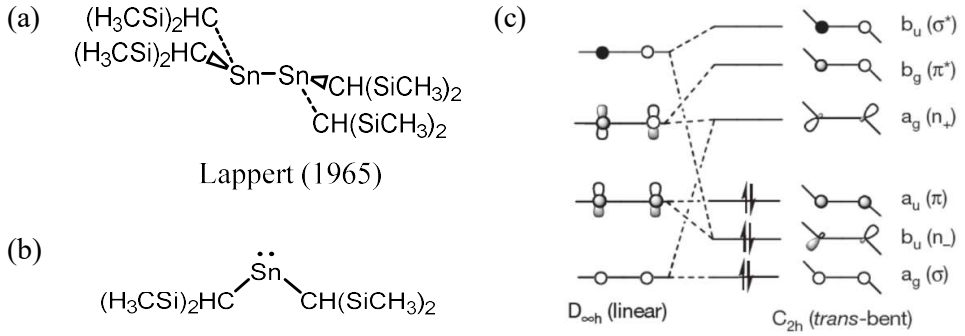

Figure 3: (a) Trans-bent structure of the tin(II)-tin(II) complex by Lappert et al. (b) Monomeric form of the tin(II) complex in solution. (c) Molecular orbital diagram of a linear and trans-bent structure of multiply bonded main group complex.

Subsequently, the activation of small molecules with main group complexes was first explored in 2005 when Power et al. synthesised a Ar-Ge≡Ge-Ar (Ar = terphenyl) that reacted cleanly with H_2 gas under ambient conditions to give a mixture of digermene, digermane and germane (Scheme 1a),[38] which then sparked the investigation of small molecule activation with main group complexes in the following decades.

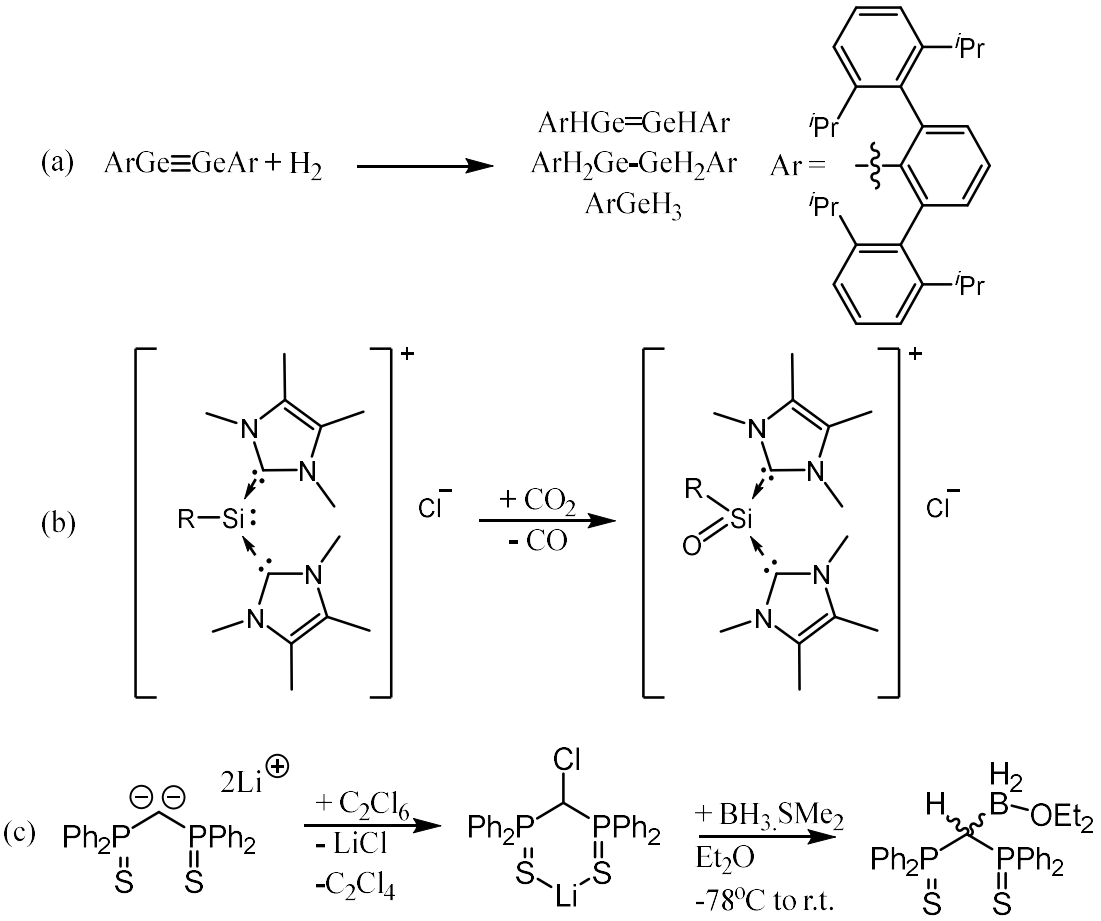

Scheme 1

It was later discovered that highly reactive main-group complexes are capable of undergoing catalysis. These include a germanium hydride synthesized by Jones et al. that catalysed the hydroboration of carbonyl compounds (Scheme 2a),[47] a diazaphospholene reported by Kinjo et al. capable of catalysing the hydroboration of carbonyl compounds (Scheme 2b),[48] an aluminium hydride shown by Roesky et al. capable of catalysing the hydroboration and the addition of trimethylsilyl cyanide (TMSCN) to carbonyl compounds (Scheme 2c),[49] as well as an N-heterocyclic imino aluminium hydride synthesized by Inoue et al. catalysed the hydroboration of alkynes to alkenes (Scheme 3a)[1,41].

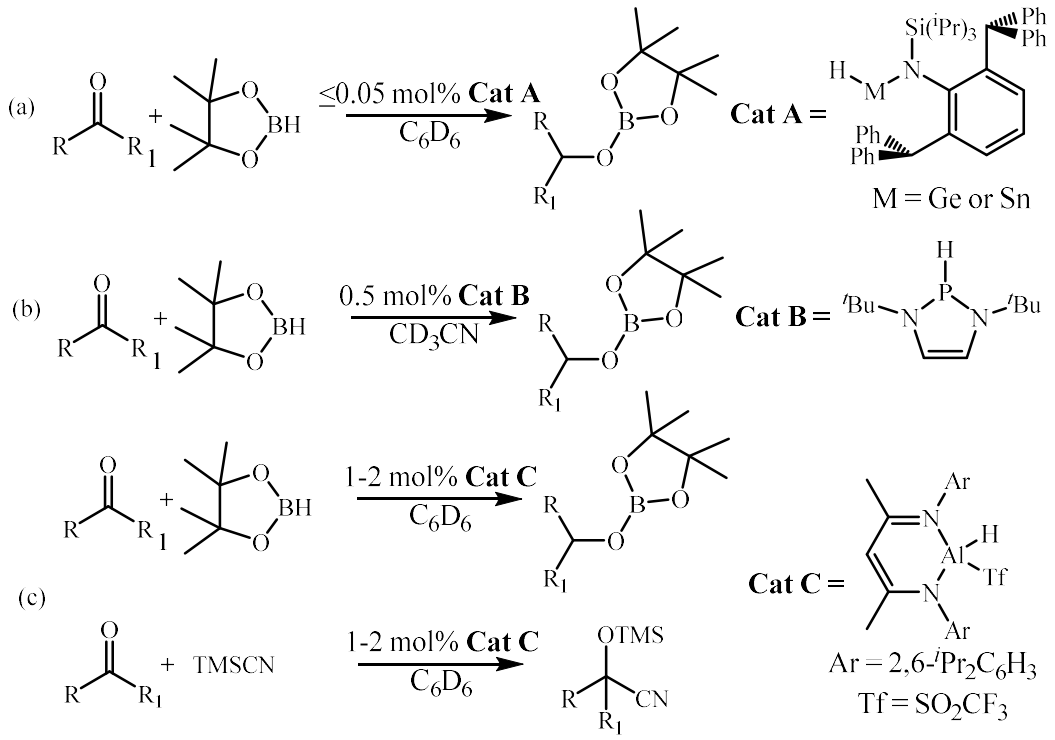

Scheme 2

Combing extraordinary properties of NHC and main-group elements, several NHC-main group complexes were synthesised by various groups for the activation of small molecules or unsaturated bonds.[39-45] This includes a sila-acylium ion stabilised by two NHCs that activates carbon dioxide to form carbon monoxide (Scheme 1b). [46] In addition, the NHC dialkylcalcium complex can catalyse the cross dehydrocoupling of silanes with amines, reported by Guan et al. (Scheme 3b).[50] These examples show that NHC-main group complexes are capable of catalysing organic reactions, similar to transition metal catalysts.

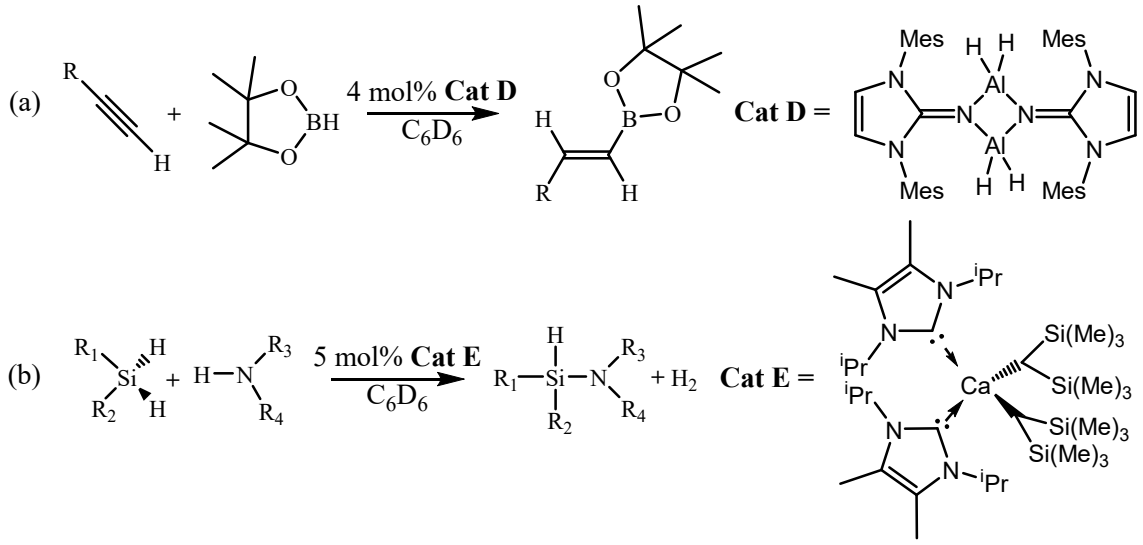

Scheme 3

NHC-silicon complexes for catalysis

Being one of the most common elements, the chemistry of silicon and its bonding have been studied since the late 1970s, with multiple review papers written on the topic.[32, 51-53] This is mainly due to silicon being isosteres of carbon with a larger covalent radius, more electropositive nature, lower toxicity than transition metals and its high relative abundance. As such, the use of silicon-based catalysts should be ideal considering the costs and sustainability.

However, among the various single site main group catalysts for hydroboration,[47-49, 54-57] there is only one report of a silicon based catalyst by Sen et al. in 2017.[58] The amidinato-silane catalyst has been reported to selectively catalyse the hydroboration of aldehydes and aldimines to the corresponding borate esters and amine boronate esters, respectively, under mild reaction conditions (Scheme 4a).

In the same year, So et al. reported the synthesis of a NHC-parent silyliumylidene cation, which is capable of slowly activating fluorobenzene to form imidazolium salt and a functionalised fluorobenzene at the ortho-position (Scheme 4b).[59]

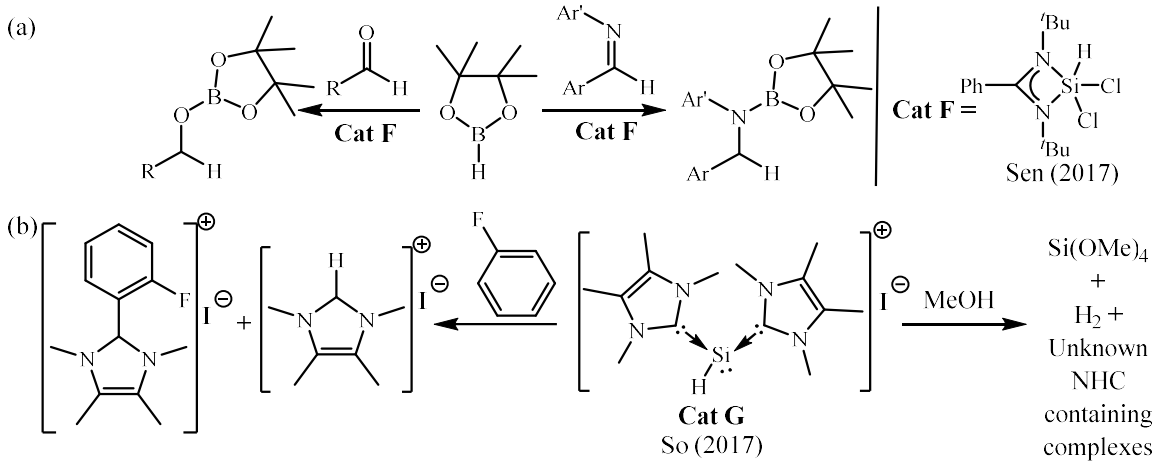

Scheme 4

The NHC-parent silyliumylidene complex also shows reactivity towards other solvents such as methanol to give $Si(OMe)_4$, hydrogen gas and other NHC containing compounds (Scheme 4b). This indicates that the Si-H bond is chemically active and could possibly be suitable for the activation of small molecules similar to other main group hydride catalysts reported by research groups of Jones and Kinjo. As such, the reactivity of the NHC-parent silyliumylidene cation (Cat G) was investigated via the reduction of carbon dioxide with 4,4,5,5-tetramethyl-1,3,2-dioxaboralane (HBpin) as the hydride source to form HCO_2Bpin (Scheme 5).[60,61-63]

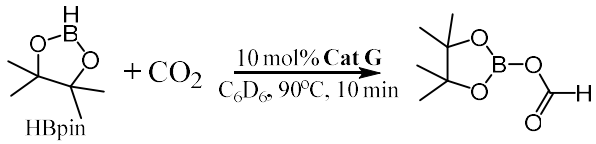

Scheme 5

Catalytic hydroboration

Organoboranes are versatile intermediates in organic synthesis due to their stability, easy handling, high functional group compatibility, and wide application in the development of new strategies for transition-metal-catalyzed carbon–carbon, carbon–oxygen, carbon–nitrogen, and carbon–halogen bond-forming reactions. The catalytic hydroboration of unsaturated organic

substrates represents a highly valuable approach for the synthesis of functionalized organoboranes. More specifically, the catalytic hydroboration of carbonyl compounds is an atom-economical and selective synthetic route to form widely used borate esters (R_2BOCHR_2), which are important intermediates for the synthesis of functionalized alcohols. Conventionally, hydroboration of C=O bonds can be achieved with stoichiometric amounts of hazardous metal hydrides, such as $LiAlH_4$ and $NaBH_4$ or the stoichiometric addition of reactive BH_3 to form borates. However, this is not ideal as the metal hydrides are still required in stochiometric amounts, leading to atom inefficiency. In addition, the catalytic hydroboration of pyridine compounds is another atom-economical and selective synthetic route to form N-boryl-dihydropyridine derivatives, which are important intermediates for the synthesis of functionalized dihydropyridine derivatives being found in naturally occurring molecules, biologically active agents and pharmaceutically important molecules. However, these catalytic hydroboration was usually achieved using toxic and low abundant transition metal catalysts. As a result, it is indispensable to look for an environmentally friendly, low cost, high abundant element for such catalysis. Silicon is one of the options, however, silicon is unlike transition metal, which do not comprise filled and empty orbitals for performing catalysis.

Given the success of the catalytic reduction of carbon dioxide by HBpin using the NHC-parent silyliumylidene complex, the catalytic hydroboration towards other unsaturated bonds, such as C=O double bond in carbonyl compounds, and C=N double bond in pyridine derivatives were investigated and will be reported in the following section.[60]

Results and discussion

Catalytic hydroboration of aldehydes: Optimization

Optimisation of the NHC-parent silyliumylidene cation-catalysed hydroboration reaction was first carried out using benzaldehyde in deuterated benzene (C_6D_6). The reaction monitored via ^{1}H NMR spectroscopy by the disappearance of the C*H*O proton resonance and the appearance of the -C*H*$_2$OBpin proton resonance of the corresponding borate ester. Preliminary investigations indicated that the catalysis was found to proceed at 24 ^{O}C with 5 mmol % of the NHC-parent silyliumylidene cation under vigorous mixing (Table 1, entry 11). Further investigations showed that doubling the catalyst loading to 10 mmol % reduced the time taken for the reaction by half (Table 1, entry 12). Upon increasing the reaction temperatures, contradictory results were observed for the hydroboration of n-butrylaldehyde where an increased catalyst loading of 10 mmol % and higher reaction temperature of 90°C resulted in a lower conversion of the aldehyde to the corresponding borate ester [Table 1, entry 9 (57.3%) and entry 10 (37.5%)]. This could be as the higher reaction temperatures decompose the catalytic intermediate, causing the catalysis to be slower. Furthermore, triphenyl silane and triethyl silane slightly catalysed the hydroboration of benzaldehyde, while no hydroboration was observed in the absence of catalyst [Table 1, entry 6 (17 %), entry 7 (16 %) and entry 1 (0 %)]. As such, it can be concluded that the hydroboration reaction of benzaldehyde can only be achieved using the NHC-parent silyliumylidene complex as catalyst.

Table 1: Optimisation for the hydroboration reaction of aldehydes

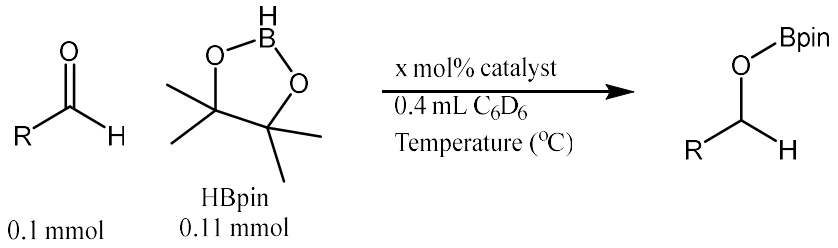

Entry	Substrate	Catalyst loading (%)	Temperature (°C)	Time (hrs)	Conversion (%)
1[a]	PhCHO	0.0	60.0	36.0	0
2	PhCHO	5.0	40.0	26.0	51
3	PhCHO	5.0	55.0	21.0	47
4[b]	PhCHO	5.0	60.0	21.0	80
5	PhCHO	5.0	60.0	73.0	>99
6[c]	PhCHO	10.0	60.0	48.0	17
7[d]	PhCHO	10.0	60.0	48.0	16
8	PhCHO	10.0	90.0	8.0	>99
9	$CH_3(CH_2)_3CHO$	5.0	40.0	26.0	57
10	$CH_3(CH_2)_3CHO$	10.0	90.0	20.5	38
11[e]	PhCHO	5.0	24.0	0.34	>99
12[e]	PhCHO	10.0	24.0	0.17	>99

[a]Performed together with Leong B.-X., [b]Initiated by Dr Li Y., [c]Triethylsilane used as catalyst instead of the NHC-parent silyliumylidene cation, [d]Triphenylsilane used as catalyst instead of the NHC-parent silyliumylidene cation, [e]Reaction mixture was mixed vigorously during the reaction, performed together with Leong B.-X.; reaction was replicated with ferrocenecarboxaldehyde by Lee J. and similar results was observed

Chemoselective hydroboration of aldehyde derivatives

Using the optimised conditions obtained, a variety of aldehyde substrates were explored and the reaction progress was monitored via ^{1}H NMR spectroscopy. ^{11}B NMR spectrum was also taken to confirm the completion of the reaction via the disappearance of the H*B*pin signal at around δ = 27.5 ppm and the appearance of the -CH_2O*B*pin signal from δ = 21.9 – 21.6 ppm.

Table 2: Substrate scope for the hydroboration of aldehyde derivatives

Entry	Substrate	Product	Time (mins)	Conversion (%)
1	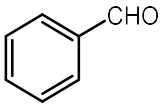	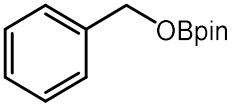	10	>99
2	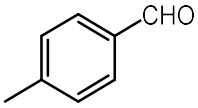	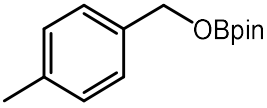	10	>99
3	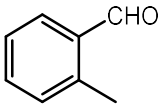	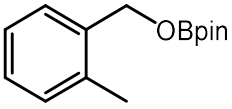	15	>99
4	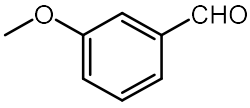	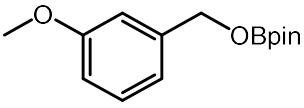	10	>99
5	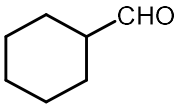	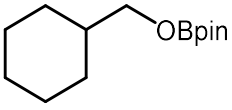	10	>99
6	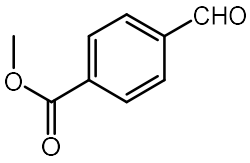	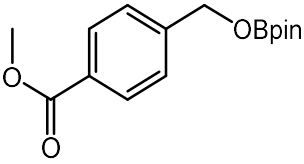	10	>99
7	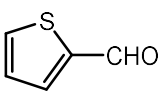	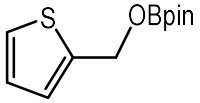	10	>99

8	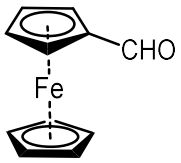	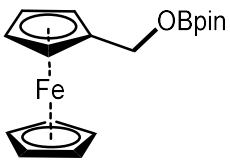	5	>99
9	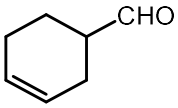	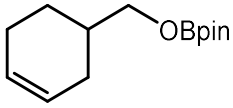	10	>99
10	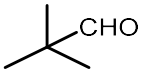	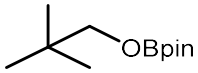	30	>99
11	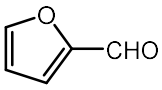	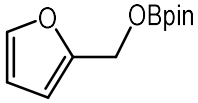	25	>99
12	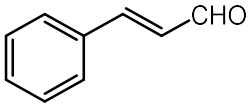	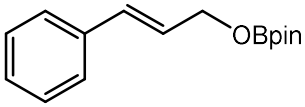	10	>99
13	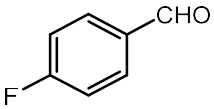	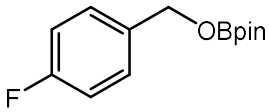	10	>99
14	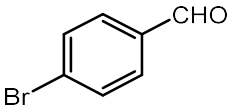	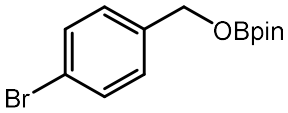	35	>99
15	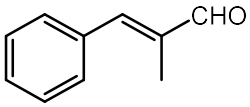	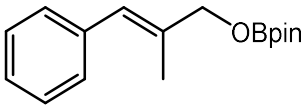	20	>99
16	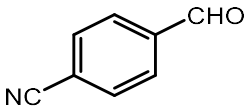	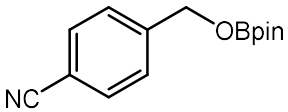	15	>99
17	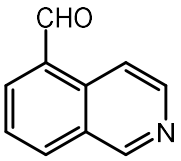	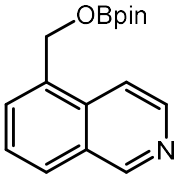	15	>99

18	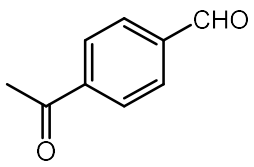	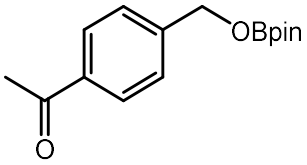	40	>99

Reaction conditions are as followed unless otherwise specified: catalyst (10 mol%), HBpin (1.1 equiv.), substrate (0.1 mmol) in 0.4 mL d-benzene in a NMR tube and shaken vigorously during the reaction. Conversion was calculated based on the ratio of aldehyde to borate ester found in the reaction mixture.

Firstly, *para*-, *ortho*- and *meta*-substituted aromatic aldehydes were tested and found to undergo catalytic hydroboration, achieving >99.0% conversion within 15 minutes (Table 2, entries 2 – 4). It was observed that hydroboration of *ortho*-methylbenzaldehyde (Table 2, entry 3) was slightly slower than *para*-methylbenzaldehyde and *meta*-methoxybenzaldehyde (Table 2, entries 2 and 4), which could be due to the slight steric hindrance of the *ortho*-methyl substituent.

Following this, hydroboration of aromatic aldehydes with electron donating and withdrawing groups was performed and found to be well tolerated, giving >99.0% conversion within 40 minutes. The hydroboration of aromatic aldehydes with electron withdrawing groups (Table 2, entries 6, 13 and 14) were found to be comparable to those with electron donating groups (Table 2, entries 2 – 4), showing that the hydroboration of aldehydes containing electron donating and withdrawing substituents are generally well tolerated. Aromatic aldehydes containing a halogen substituent were also well tolerated (Table 2, entries 13 and 14), with 4-bromobenzaldehyde being much slower than 4-fluorobenzaldehyde. This could be due to the increasing electropositive nature of the halogen atom down the group and the resultant effect exerted on the aldehyde. Chemoselectivity was also observed for aldehydes such as thiophene-2-carboxaldehyde, ferrocene carboxaldehyde and furfural (Table 2, entries 7, 8 and 11), where the thiophene, ferrocene and furan groups remain untouched during the hydroboration.

Aliphatic aldehydes were then tested and found to be suitable for hydroboration with >99.0% conversion within 30 minutes. Among the aliphatic aldehydes, those with olefinic functionalities also displayed chemoselective hydroboration, leaving the C=C double bonds intact (Table 2, entries 9, 12 and 17). Chemoselectivity was also observed for 4-carbonitrile benzaldehyde, iso-quinoline-5-carboxaldehyde and 4-acetalbenzaldehyde where the -C≡N triple bond, -C=N- double bond and C=O double bond respectively remains untouched after the catalytic reaction (Table 2, entries 16 – 18).

Catalytic hydroboration of ketone compounds: Optimization

As a carbonyl homologue of aldehydes, the catalytic hydroboration of ketones was also explored. On the basis of catalytic hydroboration of aldehydes, optimisation was attempted at elevated temperatures using acetophenone. It was observed that there was no conversion of acetophenone to the corresponding borate ester at 24 °C (Table 3, entry 1). When the reaction temperature was increased, it was observed that the full conversion of the acetophenone to the corresponding borate ester could not be achieved even after 24 hours [Table 3, entries 3 (60 °C, 66.7%) and 4 (80 °C, 85.3%)]. Subsequently, the reaction was found to proceed to >99.0% conversion within 6.0 hours at 90 °C at 10 mmol % catalyst loading. When the reaction temperature was raised to 110 °C (Table 3, entry 6), it was observed that the NHC-parent silyliumylidene cation turned white within one hour and the subsequent rate of conversion was drastically reduced. The ^{1}H NMR spectrum for the reaction at 110 °C after 12 hours also shows a significant amount of unidentified compounds that increase over time, suggesting that the catalyst decomposes at high temperatures.

Table 3: Optimisation for the hydroboration reaction of ketone using acetophenone

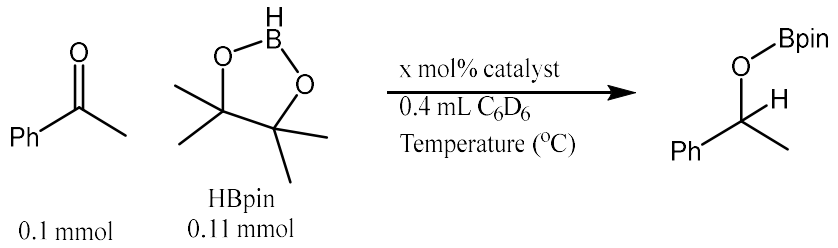

0.1 mmol HBpin 0.11 mmol

Entry	Catalyst loading (%)	Temperature (^oC)	Time (hrs)	Conversion (%)
1	10.0	24.0	24.0	0
2	10.0	40.0	24.0	36
3	10.0	60.0	24.0	67
4	10.0	80.0	24.0	85
5	10.0	90.0	6.0	>99
6	10.0	110.0	1.0	---

Chemoselective hydroboration of ketone derivatives

With the successful catalytic hydroboration of acetophenone across the C=O double bond, various ketones were selected, and the optimal reaction conditions obtained were used for the hydroboration reactions.

Table 4: Substrate scope for the hydroboration of ketone derivatives

Entry	Substrate	Product	Time (hrs)	Conversion (%)
1[a]	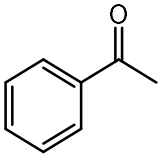	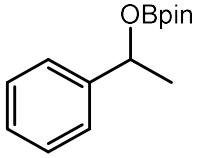	6	>99

2[a]	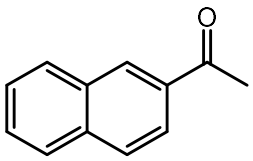	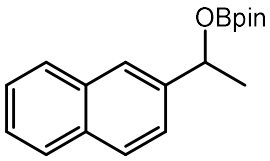	5	>99
3[a]	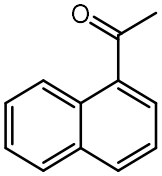	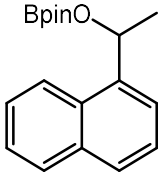	6	>99
4[a]	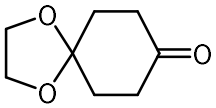	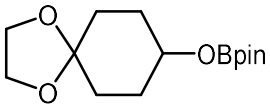	1	>99
5[a]	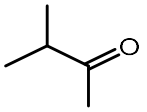	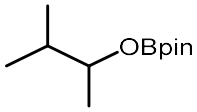	14	>99
6[a]	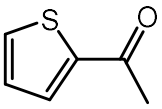	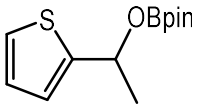	24	75
7[a]	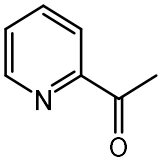	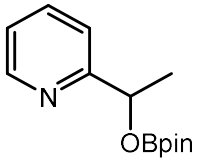	7	>99
8	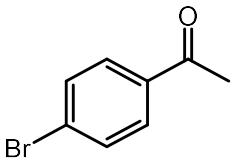	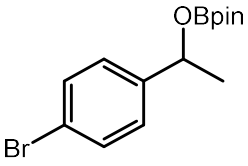	24	83
9	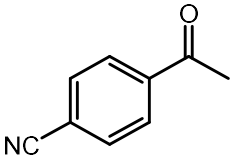	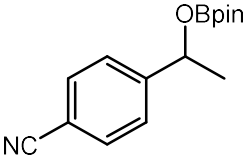	1	>99

Reaction conditions are as followed unless otherwise specified: catalyst (10 mol%), HBpin (1.1 equiv.), substrate (0.1 mmol) in 0.4 mL d-benzene in a NMR tube and shaken periodically during the reaction, [a]First tried by Dr Li Y. at 5% catalyst loading

Aromatic ketone derivatives, namely 1-(2-naphthyl) ethenone (Table 4, entry 2) and 1-acetonaphthone (Table 4, entry 3) were examined and showed >99.0% conversion. The reaction was found to be slightly faster for 1-(2-naphthyl) ethenone (Table 4, entry 2) than 1-acetonaphthone (Table 4, entry 3), which may be due to steric hindrance from the naphthyl group. Aliphatic ketones were also explored, including the cyclic 1,4-cyclohexanedione monoethylene acetal and the acyclic 3-methyl-2-butanone (Table 4, entries 4 and 5), which showed good conversion in the catalytic hydroboration.

Aromatic ketones with other functional groups were then explored and found to undergo chemoselective hydroboration. This was observed for 2-acetylpyridine and 4-acetyl benzonitrile where the pyridine and carbonitrile groups remain intact after the reaction with full conversion (Table 4, entries 7 and 9). Similar results were observed for the catalytic hydroboration of 2-acetylthiophene and 4-bromoacetophenone (Table 4, entries 6 and 8). However, full conversion was not observed within 24 hours for these reactions which may be due to the steric environment of these ketones (Table 4, entries 6 - 9). In case of 2-acetyl thiophene and 4-bromoacetophenone, prolonged heating can lead to an increase in conversion of the substrates to the corresponding borate esters (Table 4, entries 6 and 8) and no other products were formed, reflecting on the good selectivity of the NHC-parent silyliumylidene cation upon heating.

Catalytic hydroboration of pyridine derivatives: Optimisation

Following the success of the catalytic hydroboration of carbonyl derivatives, the catalytic hydroboration of pyridine derivatives was also attempted, whereby pyridine was converted into N-boryl-1,4-dihydropyridine as the sole product, displaying regioselectivity of the catalyst. Similar to the carbonyl substrates, optimisation was carried out and it was found that the optimal reaction conditions were 10 mol % catalyst loading and reaction temperature of 90 °C

(Table 5, entry 8). No catalytic hydroboration was observed when the catalysts was absent, (Table 5, entry 1), triphenyl and triethyl silane was used as the catalyst (Table 5, entries 2 and 3) or the reaction was carried out at 24 °C (Table 5, entry 4). It was also observed that the reaction did not proceed to full conversion within 24 hours until the reaction temperature was elevated to 90 °C [Table 5, entries 5 (40 °C, 28.1%), 7 (80 °C, 69.8%) and 8 (90 °C, >99.0%)]. Further increase in reaction temperature resulted in the catalyst turning white after one hour with a drastic drop in the rate of conversion. Similar to the optimisation using acetophenone (Table 3, entry 6), a significant amount of unidentified signals were observed after prolonged heating of the reaction mixture, which suggests that the catalyst has decomposed due to the high temperature.

Table 5: Optimisation for the hydroboration reaction of pyridine

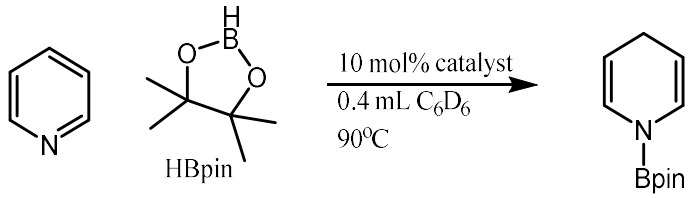

Entry	Catalyst loading (%)	Temperature (°C)	Time (hrs)	Conversion (%)
1	0.0	90.0	36.0	0
2[a]	10.0	90.0	36.0	0
3[b]	10.0	90.0	36.0	0
4	10.0	24.0	24.0	0
5	10.0	40.0	24.0	28
6	10.0	60.0	24.0	49
7	10.0	80.0	24.0	70
8	10.0	90.0	6.0	>99

9	10.0	110.0	1.0	---

Table 5: Optimisation for the hydroboration reaction of pyridine, [a]Triphenyl silane as catalyst, [b]Triethylsilane as catalyst

Chemo- and regioselective hydroboration of pyridine derivatives

After obtaining the optimal reaction conditions, other pyridine derivatives were also examined for their suitability in the catalytic hydroboration reaction. The reaction was monitored via ^{1}H NMR spectroscopy via the disappearance of the Ar-*H* peak at about $\delta = 8.53$ ppm.

Table 6: Substrate scope for the hydroboration of pyridine derivatives

Entry	**Substrate**	**Product**	**Time (hrs)**	**Conversion (%)**
1	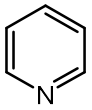	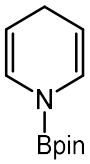	4	>99
2	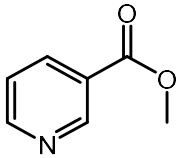	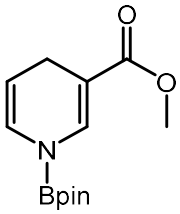	0.25	>99
3	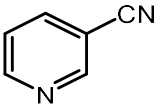	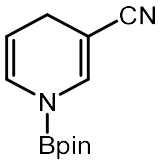	2	>99
4	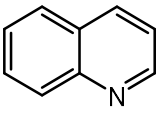	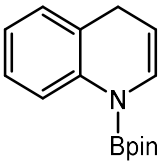	9	>99

5	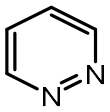	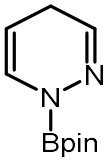	4	>99
6	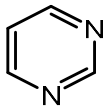	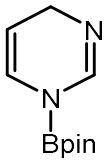	24	67

Reaction conditions are as followed unless otherwise specified: catalyst (10 mol%), HBpin (1.1 equiv.), substrate (0.1 mmol) in 0.4 mL d-benzene in a NMR tube and shaken periodically during the reaction

Substituted pyridines were found to undergo chemo- and regioselective hydroboration to yield only the corresponding N-boryl-1,4-dihydropyridine derivatives with the loss of the pyridine aromaticity. The substituents in the pyridine derivatives do not affect chemo- and regioselective hydroboration (Table 6, entries 2 and 3). It was also observed that methyl nicotinate was able to undergo catalytic hydroboration at 24°C, but the reaction conversion was <10% after one hour. Hence optimized conditions were used, whereby the reaction was finished in 15 minutes (Table 6, entry 2). The carbonitrile group remained intact after the reaction, displaying the selectivity of the catalyst.

A ring-fused pyridine was also tested to yield the corresponding N-boryl-1,4-dihydroquinoline after 9 hours (Table 6, entry 4). The reaction scope was then extended to pyrazines and 1,2-pyrazine had <99.0% conversion to N-boryl-1,4-dihydropyrazine after 4 hours (Table 6, entry 5) which was comparable to the hydroboration of pyridine (Table 6, entry 1). However, the hydroboration of 1,3-pyrazine gave a lower conversion of 67.0% after 24 hours (Table 6, entry 6), probably due to the N atom at the *meta* position which affects the attack of the catalyst at the *para* position (see below). This slows down the formation of the N-boryl-1,4-dihydropyrazine leading to slower conversion rate and longer reaction time required. Similar

to the catalytic hydroboration of ketones, prolonged heating of the reaction mixture did not yield further hydroboration products, displaying the good chemio- and regioselectivity of the catalyst.

The reaction scale of the catalytic hydroboration could also be increased to 1 mmol for both acetophenone and pyridine without a decrease in the conversion, obtaining 80% and 85% isolated yield respectively. In comparison with Sen and co-workers' amidinato silane catalyst (turnover frequency = 96.0), our catalyst has a lower turnover frequency (TOF = 59.4 h^{-1}) for the hydroboration of benzaldehyde. However, the NHC-parent silyliumylidene cation is able to catalyse hydroboration of both carbonyl compounds and pyridine derivatives, which could not be done with the amidinato silane catalyst, even after changing the reaction conditions.

Investigating catalytic mechanism[60]

Following the successful catalytic hydroboration of carbonyl and pyridine derivatives, the reaction mechanism was investigated. During the catalytic hydroboration of ketone and pyridine derivatives, it was observed that some of the spectra contain signals at about δ = 3.68, 1.76 and 1.07 ppm in the ^{1}H NMR spectra and δ = 0.91 ppm in the ^{11}B NMR spectra. These signals did not correspond to any of the reactants and products and hence, was suspected to be a new boron intermediate formed in the hydroboration. As such, stoichiometric reactions among the NHC-parent silyliumylidene cation, benzaldehyde, HBpin were carried out to determine this intermediate compound.[60] The stoichiometric reaction of the NHC-parent silyliumylidene cation and benzaldehyde under any conditions did not produce any new boron compounds. However, the stoichiometric reaction of the NHC-parent silyliumylidene cation and HBpin gave signals in both the ^{1}H and ^{11}B NMR spectra corresponding to those observed during the catalytic hydroboration of carbonyl and pyridine derivatives. Same ^{11}B NMR signal at δ 0.92 ppm (singlet) was observed, while the ^{1}H NMR spectrum shows a set of signals due

to methyl protons of I_{Me} and B*pin*. No Si-H and B-H signals were observed. On the basis of NMR spectroscopic data, the new boron compound formed in the reaction is an NHC-borylsilyliumylidene complex $[(I_{Me})_2SiBpin]I$. Its composition is also supported by the theoretical calculation and HRMS. Benzaldehyde was then added to this mixture to obtain the corresponding borate ester in 5 minutes in quantitative yields, determined via NMR spectroscopy (Scheme 6). This indicates that a NHC-borylsilyliumylidene complex was formed during the reaction of the NHC-parent silyliumylidene cation and HBpin, which was isolated as a white crystalline solid.

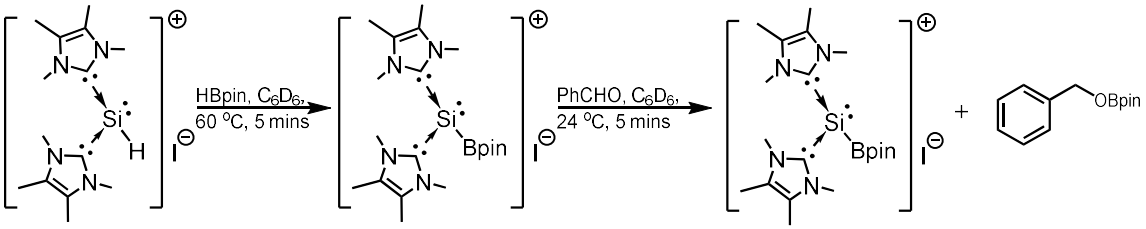

Scheme 6

The NHC-borylsilyliumylidene complex was also capable of catalysing the hydroboration of 1,4-dioxaspiro[4.5]decan-8-one and pyridine. As such, the NHC-borylsilyliumylidene complex should be a key intermediate in the catalysis. With this, the catalytic cycle was proposed as below.[60]

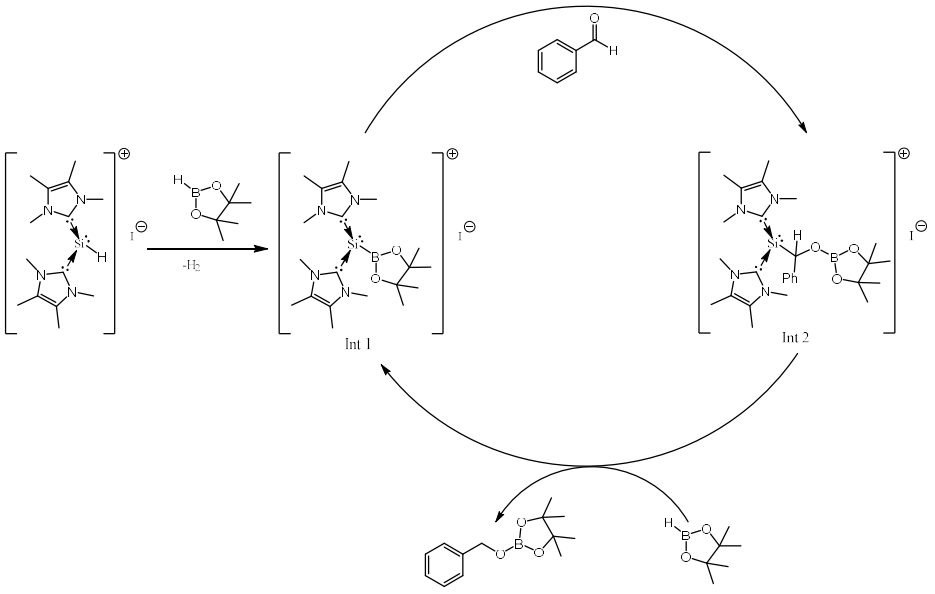

Scheme 7

The NHC-parent silyliumylidene cation first reacts with HBpin to form a NHC-borylsilyliumylidene complex, as well as hydrogen gas. The Si-B bond then inserts with the C=O bond of benzaldehyde, followed by undergoing σ-bond metathesis reaction with HBin to form the borate ester as well as to regenerate the NHC-borylsilyliumylidene complex (Scheme 7). To confirm this, a density functional theory (DFT) study at M06-2X/def2-SVP level of theory was studied to identify the feasibility of mechanism, which was collaborated with Prof. Ming-Der Su of National Chiayi University, Taiwan. Using the DFT calculation results, an energy level diagram was plotted.[60]

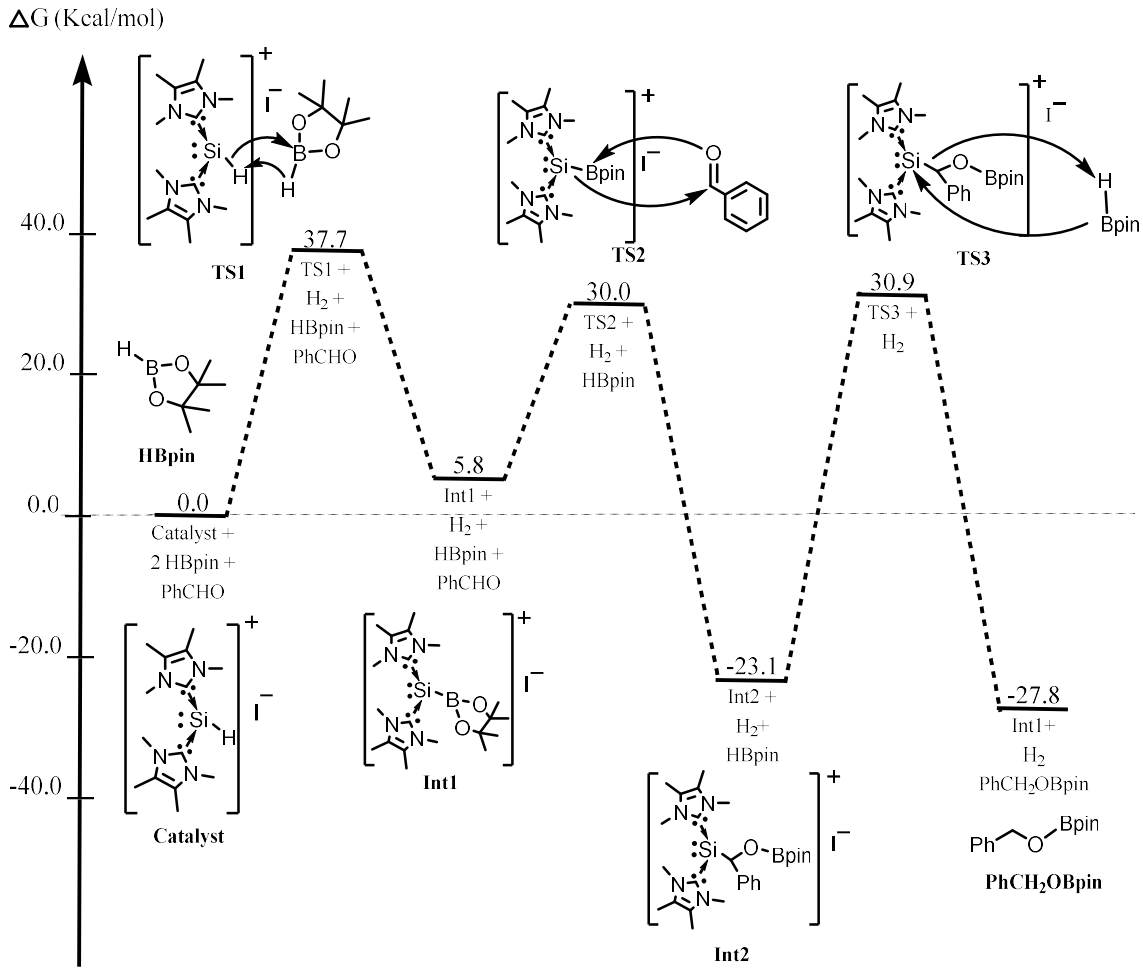

Figure 4: Energy profile diagram for catalysis via NHC-borylsilyliumylidene complex

From the energy diagram, the activation energy required for the initiation of the catalysis is 37.7 kcal/mol, where the NHC-parent silyliumylidene cation reacts with HBpin to form the NHC-borylsilyliumylidene complex (**Int1**), releasing H_2 gas in the process (Figure 4). This is consistent with the experimental data, where the NHC-parent silyliumylidene-mediated catalytic hydroboration of aldehyde derivatives could be carried out at room temperature.[60] The isolation of catalytic intermediates is currently under investigation in order to support the catalytic mechanism.

In case of pyridine derivatives, it is proposed that the catalysis proceeds through coordination of pyridine with HBpin first, which induces nucleophilic attack of the NHC-borylsilyliumylidene cation at the *para* position of pyridine due to lesser steric congestion. Subsequent dearomatization of pyridine results in displacing the hydride from the borane moiety, which then attacks at the para-position to afford N-boryl-1,4-dihydropyridine, along with the regeneration of the catalyst.

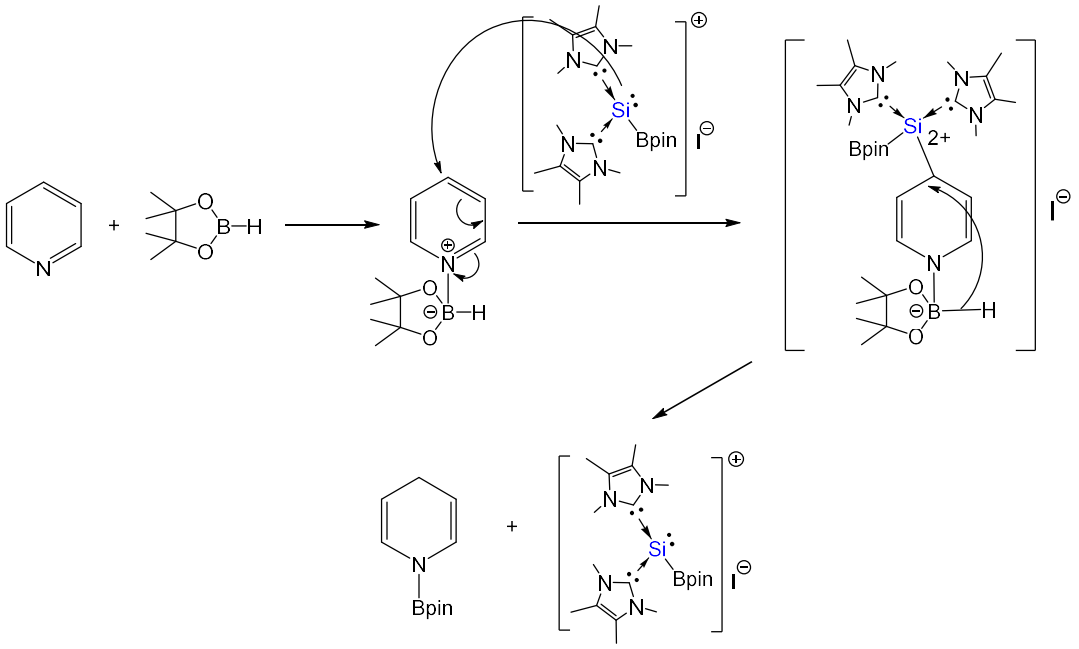

Scheme 8

Conclusion

The NHC-parent silyliumylidene cation has been shown to catalyse the hydroboration of a variety of carbonyl and pyridine derivatives under mild conditions with high chemo- and regioselectivity. The catalytic mechanism was investigated and was proposed to be via a NHC-borylsilyliumylidene complex.

References

1. Fischer, E. O.; Maasböl, A., On the Existence of a Tungsten Carbonyl Carbene Complex. *Angew. Chem. Int. Ed.* **1964,** *3* (8), 580-581.
2. Wanzlick, H.-W.; Schönherr, H.-J., Direct Synthesis of a Mercury Salt-Carbene Complex. *Angew. Chem. Int. Ed.* **1968,** *7* (2), 141-142.
3. Öfele, K., 1,3-Dimethyl-4-imidazolinyliden-(2)-pentacarbonylchrom ein neuer übergangsmetall-carben-komplex. *J. Organomet. Chem.* **1968,** *12* (3), P42-P43.
4. George, T. A.; Jones, K.; Lappert, M. F., 385. Amino-derivatives of metals and metalloids. Part II. Aminostannylation of unsaturated substrates, and the infrared spectra and structures of carbamato- and dithiocarbamato-trimethylstannanes and related compounds. *J. Chem. Soc.* **1965,** (0), 2157-2165.
5. Arduengo, A. J.; Harlow, R. L.; Kline, M., A stable crystalline carbene. *J. Am. Chem. Soc.* **1991,** *113* (1), 361-363.
6. Glorius, F., N-Heterocyclic Carbenes in Catalysis—An Introduction. In *N-Heterocyclic Carbenes in Transition Metal Catalysis*, Springer Berlin Heidelberg: Berlin, Heidelberg, 2007; pp 1-20.
7. Cazin, C. J., *N-Heterocyclic Carbenes in Transition Metal Catalysis and Organocatalysis*. Springer: 2011.
8. Lloyd, L., Handbook of Industrial Catalysts. 1 ed.; Springer US: Boston, MA, 2011; p. 490.
9. Diez-Gonzalez, S., *N-Heterocyclic Carbenes: From Laboratory Curiosities to Efficient Synthetic Tools: Edition 2*. The Royal Society of Chemistry: Cambridge, UK, 2017.
10. Mathey, F., *Transition Metal Organometallic Chemistry*. 1 ed.; Springer Singapore: Singapore, 2013; p 100.
11. Huang, J.; Schanz, H.-J.; Stevens, E. D.; Nolan, S. P., Stereoelectronic Effects Characterizing Nucleophilic Carbene Ligands Bound to the Cp*RuCl (Cp* = η5-C5Me5) Moiety: A Structural and Thermochemical Investigation. *Organometallics* **1999,** *18* (12), 2370-2375.
12. Bourissou, D.; Guerret, O.; Gabbaï, F. P.; Bertrand, G., Stable Carbenes. *Chem. Rev.* **2000,** *100* (1), 39-92.
13. Díez-González, S.; Nolan, S. P., Stereoelectronic parameters associated with N-heterocyclic carbene (NHC) ligands: A quest for understanding. *Coord. Chem. Rev.* **2007,** *251* (5), 874-883.
14. Heck, R. F., Mechanism of arylation and carbomethoxylation of olefins with organopalladium compounds. *J. Am. Chem. Soc.* **1969,** *91* (24), 6707-6714.
15. Dieck, H. A.; Heck, R. F., Organophosphinepalladium complexes as catalysts for vinylic hydrogen substitution reactions. *J. Am. Chem. Soc.* **1974,** *96* (4), 1133-1136.
16. Herrmann, W. A.; Elison, M.; Fischer, J.; Köcher, C.; Artus, G. R. J., Metal Complexes of N-Heterocyclic Carbenes—A New Structural Principle for Catalysts in Homogeneous Catalysis. *Angew. Chem. Int. Ed.* **1995,** *34* (21), 2371-2374.
17. Khramov, D. M.; Lynch, V. M.; Bielawski, C. W., N-Heterocyclic Carbene−Transition Metal Complexes: Spectroscopic and Crystallographic Analyses of π-Back-bonding Interactions. *Organometallics* **2007,** *26* (24), 6042-6049.
18. Herrmann, W. A., N-Heterocyclic Carbenes: A New Concept in Organometallic Catalysis. *Angew. Chem. Int. Ed.* **2002,** *41* (8), 1290-1309.
19. Schwab, P.; France, M. B.; Ziller, J. W.; Grubbs, R. H., A Series of Well-Defined Metathesis Catalysts–Synthesis of [RuCl2(□CHR′)(PR3)2] and Its Reactions. *Angew. Chem. Int. Ed.* **1995,** *34* (18), 2039-2041.

20. Schwab, P.; Grubbs, R. H.; Ziller, J. W., Synthesis and Applications of RuCl2(CHR')(PR3)2: The Influence of the Alkylidene Moiety on Metathesis Activity. *J. Am. Chem. Soc.* **1996,** *118* (1), 100-110.
21. Scholl, M.; Trnka, T. M.; Morgan, J. P.; Grubbs, R. H., Increased ring closing metathesis activity of ruthenium-based olefin metathesis catalysts coordinated with imidazolin-2-ylidene ligands. *Tetrahedron Lett.* **1999,** *40* (12), 2247-2250.
22. Markó, I. E.; Stérin, S.; Buisine, O.; Mignani, G.; Branlard, P.; Tinant, B.; Declercq, J.-P., Selective and Efficient Platinum(0)-Carbene Complexes As Hydrosilylation Catalysts. *Science* **2002,** *298* (5591), 204.
23. Brenner, E.; Fort, Y., New efficient nickel(0) catalysed amination of aryl chlorides. *Tetrahedron Lett.* **1998,** *39* (30), 5359-5362.
24. Kuhl, S.; Schneider, R.; Fort, Y., Catalytic Carbon-Fluorine Bond Activation with Monocoordinated Nickel-Carbene Complexes: Reduction of Fluoroarenes. *Adv. Synth. Catal.* **2003,** *345* (3), 341-344.
25. Gradel, B. t.; Brenner, E.; Schneider, R.; Fort, Y., Nickel-catalysed amination of aryl chlorides using a dihydroimidazoline carbene ligand. *Tetrahedron Lett.* **2001,** *42* (33), 5689-5692.
26. Desmarets, C.; Schneider, R.; Fort, Y., Nickel(0)/Dihydroimidazol-2-ylidene Complex Catalyzed Coupling of Aryl Chlorides and Amines. *J. Org. Chem.* **2002,** *67* (9), 3029-3036.
27. Davies, C. J. E.; Page, M. J.; Ellul, C. E.; Mahon, M. F.; Whittlesey, M. K., Ni(i) and Ni(ii) ring-expanded N-heterocyclic carbene complexes: C–H activation, indole elimination and catalytic hydrodehalogenation. *Chem. Commun.* **2010,** *46* (28), 5151-5153.
28. Power, P. P., Main-group elements as transition metals. *Nature* **2010,** *463*, 171.
29. Cotton, J. D.; Davidson, P. J.; Lappert, M. F., Subvalent Group 4B metal alkyls and amides. Part II. The chemistry and properties of bis[bis(trimethylsilyl)methyl]tin(II) and its lead analogue. *J. Chem. Soc., Dalton Trans.* **1976,** (21), 2275-2286.
30. Davidson, P. J.; Harris, D. H.; Lappert, M. F., Subvalent Group 4B metal alkyls and amides. Part I. The synthesis and physical properties of kinetically stable bis[bis(trimethysilyl)methyl]-germanium(II), -tin(II), and -lead(II). *J. Chem. Soc., Dalton Trans.* **1976,** (21), 2268-2274.
31. Grev, R. S., Structure and Bonding in the Parent Hydrides and Multiply Bonded Silicon and Germanium Compounds: From Mhn to R2M = M′ R2 and RM ≡ M′ R. In *Advances in Organometallic Chemistry*, Stone, F. G. A.; West, R., Eds. Academic Press: 1991; Vol. 33, pp 125-170.
32. Nesterov, V.; Reiter, D.; Bag, P.; Frisch, P.; Holzner, R.; Porzelt, A.; Inoue, S., NHCs in Main Group Chemistry. *Chem. Rev.* **2018,** *118* (19), 9678-9842.
33. Wang, Y.; Robinson, G. H., N-Heterocyclic Carbene—Main-Group Chemistry: A Rapidly Evolving Field. *Inorg. Chem.* **2014,** *53* (22), 11815-11832.
34. Power, P. P., Interaction of Multiple Bonded and Unsaturated Heavier Main Group Compounds with Hydrogen, Ammonia, Olefins, and Related Molecules. *Acc. Chem. Res.* **2011,** *44* (8), 627-637.
35. Sarmah, S.; Guha, A. K.; Phukan, A. K., Donor–Acceptor Complexes of Normal and Abnormal N-Heterocyclic Carbenes with Group 13 (B, Al, Ga) Elements: A Combined DFT and Atoms-in-Molecules Study. *Eur. J. Inorg. Chem.* **2013,** *2013* (18), 3233-3239.
36. Bayat, M.; Soltani, E., Stabilization of group 14 tetrylene compounds by N-heterocyclic carbene: A theoretical study. *Polyhedron* **2017,** *123*, 39-46.
37. Fischer, R. C.; Power, P. P., π-Bonding and the Lone Pair Effect in Multiple Bonds Involving Heavier Main Group Elements: Developments in the New Millennium. *Chem. Rev.* **2010,** *110* (7), 3877-3923.

38. Spikes, G. H.; Fettinger, J. C.; Power, P. P., Facile Activation of Dihydrogen by an Unsaturated Heavier Main Group Compound. *J. Am. Chem. Soc.* **2005,** *127* (35), 12232-12233.
39. Wilkins, L. C.; Melen, R. L., Enantioselective Main Group Catalysis: Modern Catalysts for Organic Transformations. *Coord. Chem. Rev.* **2016,** *324*, 123-139.
40. Sen, T. K.; Sau, S. C.; Mukherjee, A.; Hota, P. K.; Mandal, S. K.; Maity, B.; Koley, D., Abnormal N-heterocyclic carbene main group organometallic chemistry: a debut to the homogeneous catalysis. *Dalton Trans.* **2013,** *42* (39), 14253-14260.
41. Franz, D.; Sirtl, L.; Pöthig, A.; Inoue, S., Aluminum Hydrides Stabilized by N-Heterocyclic Imines as Catalysts for Hydroborations with Pinacolborane. *Z. Anorg. Allg. Chem.* **2016,** *642* (22), 1245-1250.
42. Ahmad, S. U.; Szilvási, T.; Irran, E.; Inoue, S., An NHC-Stabilized Silicon Analogue of Acylium Ion: Synthesis, Structure, Reactivity, and Theoretical Studies. *J. Am. Chem. Soc.* **2015,** *137* (17), 5828-5836.
43. Ahmad, S. U.; Szilvási, T.; Inoue, S., A facile access to a novel NHC-stabilized silyliumylidene ion and C–H activation of phenylacetylene. *Chem. Commun.* **2014,** *50* (84), 12619-12622.
44. Macdonald, C. L. B.; Binder, J. F.; Swidan, A. a.; Nguyen, J. H.; Kosnik, S. C.; Ellis, B. D., Convenient Preparation and Detailed Analysis of a Series of NHC-Stabilized Phosphorus(I) Dyes and Their Derivatives. *Inorg. Chem.* **2016,** *55* (14), 7152-7166.
45. Chu, T.; Nikonov, G. I., Oxidative Addition and Reductive Elimination at Main-Group Element Centers. *Chem. Rev.* **2018,** *118* (7), 3608-3680.
46. Heuclin, H.; Ho, S. Y. F.; Le Goff, X. F.; So, C.-W.; Mézailles, N., Facile B–H Bond Activation of Borane by Stable Carbenoid Species. *J. Am. Chem. Soc.* **2013,** *135* (24), 8774-8777.
47. Hadlington, T. J.; Hermann, M.; Frenking, G.; Jones, C., Low Coordinate Germanium(II) and Tin(II) Hydride Complexes: Efficient Catalysts for the Hydroboration of Carbonyl Compounds. *J. Am. Chem. Soc.* **2014,** *136* (8), 3028-3031.
48. Chong, C. C.; Hirao, H.; Kinjo, R., Metal-Free σ-Bond Metathesis in 1,3,2-Diazaphospholene-Catalyzed Hydroboration of Carbonyl Compounds. *Angew. Chem. Int. Ed.* **2015,** *54* (1), 190-194.
49. Yang, Z.; Zhong, M.; Ma, X.; De, S.; Anusha, C.; Parameswaran, P.; Roesky, H. W., An Aluminum Hydride That Functions like a Transition-Metal Catalyst. *Angew. Chem. Int. Ed.* **2015,** *54* (35), 10225-10229.
50. Li, N.; Guan, B.-T., A Dialkyl Calcium Carbene Adduct: Synthesis, Structure, and Catalytic Cross-Dehydrocoupling of Silanes with Amines. *Eur. J. Inorg. Chem.* **2019,** *2019* (16), 2231-2235.
51. Raabe, G.; Michl, J., Multiple bonding to silicon. *Chem. Rev.* **1985,** *85* (5), 419-509.
52. Colvin, E. W., Silicon in organic synthesis. *Chem. Soc. Rev.* **1978,** *7* (1), 15-64.
53. Michl, J., Editorial. Silicon Chemistry. *Chem. Rev.* **1995,** *95* (5), 1135-1135.
54. Asay, M.; Jones, C.; Driess, M., N-Heterocyclic Carbene Analogues with Low-Valent Group 13 and Group 14 Elements: Syntheses, Structures, and Reactivities of a New Generation of Multitalented Ligands. *Chem. Rev.* **2011,** *111* (2), 354-396.
55. Schneider, J.; Sindlinger, C. P.; Freitag, S. M.; Schubert, H.; Wesemann, L., Diverse Activation Modes in the Hydroboration of Aldehydes and Ketones with Germanium, Tin, and Lead Lewis Pairs. *Angew. Chem. Int. Ed.* **2017,** *56* (1), 333-337.
56. Wu, Y.; Shan, C.; Sun, Y.; Chen, P.; Ying, J.; Zhu, J.; Liu, L.; Zhao, Y., Main group metal–ligand cooperation of N-heterocyclic germylene: an efficient catalyst for hydroboration of carbonyl compounds. *Chem. Commun.* **2016,** *52* (95), 13799-13802.
57. Jakhar, V. K.; Barman, M. K.; Nembenna, S., Aluminum Monohydride Catalyzed Selective Hydroboration of Carbonyl Compounds. *Org. Lett.* **2016,** *18* (18), 4710-4713.

58. Bisai, M. K.; Pahar, S.; Das, T.; Vanka, K.; Sen, S. S., Transition metal free catalytic hydroboration of aldehydes and aldimines by amidinato silane. *Dalton Trans.* **2017,** *46* (8), 2420-2424.
59. Li, Y.; Chan, Y.-C.; Leong, B.-X.; Li, Y.; Richards, E.; Purushothaman, I.; De, S.; Parameswaran, P.; So, C.-W., Trapping a Silicon(I) Radical with Carbenes: A Cationic cAAC–Silicon(I) Radical and an NHC–Parent-Silyliumylidene Cation. *Angew. Chem. Int. Ed.* **2017,** *56* (26), 7573-7578.
60. Leong, B.-X.; Lee, J.; Li, Y.; Yang, M.-C.; Siu, C.-K.; Su, M.-D.; So, C.-W., A Versatile NHC-Parent Silyliumylidene Cation for Catalytic Chemo- and Regioselective Hydroboration. *Manuscript submitted for publication* **2019**.
61. Anker, M. D.; Arrowsmith, M.; Bellham, P.; Hill, M. S.; Kociok-Köhn, G.; Liptrot, D. J.; Mahon, M. F.; Weetman, C., Selective reduction of CO2 to a methanol equivalent by B(C6F5)3-activated alkaline earth catalysis. *Chem. Sci.* **2014,** *5* (7), 2826-2830.
62. Abdalla, J. A. B.; Riddlestone, I. M.; Tirfoin, R.; Aldridge, S., Cooperative Bond Activation and Catalytic Reduction of Carbon Dioxide at a Group 13 Metal Center. *Angew. Chem. Int. Ed.* **2015,** *54* (17), 5098-5102.
63. Hadlington, T. J.; Kefalidis, C. E.; Maron, L.; Jones, C., Efficient Reduction of Carbon Dioxide to Methanol Equivalents Catalyzed by Two-Coordinate Amido–Germanium(II) and −Tin(II) Hydride Complexes. *ACS Catal.* **2017,** *7* (3), 1853-1859.

Appendix

General experimental procedures:

All manipulations were carried out under an inert atmosphere of argon gas by standard Schlenk techniques. The catalyst was prepared according to the literature procedure. Toluene, hexane and diethyl ether was dried over Na/K alloy and distilled prior to use. C_6D_6 were dried over K metal and distilled prior to use. Chemicals were purchased and dried over CaH_2 prior to usage.

The ^{1}H and ^{11}B NMR spectra were recorded on a JEOL ECA 400 spectrometer. The NMR spectra were recorded in C_6D_6 and referenced to the residual proton peak of C_6D_6 relative to $SiMe_4$ for ^{1}H and $BF_3{\cdot}Et_2O$ for ^{11}B. The following abbreviations are used to describe signal multiplicities: s = singlet, d = doublet, t = triplet, q = quartet and m = multiplet. Coupling constants *J* are given in Hertz (Hz).

General procedures for the catalytic hydroboration of carbonyl and pyridine derivatives[60]

HBpin (16.0 µL, 0.11 mmol, 1.1 equiv.) was added to a J-Young NMR tube containing the catalyst (4.0 mg, 0.01 mmol, 10 mol%) and 0.4 mL of C_6D_6. The substrate (0.1 mmol, 1.0 equiv.) was then added and the reaction mixture was mixed vigorously. The reaction conditions follow those in Table 2 – 4 and the reaction monitored via NMR spectroscopy. The conversion was calculated based on the presence of the substrate and the corresponding product. The chemical shifts of the products agree with the reported values in the literature.

Isolation of the borate ester product (hydroboration of carbonyl derivatives)[60]

After the completion of the catalyses, the crude solution was filtered and the filtrate dried under vacuum. The dried residue was then extracted with hexane and the resultant borate ester solution was dried under vacuum for at least one hour to remove the volatiles.

Isolation of the N-boryl-1,4-dihydropyridine product (hydroboration of pyridine derivatives)

After the completion of the catalyses, the crude solution was filtered and the filtrate dried under vacuum. The dried residue was then extracted with diethyl ether and the resultant N-boryl-1,4-dihydropyridine solution was dried under vacuum for at least one hour to remove the volatiles.

Table A1: NMR Spectroscopic data for the hydroboration of aldehyde derivatives

Entry	Product	NMR Chemical shifts
1	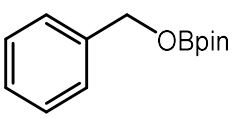	^{1}H NMR (395.9 MHz, 24 °C, C_6D_6, ppm): δ = 7.30 (d, 2H, Ar-*H*, $^{3}J_{H,H}$ = 7.2 Hz,), 7.15 – 7.11 (m, 2H, Ar-*H*), 7.07 – 7.03 (m, 1H, Ar-*H*), 4.93 (s, 2H, O-C*H*$_2$), 1.04 (s, 12H, Bpin-C*H*$_3$). ^{11}B{^{1}H} NMR (128.41 MHz, 24 °C, C_6D_6, ppm): δ = 21.8.
2	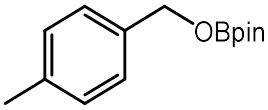	^{1}H NMR (395.9 MHz, 24 °C, C_6D_6, ppm): δ = 7.25 (d, 2H, Ar-*H*, $^{3}J_{H,H}$ = 7.7 Hz), 6.96 (d, 2H, Ar-*H*, $^{3}J_{H,H}$ = 8.2 Hz), 4.95 (s, 2H, O-C*H*$_2$), 2.08 (s, 3H, -C*H*$_3$), 1.05 (s, 12H, Bpin-C*H*$_3$). ^{11}B{^{1}H} NMR (128.41 MHz, 24 °C, C_6D_6, ppm): δ = 21.9.
3	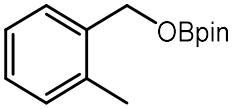	^{1}H NMR (395.9 MHz, 24 °C, C_6D_6, ppm): δ = 7.54 (d, 1H, Ar-*H*, $^{3}J_{H,H}$ = 7.2 Hz), 7.12 – 7.03 (m, 2H, Ar-*H*), 6.95 (d, 1H, Ar-H, $^{3}J_{H,H}$ = 6.8 Hz), 4.97 (s, 2H, O-C*H*$_2$), 2.07 (s, 3H, -C*H*$_3$), 1.05 (s, 12H, Bpin-C*H*$_3$). ^{11}B{^{1}H} NMR (128.41 MHz, 24 °C, C_6D_6, ppm): δ = 21.9.
4	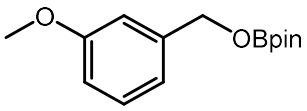	^{1}H NMR (395.9 MHz, 24 °C, C_6D_6, ppm): δ = 7.09 – 7.06 (m, 1H, Ar-*H*), 6.99 (s, 1H, Ar-*H*), 6.92 (d, 1H, Ar-*H*, $^{3}J_{H,H}$ = 7.2 Hz), 6.71 (dd, 1H, Ar-*H*, $^{3}J_{H,H}$ = 2.3, 8.2 Hz), 4.94 (s, 2H, O-C*H*$_2$), 3.32 (s, 3H, O-C*H*$_3$), 1.05 (s, 12H, Bpin-C*H*$_3$). ^{11}B{^{1}H} NMR (128.41 MHz, 24 °C, C_6D_6, ppm): δ = 21.8.
5	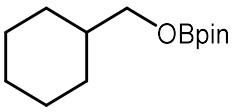	^{1}H NMR (395.9 MHz, 24 °C, C_6D_6, ppm): δ = 3.73 (d, 2H, O-C*H*$_2$, $^{3}J_{H,H}$ = 4.5 Hz), 1.71 – 1.38 (m, 11H, Cy-*H*), 1.07 (s, 12H, Bpin-C*H*$_3$). ^{11}B{^{1}H} NMR (128.41 MHz, 24 °C, C_6D_6, ppm): δ = 21.6.
6	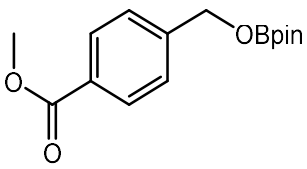	^{1}H NMR (395.9 MHz, 24 °C, C_6D_6, ppm): δ = 8.02 (d, 2H, Ar-*H*, $^{3}J_{H,H}$ = 8.2 Hz), 7.22 (d, 2H, Ar-*H*, $^{3}J_{H,H}$ = 6.8 Hz), 4.85 (s, 2H, O-C*H*$_2$), 3.51 (s, 3H, O-C*H*$_3$), 1.04 (s, 12H, Bpin-C*H*$_3$). ^{11}B{^{1}H} NMR (128.41 MHz, 24 °C, C_6D_6, ppm): δ = 21.7.

7 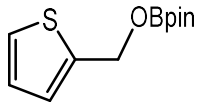

^{1}H NMR (395.9 MHz, 24 ºC, C_6D_6, ppm): δ = 6.88 (d, 1H, Ar-*H*, $^{3}J_{H,H}$ = 5.0 Hz), 6.82 (d, 1H, Ar-*H*, $^{3}J_{H,H}$ = 3.2 Hz), 6.69 – 6.67 (m, 1H, Ar-*H*), 4.98 (s, 2H, O-C*H*$_2$), 1.04 (s, 12H, Bpin-C*H*$_3$).
^{11}B{^{1}H} NMR (128.41 MHz, 24 ºC, C_6D_6, ppm): δ = 21.8.

8 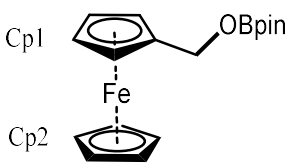

^{1}H NMR (395.9 MHz, 24 ºC, C_6D_6, ppm): δ = 4.75 (s, 2H, O-C*H*$_2$), 4.21 (t, 2H, Cp1-*H,* $^{3}J_{H,H}$ = 1.8 Hz), 3.98 (s, 5H, Cp2-*H*), 3.95 (t, 2H, Cp1-*H,* $^{3}J_{H,H}$ = 1.8 Hz), 1.07 (s, 12H, Bpin-C*H*$_3$).
^{11}B{^{1}H} NMR (128.41 MHz, 24 ºC, C_6D_6, ppm): δ = 21.9.

9 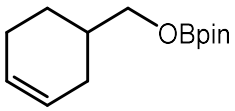

^{1}H NMR (395.9 MHz, 24 ºC, C_6D_6, ppm): δ = 5.59 (s, 2H, C=C*H*), 3.78 (d, 2H, O-C*H*$_2$, $^{3}J_{H,H}$ = 5.9 Hz), 2.03 – 1.67 (m, 7H, Cy-*H*), 1.06 (s, 12H, Bpin-C*H*$_3$).
^{11}B{^{1}H} NMR (128.41 MHz, 24 ºC, C_6D_6, ppm): δ = 21.6.

10 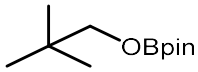

^{1}H NMR (395.9 MHz, 24 ºC, C_6D_6, ppm): δ = 3.65 (s, 2H, O-C*H*$_2$), 1.07 (s, 12H, Bpin-C*H*$_3$), 0.90 (s, 9H, -C*H*$_3$).
^{11}B{^{1}H} NMR (128.41 MHz, 24 ºC, C_6D_6, ppm): δ = 21.7.

11 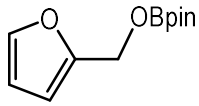

^{1}H NMR (395.9 MHz, 24 ºC, C_6D_6, ppm): δ = 7.05 (m, 1H, Ar-*H*), 6.13 (d, 1H, Ar-*H*, $^{3}J_{H,H}$ = 3.2 Hz), 6.02 – 6.01 (m, 1H, Ar-*H*), 4.85 (s, 2H, O-C*H*$_2$), 1.03 (s, 12H, Bpin-C*H*$_3$).
^{11}B{^{1}H} NMR (128.41 MHz, 24 ºC, C_6D_6, ppm): δ = 21.8.

12 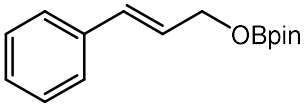

^{1}H NMR (395.9 MHz, 24 ºC, C_6D_6, ppm): δ = 7.18 (d, 2H, Ar-*H*, $^{3}J_{H,H}$ = 7.2 Hz), 7.08 (t, 2H, Ar-*H*, $^{3}J_{H,H}$ = 7.2 Hz), 7.03 – 6.99 (m, 1H, Ar-*H*), 6.61 (d, 1H, Ar-C*H*, $^{3}J_{H,H}$ = 16.3 Hz), 6.17 (dt, 1H, Ar-C=C*H*, $^{3}J_{H,H}$ = 5.2, 15.9 Hz), 4.54 (dd, 2H, O-C*H*$_2$, $^{3}J_{H,H}$ = 5.2 Hz, $^{4}J_{H,H}$ = 1.6 Hz), 1.06 (s, 12H, Bpin-C*H*$_3$).
^{11}B{^{1}H} NMR (128.41 MHz, 24 ºC, C_6D_6, ppm): δ = 21.8.

13 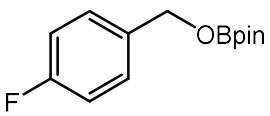

^{1}H NMR (395.9 MHz, 24 ºC, C_6D_6, ppm): δ = 7.09 – 7.05 (m, 2H, Ar-*H*), 6.78 – 6.74 (m, 2H, Ar-*H*), 4.80 (s, 2H, O-C*H*$_2$), 1.04 (s, 12H, Bpin-C*H*$_3$).
^{11}B{^{1}H} NMR (128.41 MHz, 24 ºC, C_6D_6, ppm): δ = 21.8.

14	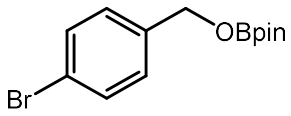	^{1}H NMR (395.9 MHz, 24 ºC, C_6D_6, ppm): δ = 7.21 (d, 2H, Ar-*H*, $^{3}J_{H,H}$ = 8.6 Hz), 6.93 (d, 2H, Ar-*H*, $^{3}J_{H,H}$ = 8.6 Hz), 4.73 (s, 2H, O-C*H*$_2$), 1.03 (s, 12H, Bpin-C*H*$_3$). ^{11}B{^{1}H} NMR (128.41 MHz, 24 ºC, C_6D_6, ppm): δ = 21.8.
15	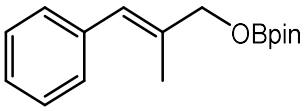	^{1}H NMR (395.9 MHz, 24 ºC, C_6D_6, ppm): δ = 7.20 – 7.12 (m, 4H [overlap with C_6D_6], Ar-*H*), 7.06 – 7.02 (m, 1H, Ar-*H*), 6.69 (s, 1H, C=C*H*), 4.46 (s, 2H, O-C*H*$_2$), 1.72 (s, 3H, C-C*H*$_3$), 1.08 (s, 12H, Bpin-C*H*$_3$). ^{11}B{^{1}H} NMR (128.41 MHz, 24 ºC, C_6D_6, ppm): δ = 21.9.
16	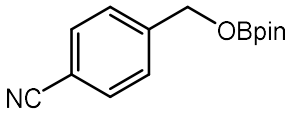	^{1}H NMR (395.9 MHz, 24 ºC, C_6D_6, ppm): δ = 6.99 (d, 2H, Ar-*H*, $^{3}J_{H,H}$ = 4.6 Hz), 6.87 (d, 2H, Ar-*H*, $^{3}J_{H,H}$ = 5.4 Hz), 4.67 (s, 2H, O-C*H*$_2$), 1.04 (s, 12H, Bpin-C*H*$_3$). ^{11}B{^{1}H} NMR (128.41 MHz, 24 ºC, C_6D_6, ppm): δ = 21.8.
17	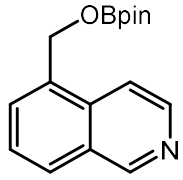	^{1}H NMR (395.9 MHz, 24 ºC, C_6D_6, ppm): δ = 9.17 (s, 1H, Ar-*H*), 8.54 (d, 1H, Ar-*H*, $^{3}J_{H,H}$ = 5.9 Hz), 7.64 (d, 1H, Ar-*H*, $^{3}J_{H,H}$ = 7.2 Hz), 7.43 (d, 1H, Ar-*H*, $^{3}J_{H,H}$ = 5.9 Hz), 7.35 (d, 1H, Ar-*H*, $^{3}J_{H,H}$ = 8.2 Hz), 7.10 (t, 1H, Ar-*H*, $^{3}J_{H,H}$ = 7.5 Hz), 5.23 (s, 2H, O-C*H*$_2$), 1.05 (s, 12H, Bpin-C*H*$_3$). ^{11}B{^{1}H} NMR (128.41 MHz, 24 ºC, C_6D_6, ppm): δ = 21.9.
18	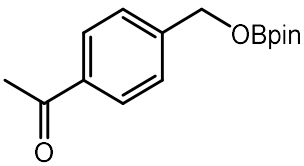	^{1}H NMR (395.9 MHz, 24 ºC, C_6D_6, ppm): δ = 7.75 (d, 2H, Ar-*H*, $^{3}J_{H,H}$ = 8.2 Hz), 7.21 (d, 2H, Ar-*H*, $^{3}J_{H,H}$ = 8.6 Hz), 4.88 (s, 2H, O-C*H*$_2$), 2.08 (s, 3H, C-C*H*$_3$), 1.05 (s 12H, Bpin-C*H*$_3$). ^{11}B{^{1}H} NMR (128.41 MHz, 24 ºC, C_6D_6, ppm): δ = 21.9.

Table A2: NMR Spectroscopic data for the hydroboration of ketone derivatives

Entry	Product	NMR Chemical shifts
1	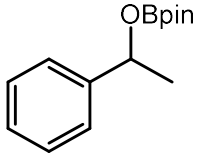	^{1}H NMR (395.9 MHz, 24 ºC, C_6D_6, ppm): δ = 7.37 (d, 2H, Ar-*H*, $^{3}J_{H,H}$ = 7.2 Hz), 7.16 – 7.12 (m, 2H [overlap with C_6D_6], Ar-*H*), 7.07 – 7.03 (m, 1H, Ar-*H*), 5.41 (q, 1H, O-C*H*, $^{3}J_{H,H}$ = 6.8 Hz), 1.46 (d, 3H, OCH-CH_3, $^{3}J_{H,H}$ = 6.3 Hz), 1.03 (s, 6H, Bpin-CH_3), 1.00 (s, 6H, Bpin-CH_3). ^{11}B{^{1}H} NMR (128.41 MHz, 24 ºC, C_6D_6, ppm): δ = 21.7.
2	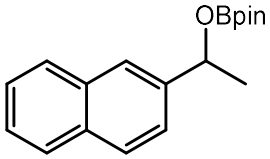	^{1}H NMR (395.9 MHz, 24 ºC, C_6D_6, ppm): δ = 7.85 (s, 1H, Ar-*H*), 7.62 – 7.59 (m, 3H, Ar-*H*), 7.47 (dd, 1H, Ar-*H*, $^{3}J_{H,H}$ = 1.8, 8.6 Hz), 7.26 – 7.20 (m, 2H, Ar-*H*), 5.58 (q, 1H, O-C*H*, $^{3}J_{H,H}$ = 6.3 Hz), 1.55 (d, 3H, OCH-CH_3, $^{3}J_{H,H}$ = 6.4 Hz), 1.03 (s, 6H, Bpin-CH_3), 1.00 (s, 6H, Bpin-CH_3). ^{11}B{^{1}H} NMR (128.41 MHz, 24 ºC, C_6D_6, ppm): δ = 21.6.
3	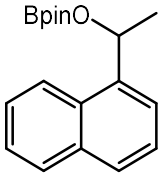	^{1}H NMR (395.9 MHz, 24 ºC, C_6D_6, ppm): δ = 7.97 – 7.95 (m, 1H, Ar-*H*), 7.88 (d, 1H, Ar-*H*, $^{3}J_{H,H}$ = 7.2 Hz), 7.64 – 7.62 (m, 1H, Ar-*H*), 7.54 (d, 1H, Ar-*H*, $^{3}J_{H,H}$ = 8.2 Hz), 7.30 – 7.26 (m, 1H, Ar-*H*), 7.25 – 7.20 (m, 2H, Ar-*H*), 6.19 (q, 1H, O-C*H*, $^{3}J_{H,H}$ = 6.3 Hz), 1.63 (d, 3H, OCH-CH_3, $^{3}J_{H,H}$ = 6.3 Hz), 1.02 (s, 6H, Bpin-CH_3), 0.98 (s, 6H, Bpin-CH_3). ^{11}B{^{1}H} NMR (128.41 MHz, 24 ºC, C_6D_6, ppm): δ = 21.7.
4	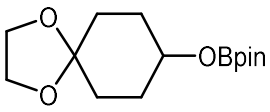	^{1}H NMR (395.9 MHz, 24 ºC, C_6D_6, ppm): δ = 4.35 – 4.29 (m, 1H, O-C*H*), 3.53 – 3.46 (m, 4H, O-CH_2), 1.92 – 1.85 (m, 6H, Cy-*H*), 1.58 – 1.47 (m, 2H, Cy-*H*), 1.06 (s, 12H, Bpin-CH_3). ^{11}B{^{1}H} NMR (128.41 MHz, 24 ºC, C_6D_6, ppm): δ = 21.3.
5	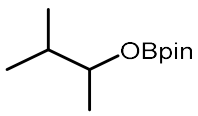	^{1}H NMR (395.9 MHz, 24 ºC, C_6D_6, ppm): δ = 4.15 (dq, 1H, O-C*H*, $^{3}J_{H,H}$ = 6.1 Hz), 1.69 – 1.61 (m, 1H, $(CH_3)_2CH$), 1.16 (d, 3H, -CH_3, $^{3}J_{H,H}$ = 6.3 Hz), 1.07 (s, 12H, Bpin-CH_3), 0.92 (d, 3H, -CH_3, $^{3}J_{H,H}$ = 6.4 Hz), 0.86 (d, 3H, -CH_3, $^{3}J_{H,H}$ = 6.8 Hz). ^{11}B{^{1}H} NMR (128.41 MHz, 24 ºC, C_6D_6, ppm): δ = 21.5.

6	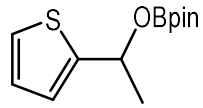	^{1}H NMR (395.9 MHz, 24 ºC, C_6D_6, ppm): δ = 6.86 – 6.85 (m, 1H, Ar-*H*), 6.84 – 6.82 (m, 1H, Ar-*H*), 6.70 – 6.68 (m, 1H, Ar-*H*), 5.63 (q, 1H, O-C*H*, $^{3}J_{H,H}$ = 6.5 Hz), 1.52 (d, 3H, OCH-CH_3, $^{3}J_{H,H}$ = 6.4 Hz), 1.03 (s, 12H, Bpin-CH_3). ^{11}B{^{1}H} NMR (128.41 MHz, 24 ºC, C_6D_6, ppm): δ = 21.6.
7	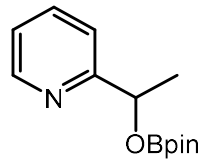	^{1}H NMR (395.9 MHz, 24 ºC, C_6D_6, ppm): δ = 8.38 (d, 1H, Ar-*H*, $^{3}J_{H,H}$ = 5.0 Hz), 7.30 (d, 1H, Ar-*H*, $^{3}J_{H,H}$ = 7.7 Hz), 7.15 – 7.10 (m, 1H, Ar-*H*), 6.64 – 6.61 (m, 1H, Ar-*H*), 5.54 (q, 1H, O-C*H*, $^{3}J_{H,H}$ = 6.7 Hz), 1.60 (d, 3H, OCH-CH_3, $^{3}J_{H,H}$ = 6.3 Hz), 1.13 (s, 6H, Bpin-CH_3), 1.11 (s, 6H, Bpin-CH_3). ^{11}B{^{1}H} NMR (128.41 MHz, 24 ºC, C_6D_6, ppm): δ = 19.5.
8	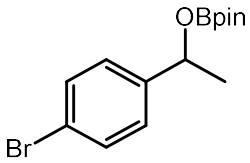	^{1}H NMR (395.9 MHz, 24 ºC, C_6D_6, ppm): δ 7.23 (d, 2H, Ar-*H*, $^{3}J_{H,H}$ = 8.6 Hz), 6.99, (d, 2H, Ar-*H*, $^{3}J_{H,H}$ = 8.6 Hz), 5.23 (q, 1H, O-C*H*, $^{3}J_{H,H}$ = 6.6 Hz), 1.33 (d, 3H, OCH-CH_3, $^{3}J_{H,H}$ = 6.4 Hz), 1.02 (s, 12H, Bpin-CH_3) ^{11}B{^{1}H} NMR (128.41 MHz, 24 ºC, C_6D_6, ppm): δ = 21.5.
9	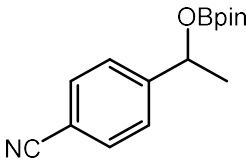	^{1}H NMR (395.9 MHz, 24 ºC, C_6D_6, ppm): δ = 7.02 – 6.94 (m, 4H, Ar-*H*), 5.15 (q, 1H, O-C*H*, $^{3}J_{H,H}$ = 6.5 Hz), 1.23 (d, 3H, OCH-CH_3, $^{3}J_{H,H}$ = 6.3 Hz), 1.02 (s, 6H, Bpin-CH_3), 0.99 (s, 6H, Bpin-CH_3). ^{11}B{^{1}H} NMR (128.41 MHz, 24 ºC, C_6D_6, ppm): δ = 21.6.

Table A3: NMR Spectroscopic data for the hydroboration of pyridine derivatives

Entry	Product	NMR Chemical shifts
1	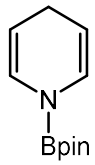	^{1}H NMR (395.9 MHz, 24 ºC, C_6D_6, ppm): δ = 6.52 – 6.50 (m, 2H, N=C*H*), 4.59 – 4.55 (m, 2H, C=C*H*), 2.83 – 2.81 (m, 2H, -CH_2), 0.98 (s, 12H, Bpin-CH_3). ^{11}B{^{1}H} NMR (128.41 MHz, 24 ºC, C_6D_6, ppm): δ = 23.1.
2	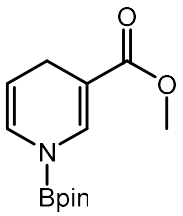	^{1}H NMR (395.9 MHz, 24 ºC, C_6D_6, ppm): δ = 7.83 (s, 1H, N=C*H*), 6.33 (d, 1H, N=C*H*, $^{3}J_{H,H}$ = 6.8 Hz), 4.70 – 4.68 (m, 1H, C=C*H*), 3.40 (s, 3H, O-CH_3), 3.20 (s, 2H, -CH_2), 0.93 (s, 12H, Bpin-CH_3). ^{11}B{^{1}H} NMR (128.41 MHz, 24 ºC, C_6D_6, ppm): δ = 23.1.
3	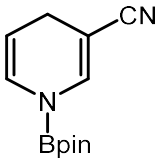	^{1}H NMR (395.9 MHz, 24 ºC, C_6D_6, ppm): δ = 6.87 (s, 1H, N=C*H*), 6.07 (d, 1H, N=C*H* ,$^{3}J_{H,H}$ = 8.2 Hz), 4.28 – 4.23 (m, 1H, C=C*H*), 2.61 – 2.59 (m, 2H, -CH_2), 0.91 (s, 12H, Bpin-CH_3). ^{11}B{^{1}H} NMR (128.41 MHz, 24 ºC, C_6D_6, ppm): δ = 22.8.
4	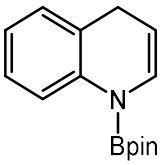	^{1}H NMR (395.9 MHz, 24 ºC, C_6D_6, ppm): δ = 7.78 (d, 1H, N=C*H*, $^{3}J_{H,H}$ = 8.2 Hz), 7.10 – 7.06 (m, 1H, Ar-*H*), 6.85 – 6.77 (m, 2H, Ar-*H*), 6.25 (d, 1H, Ar-*H*, $^{3}J_{H,H}$ = 10.0 Hz), 5.58 (dt, 1H, C=C*H*, $^{3}J_{H,H}$ = 4.5, 9.5 Hz), 4.14 (dt, 2H, -CH_2, $^{3}J_{H,H}$ = 1.8, 4.1 Hz), 1.04 (s, 12H, Bpin-CH_3). ^{11}B{^{1}H} NMR (128.41 MHz, 24 ºC, C_6D_6, ppm): δ = 22.8.
5	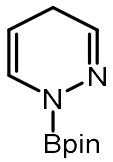	^{1}H NMR (395.9 MHz, 24 ºC, C_6D_6, ppm): δ = 6.62 – 6.61 (m, 1H, N=C*H*), 6.48 (d, 1H, N=C*H*, $^{3}J_{H,H}$ = 1.8 Hz), 4.32 – 4.30 (m, 1H, C=C*H*), 2.30 (s, 2H, -CH_2), 1.04 (s, 12H, Bpin-CH_3). ^{11}B{^{1}H} NMR (128.41 MHz, 24 ºC, C_6D_6, ppm): δ = 23.6.

6	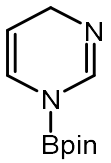	^{1}H NMR (395.9 MHz, 24 ºC, C_6D_6, ppm): δ = 8.17 (d, 1H, N=C*H*, $^{3}J_{H,H}$ = 4.5 Hz), 6.28 (dt, 1H, C=C*H*, $^{3}J_{H,H}$ = 1.5, 4.9 Hz), 4.82 (s, 1H, N=C*H*), 3.83 – 3.81 (m, 2H, -CH_2), 1.06 (s, 12H, Bpin-CH_3). ^{11}B{^{1}H} NMR (128.41 MHz, 24 ºC, C_6D_6, ppm): δ = 23.2.

Table S1 Entry 1, ^{1}H, $^{11}B\{^{1}H\}$ NMR Spectra of crude product

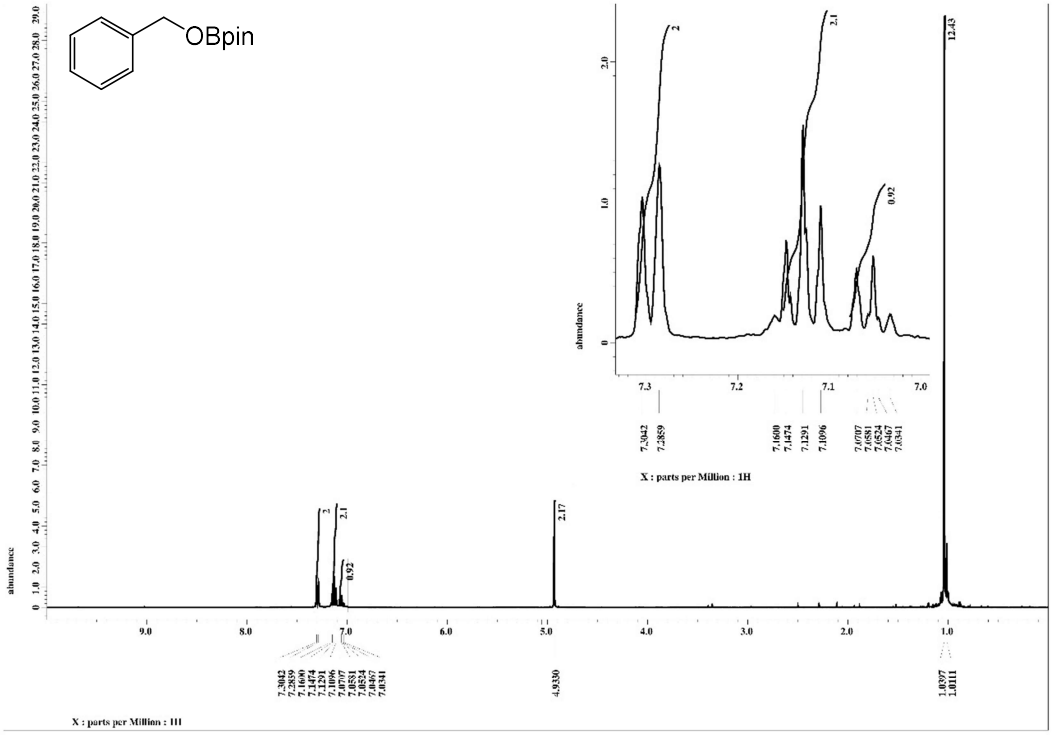

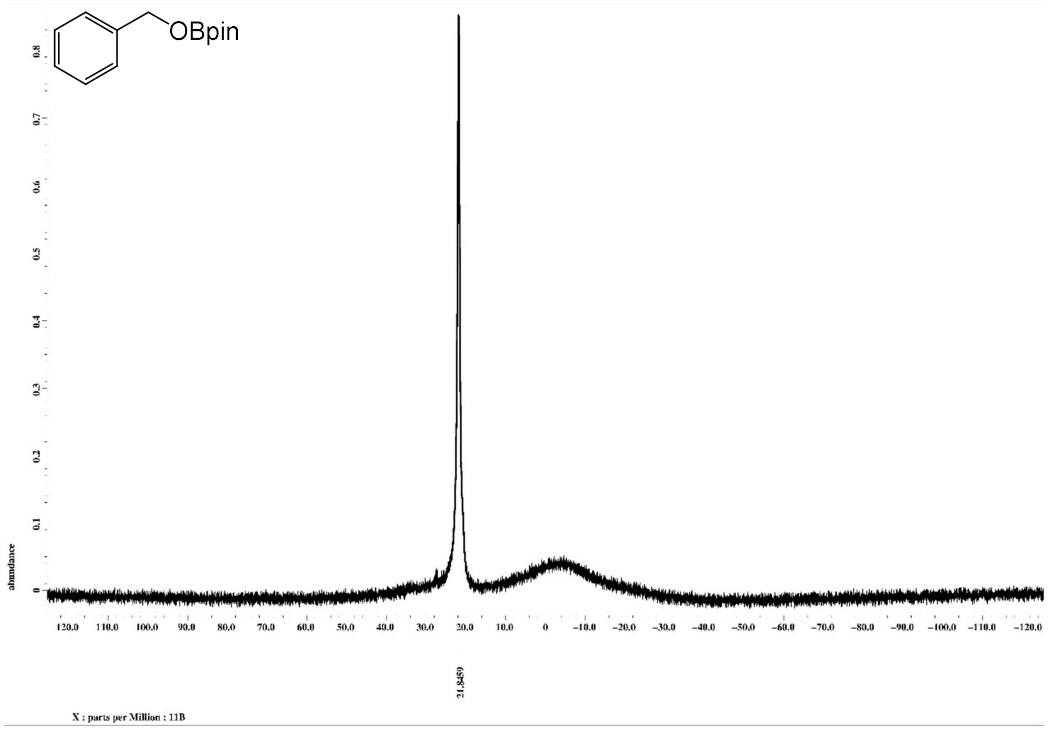

Table S1 Entry 2, ^{1}H, $^{11}B\{^{1}H\}$ NMR Spectra of crude product

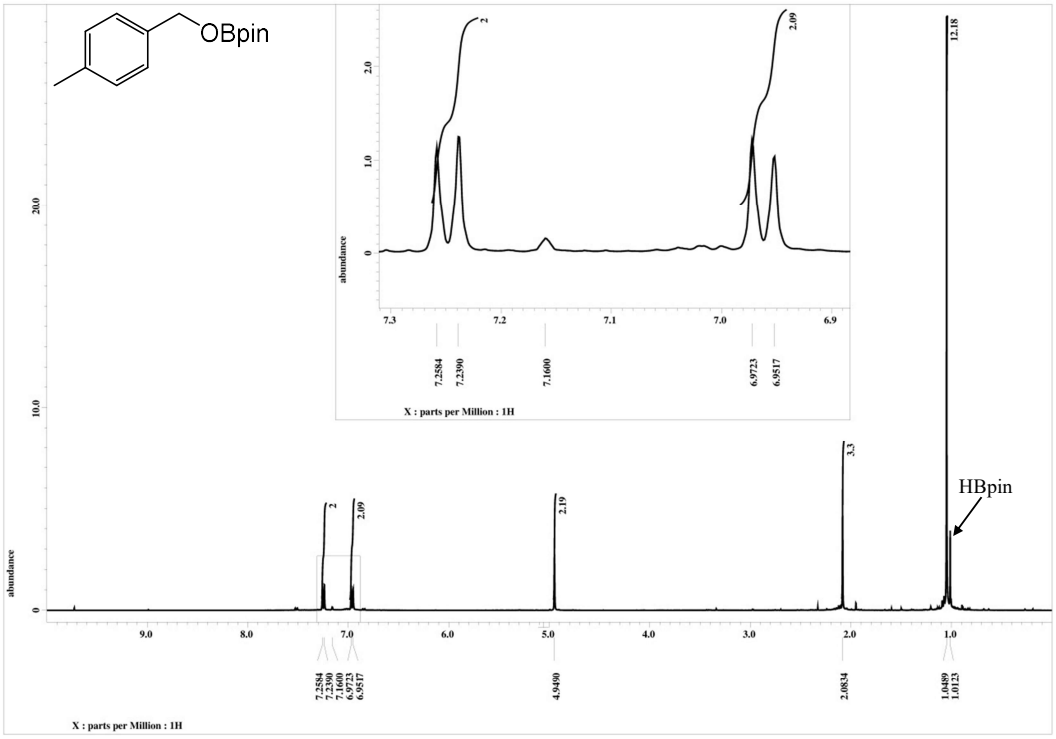

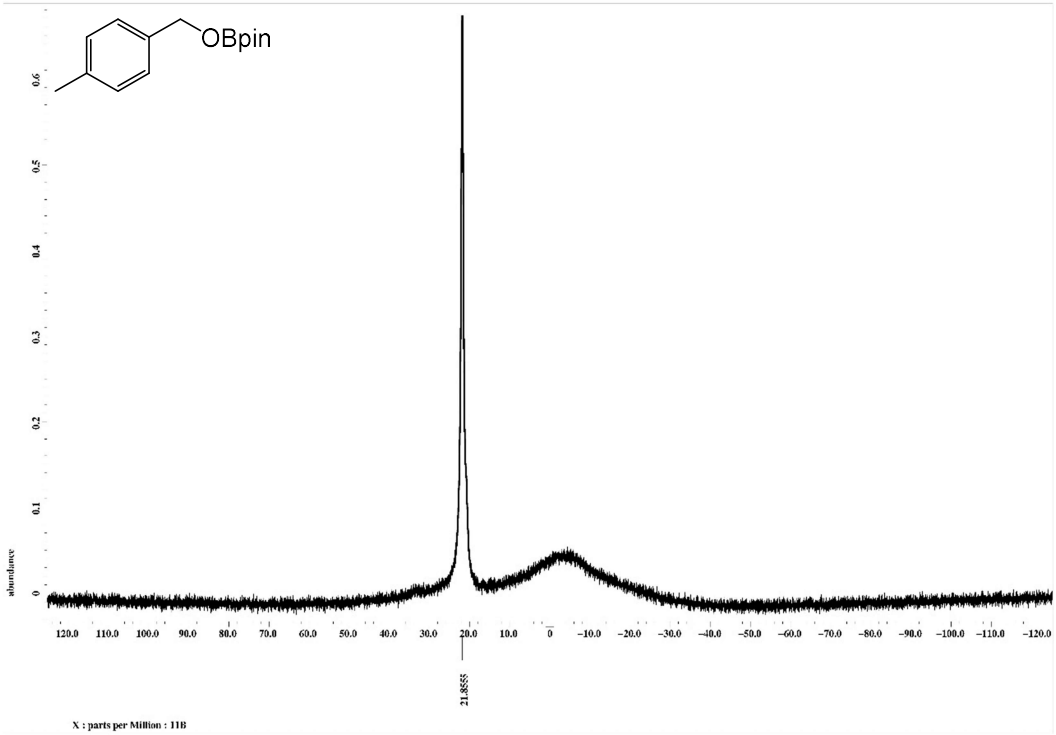

Table S1 Entry 3, ^{1}H, $^{11}B\{^{1}H\}$ NMR Spectra of crude product

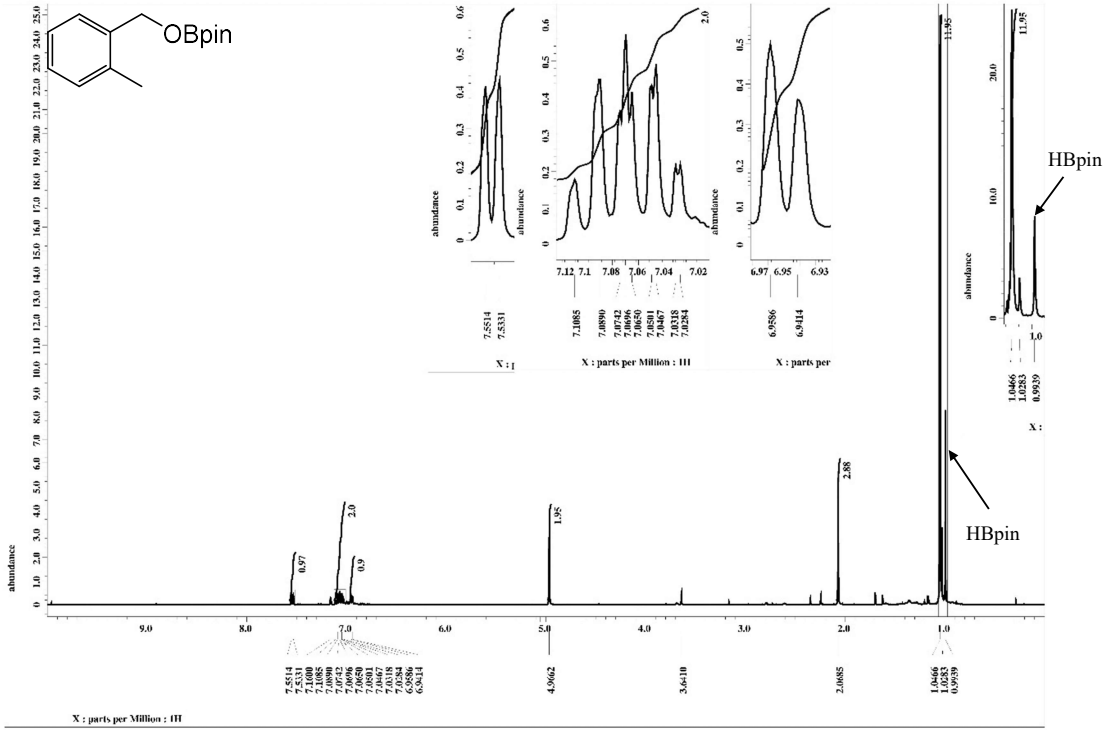

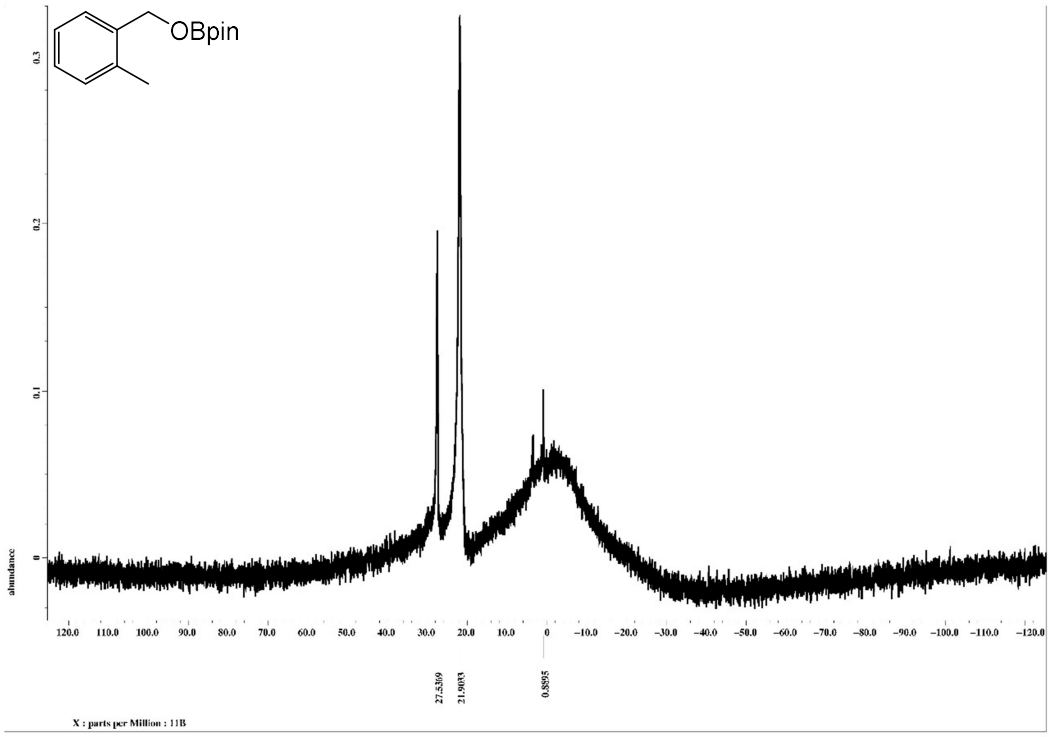

Table S1 Entry 4, ^{1}H, $^{11}B\{^{1}H\}$ NMR Spectra of crude product

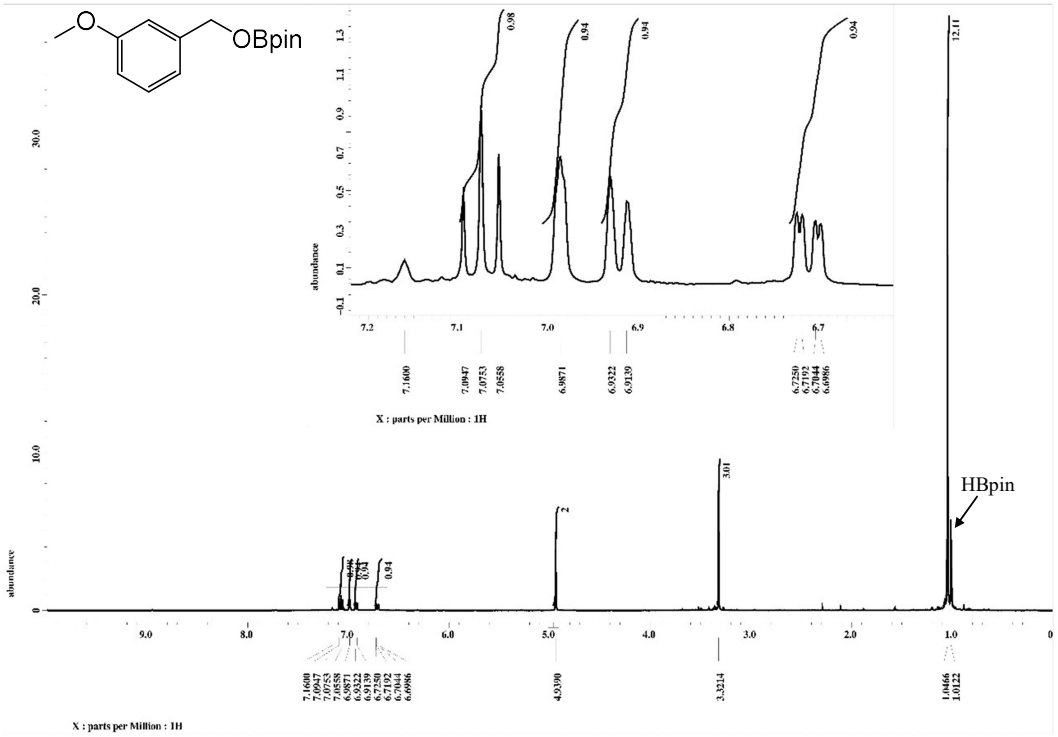

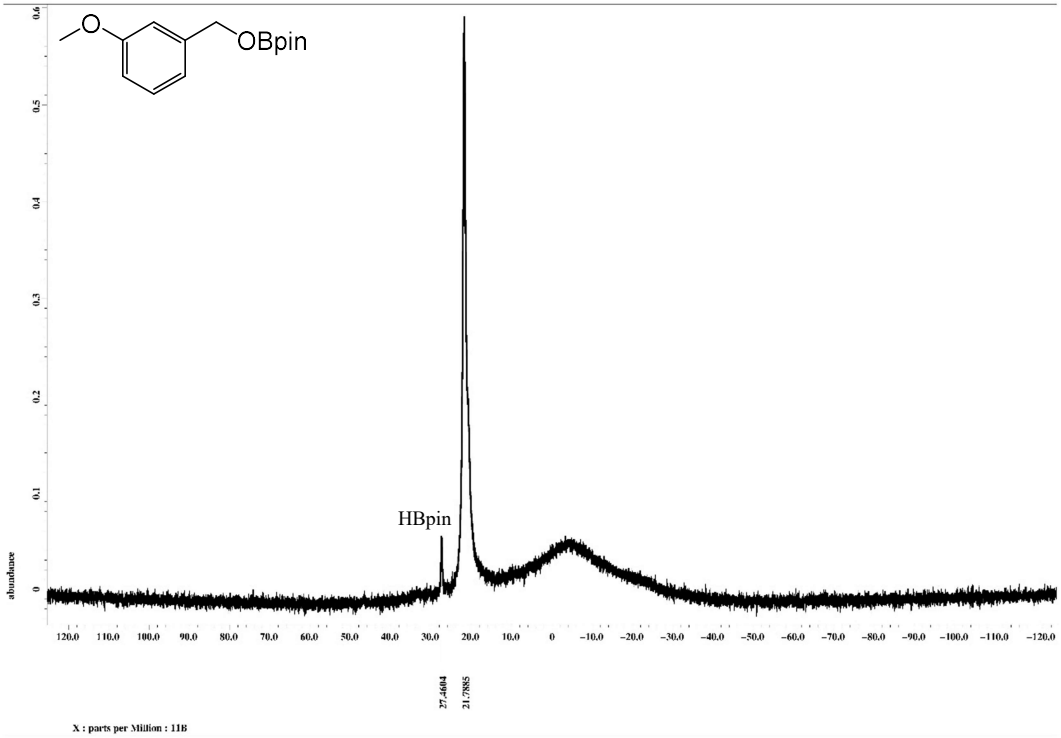

Table S1 Entry 5, ^{1}H, $^{11}B\{^{1}H\}$ NMR Spectra of crude product

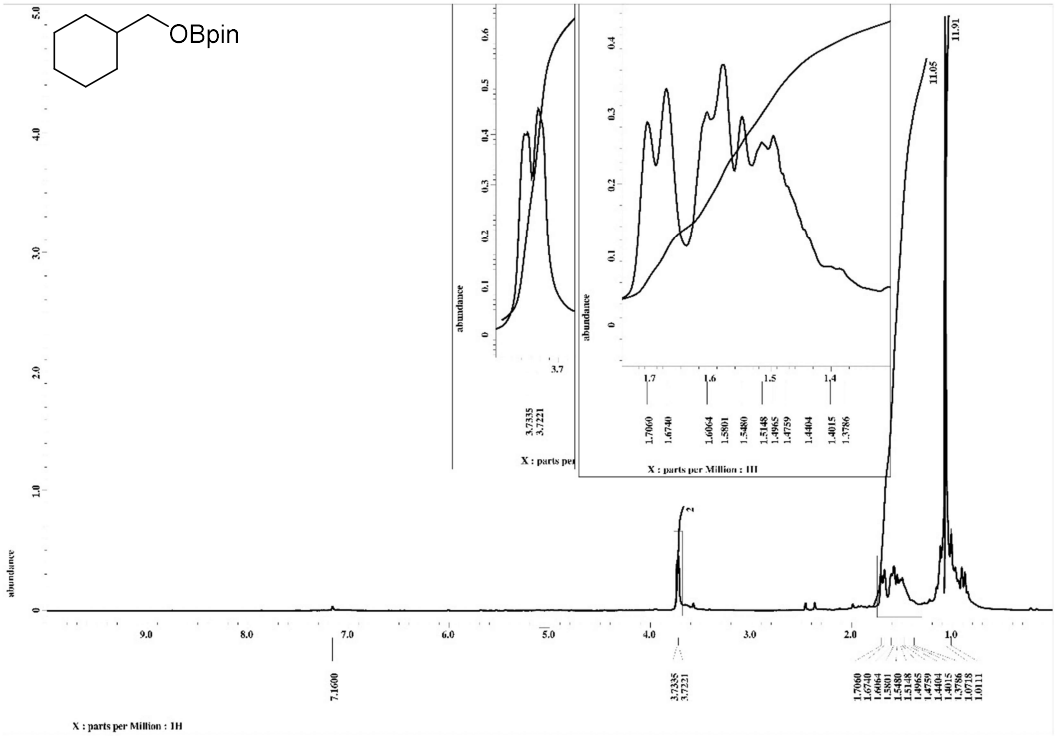

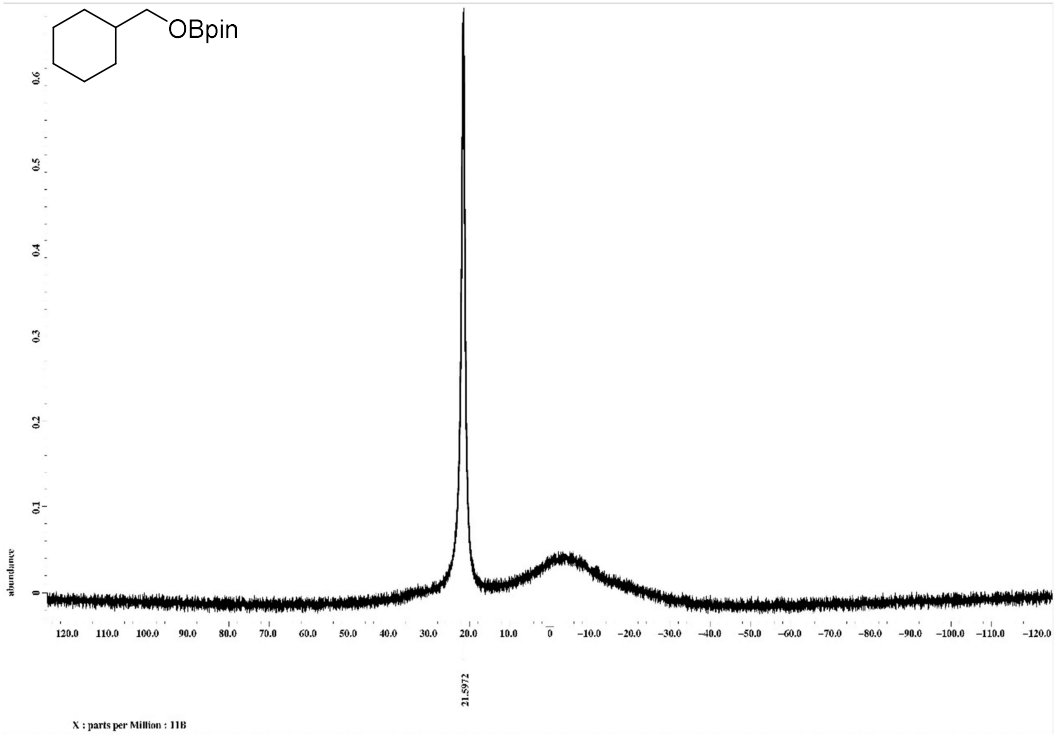

Table S1 Entry 6, ^{1}H, $^{11}B\{^{1}H\}$ NMR Spectra of crude product

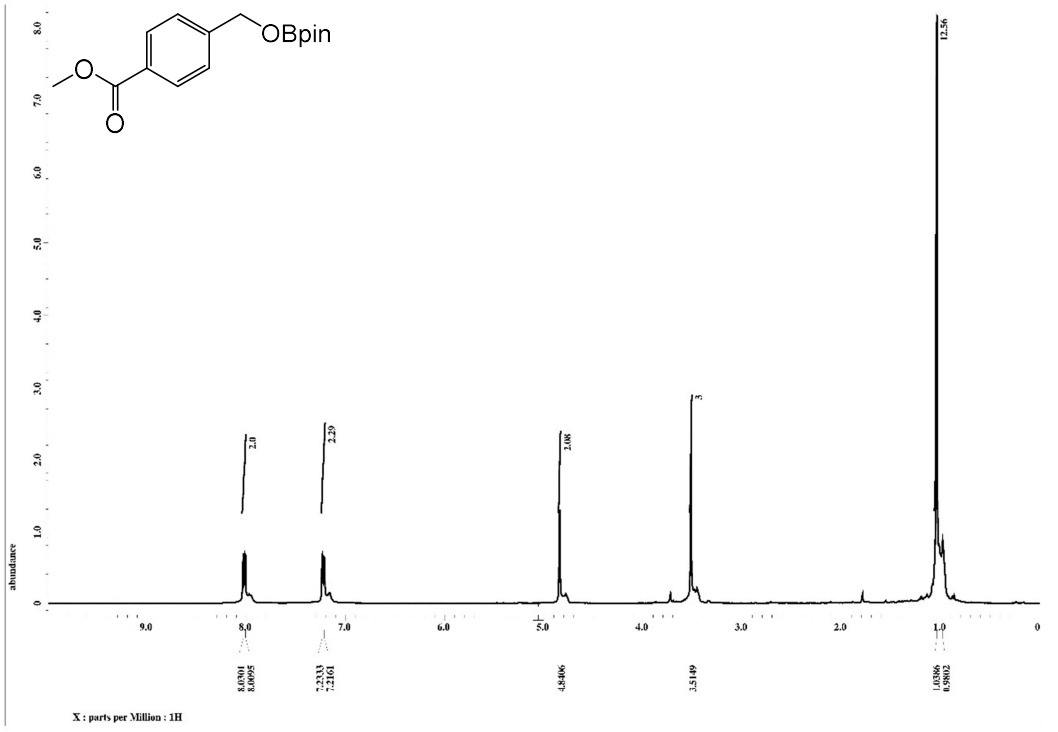

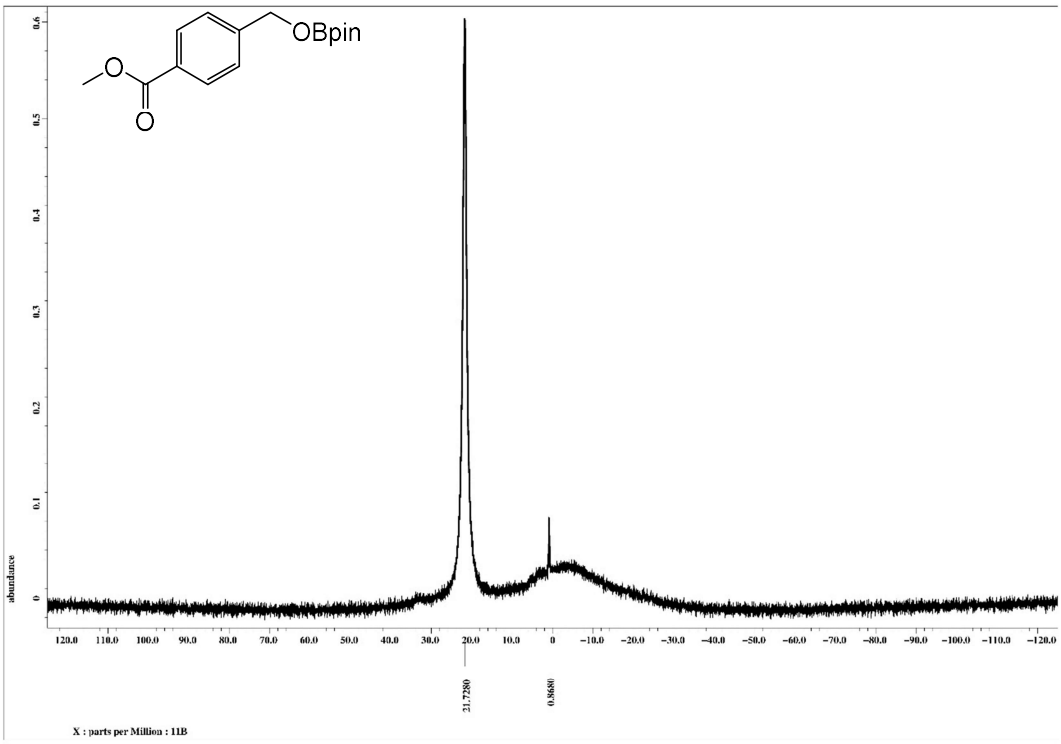

Table S1 Entry 7, ^{1}H, $^{11}B\{^{1}H\}$ NMR Spectra of crude product

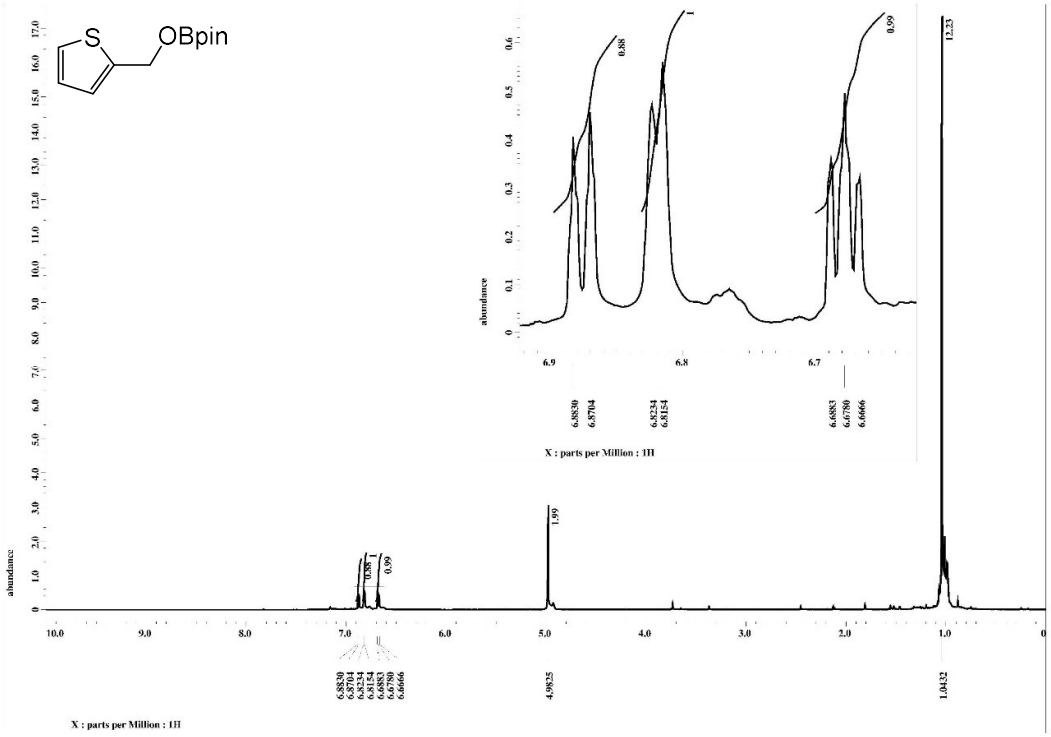

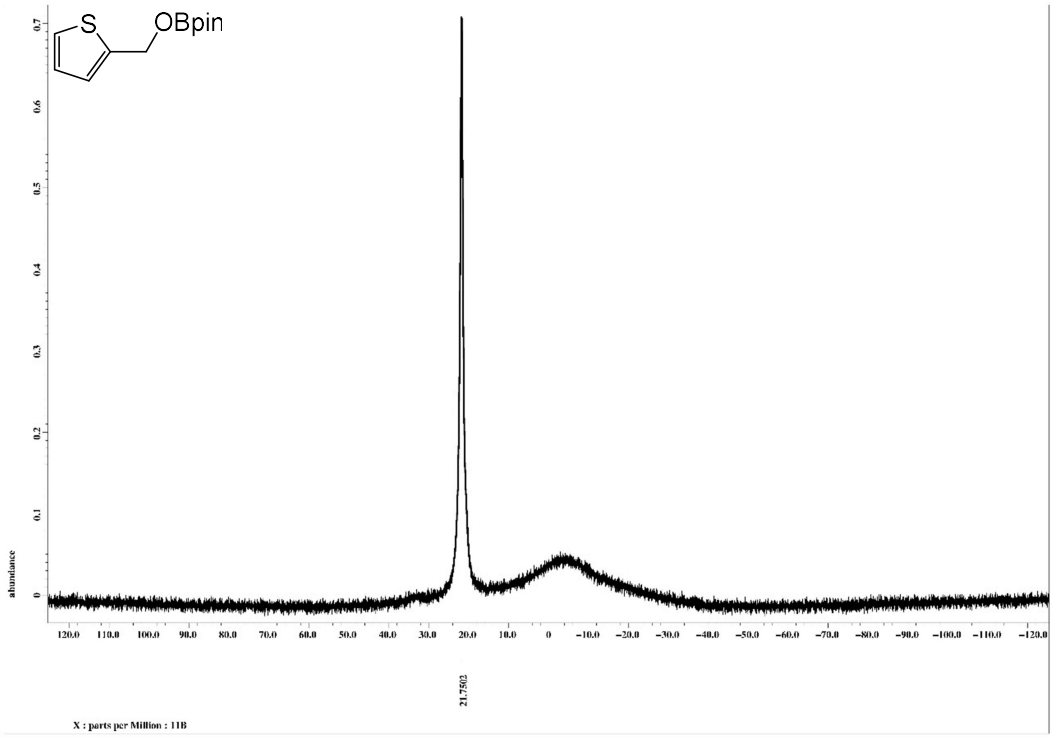

Table S1 Entry 8, ^{1}H, $^{11}B\{^{1}H\}$ NMR Spectra of crude product

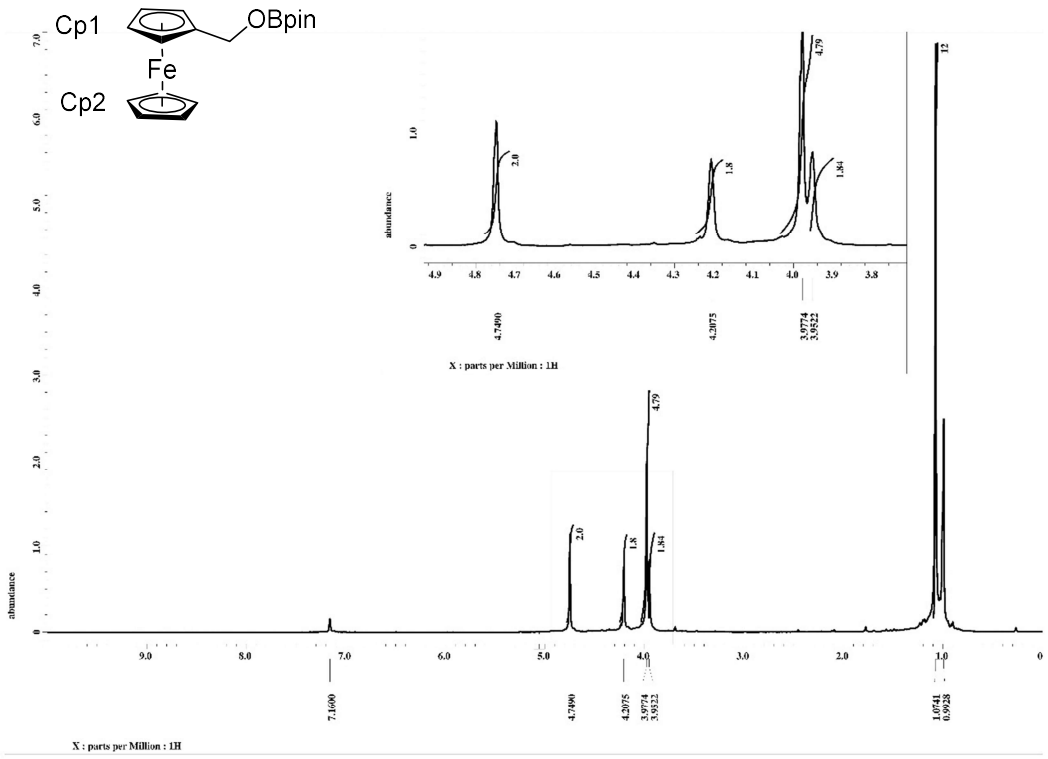

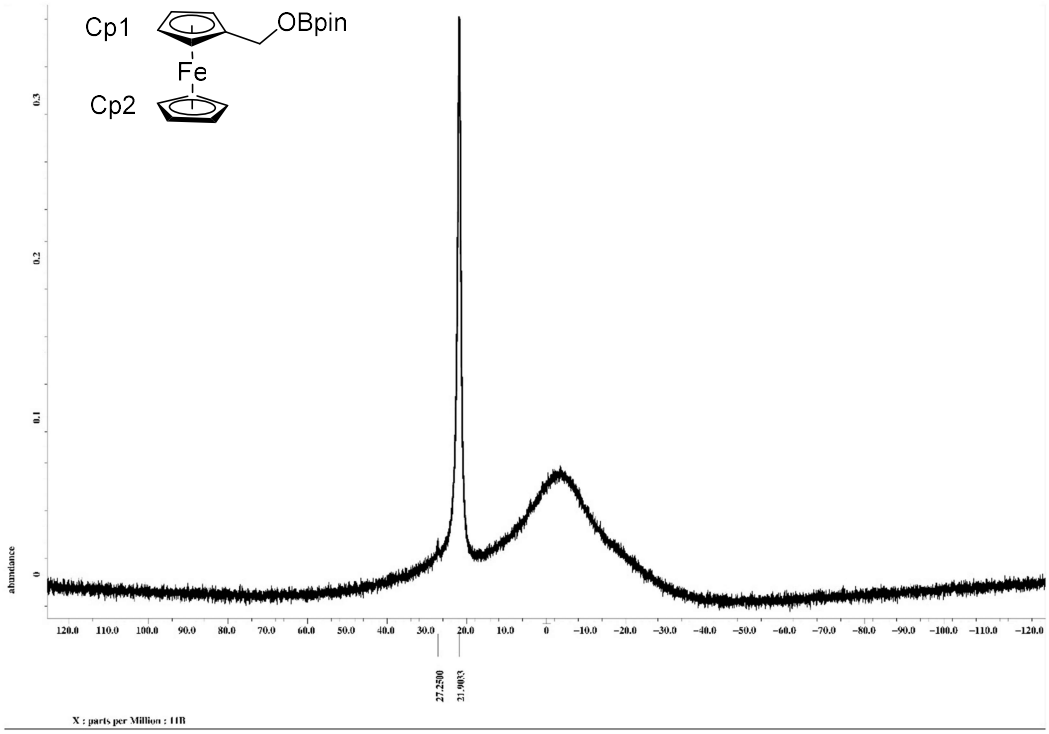

Table S1 Entry 9, ^{1}H, $^{11}B\{^{1}H\}$ NMR Spectra of crude product

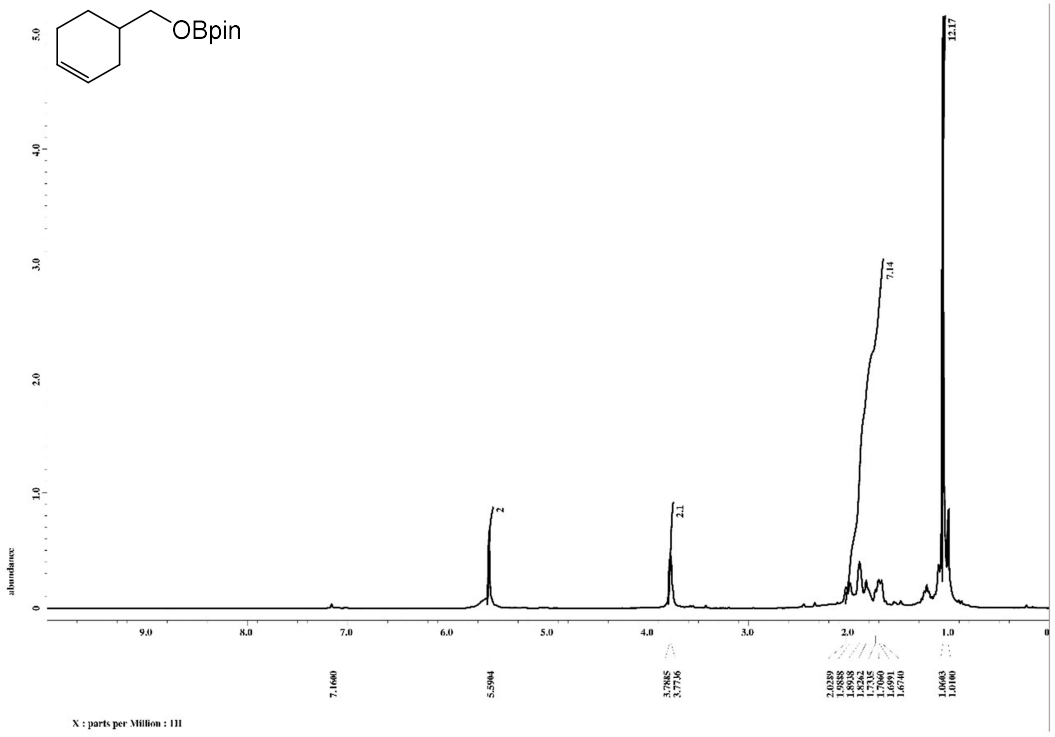

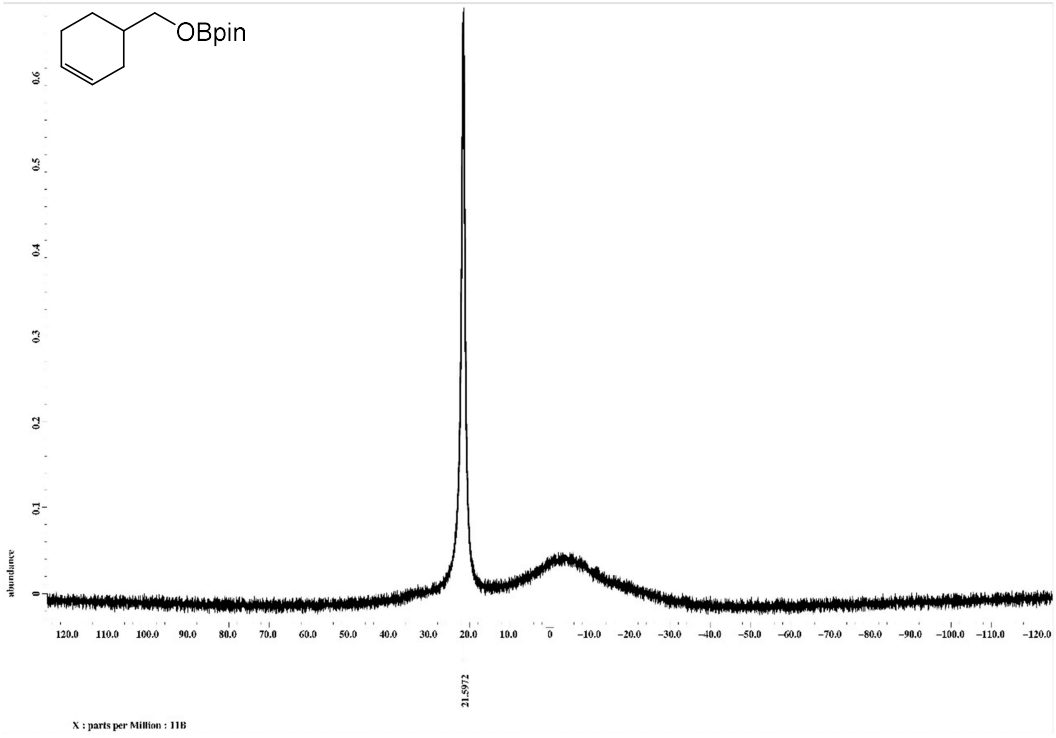

Table S1 Entry 10, ^{1}H, $^{13}C\{^{1}H\}$ NMR Spectra of crude product

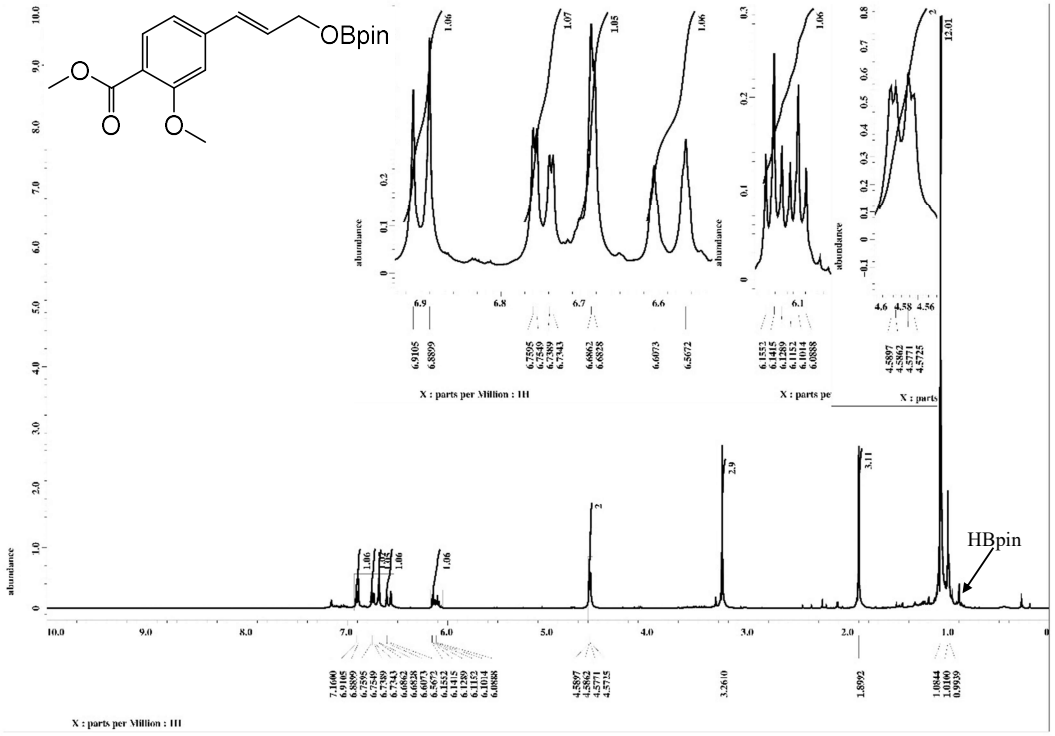

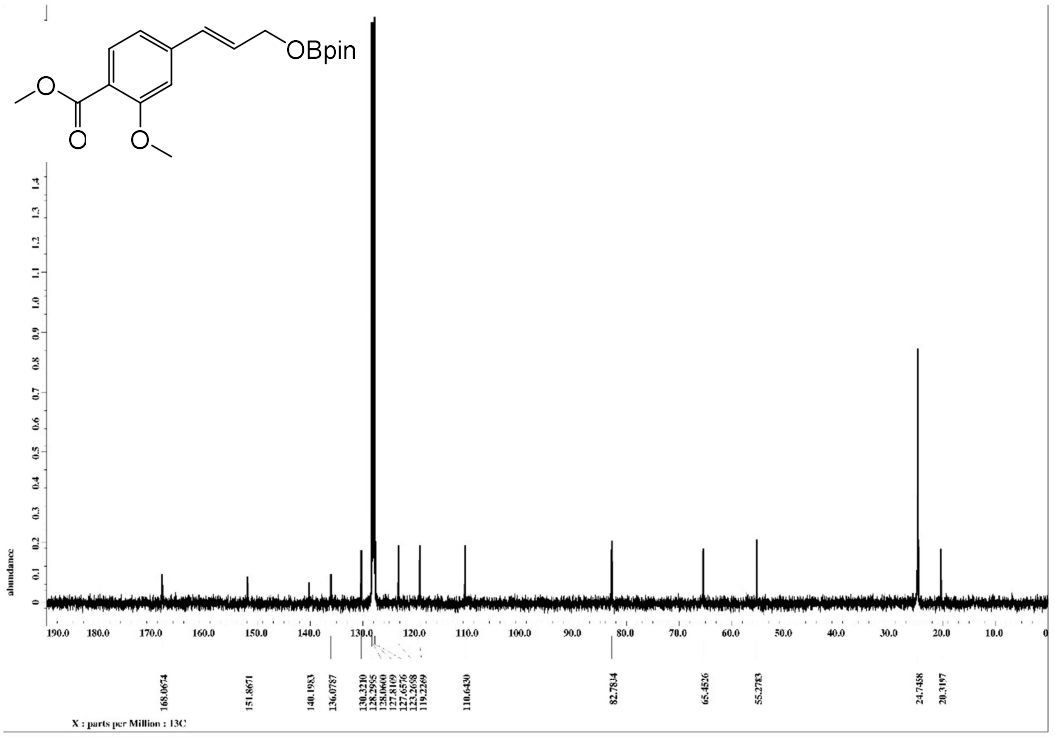

Table S1 Entry 11, ^{1}H, $^{11}B\{^{1}H\}$ NMR Spectra of crude product

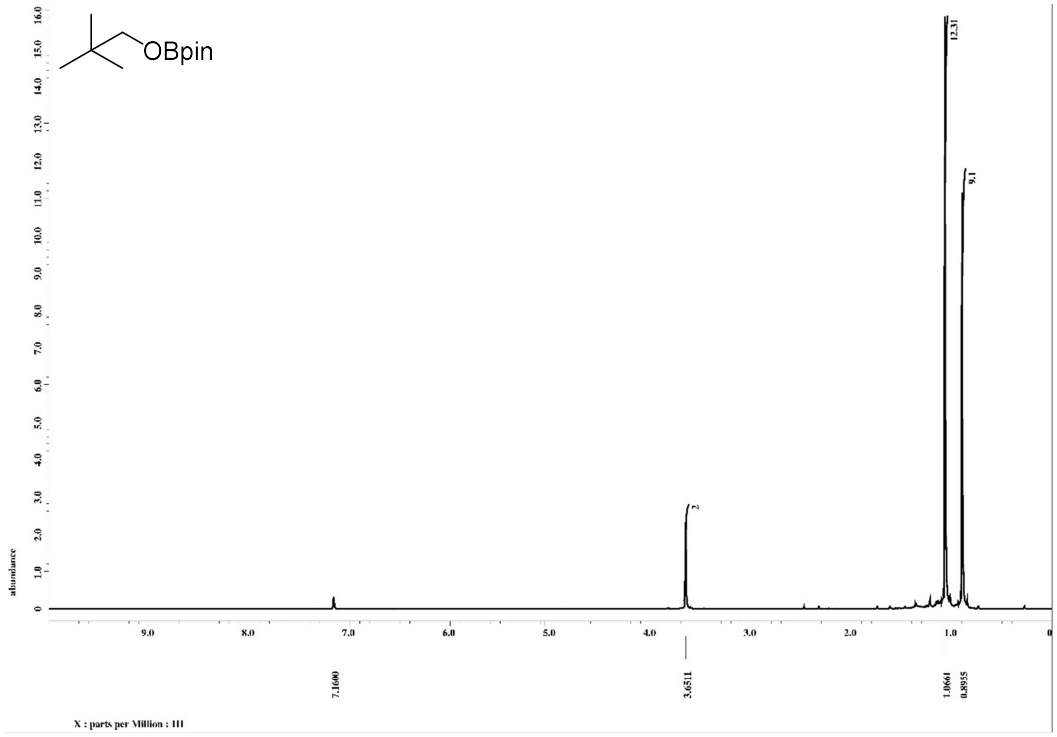

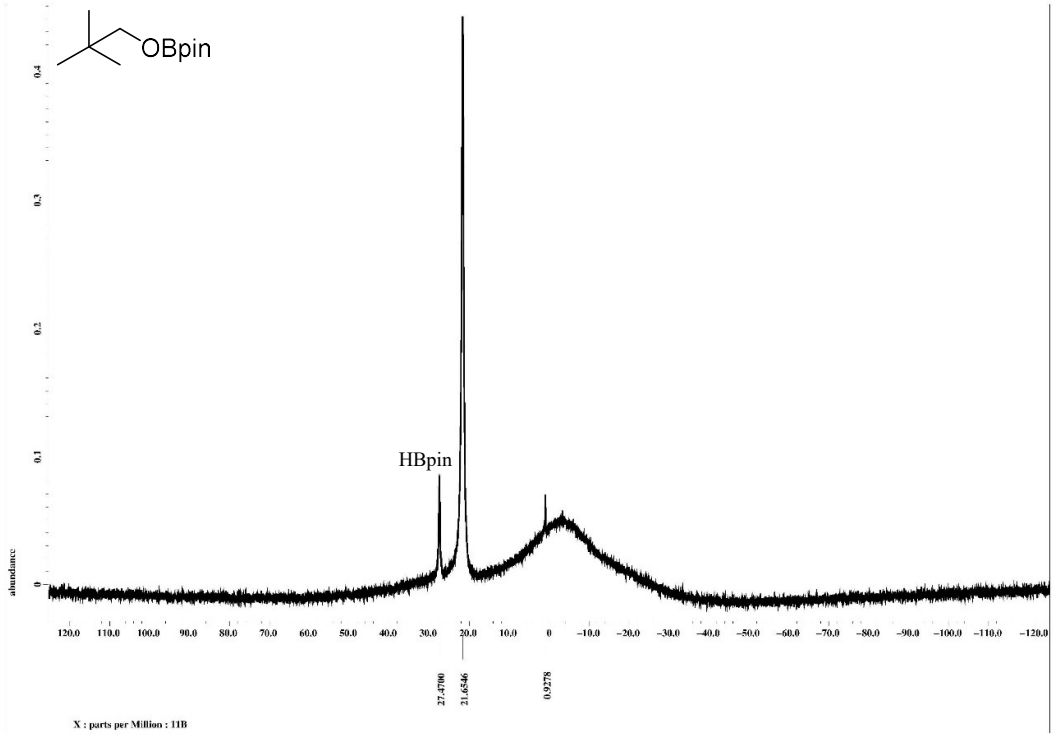

Table S1 Entry 12, ^{1}H, $^{11}B\{^{1}H\}$ NMR Spectra of crude product

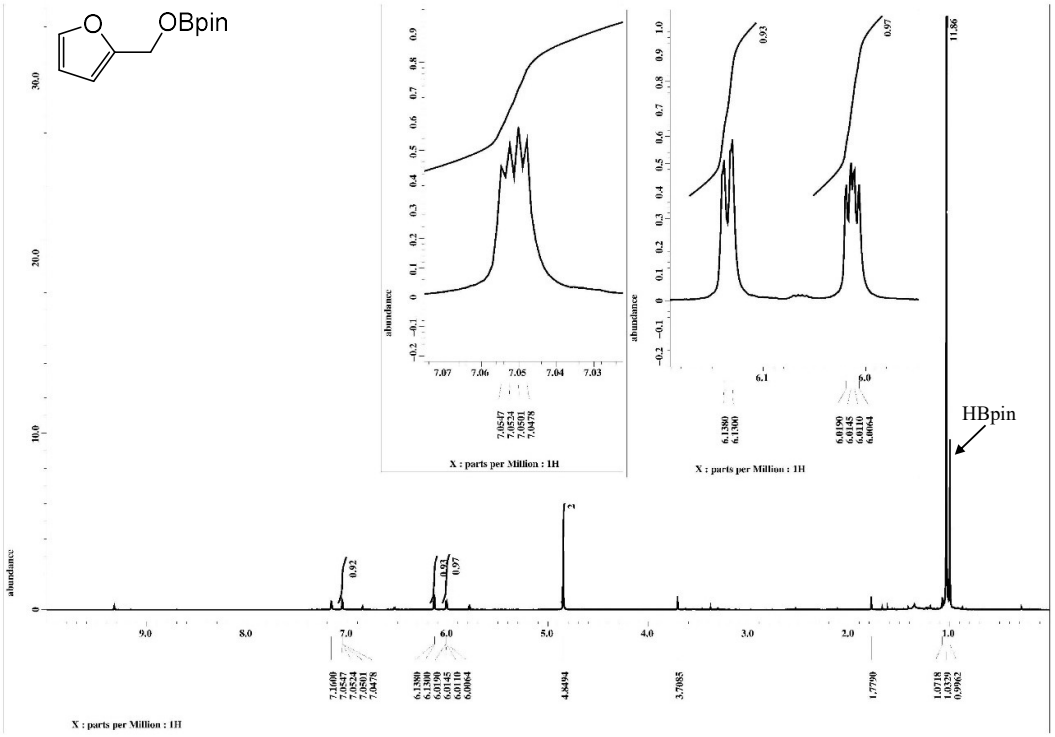

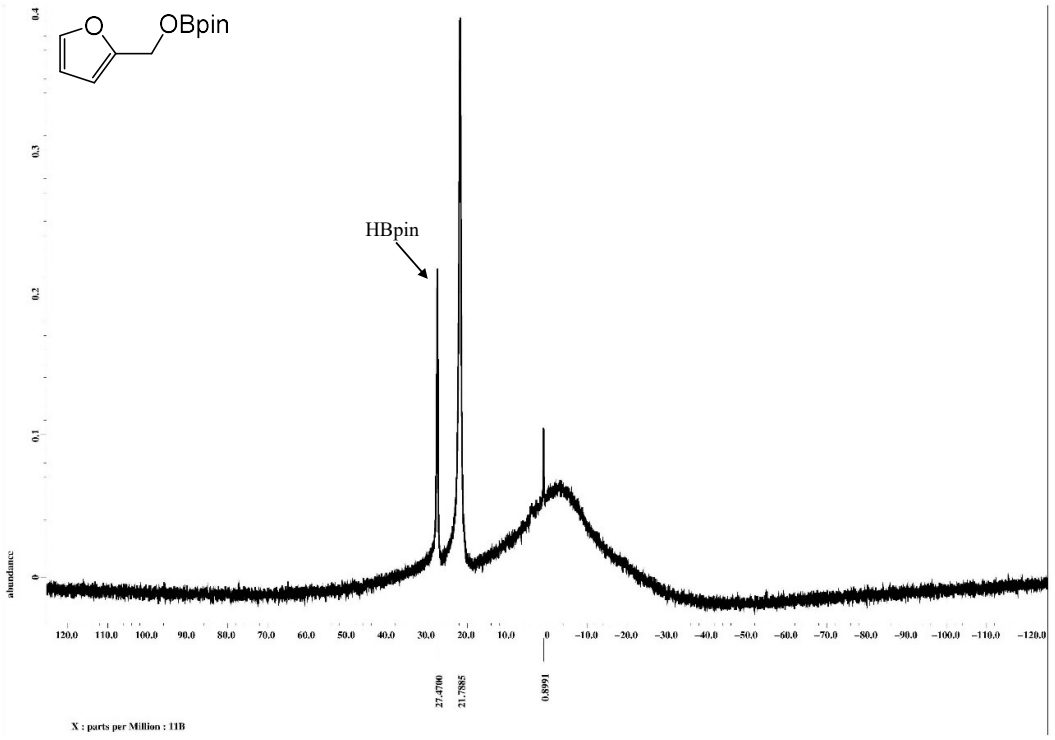

Table S1 Entry 13, ^{1}H, $^{11}B\{^{1}H\}$ NMR Spectra of crude product

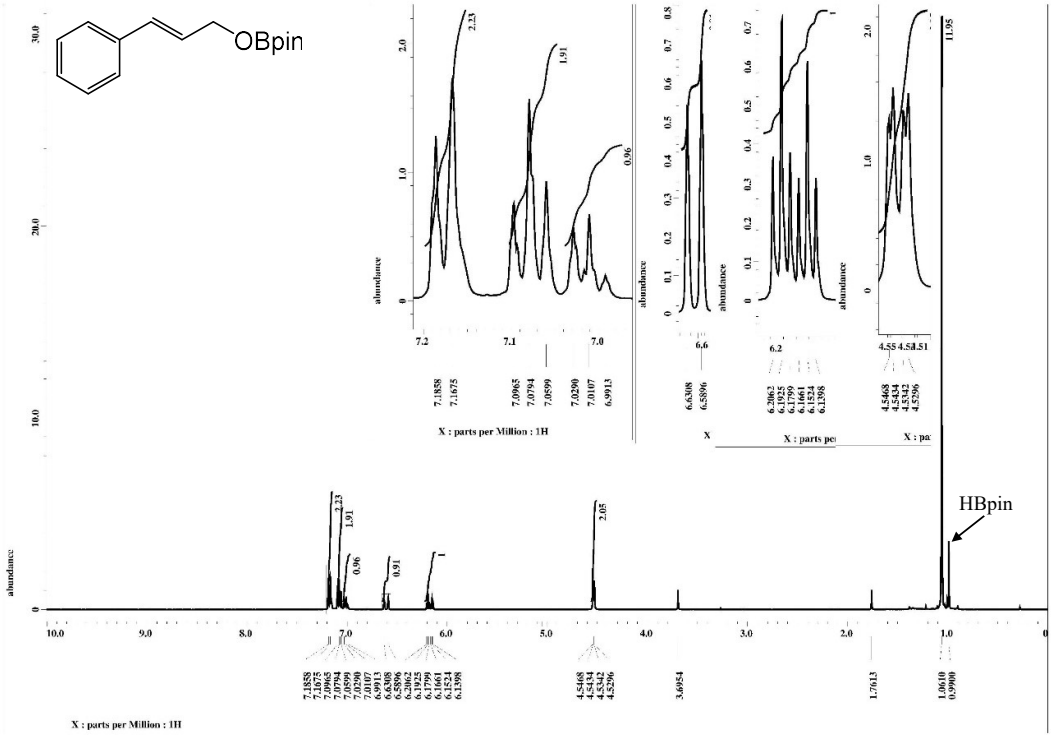

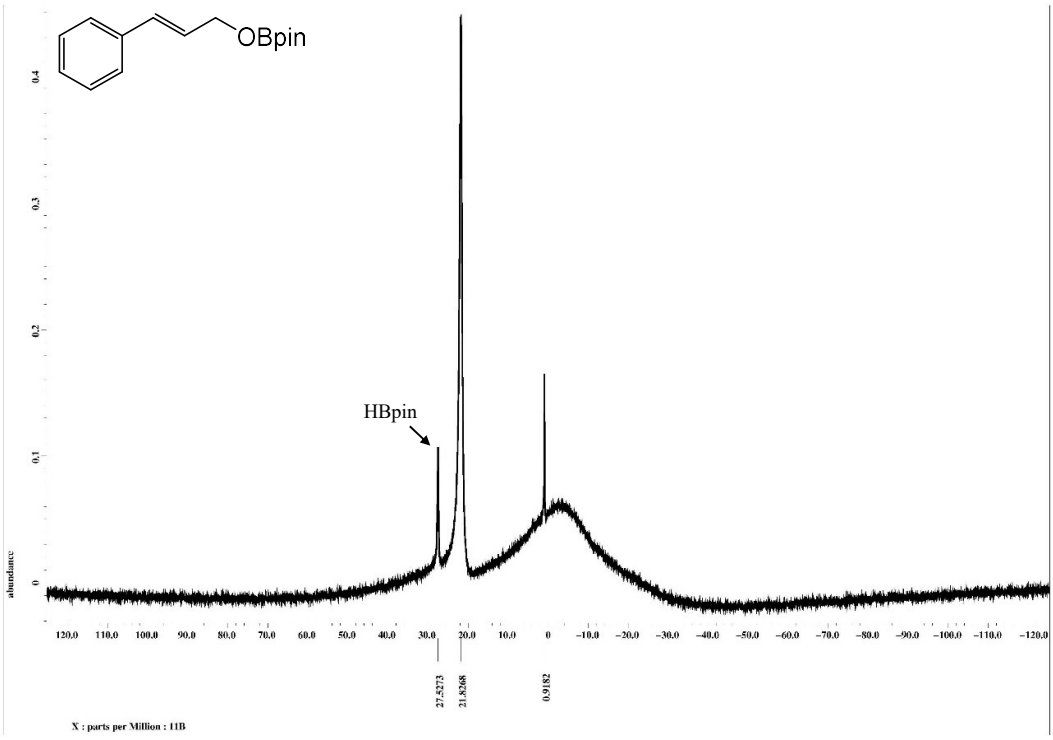

Table S1 Entry 14, ^{1}H, $^{11}B\{^{1}H\}$ NMR Spectra of crude product

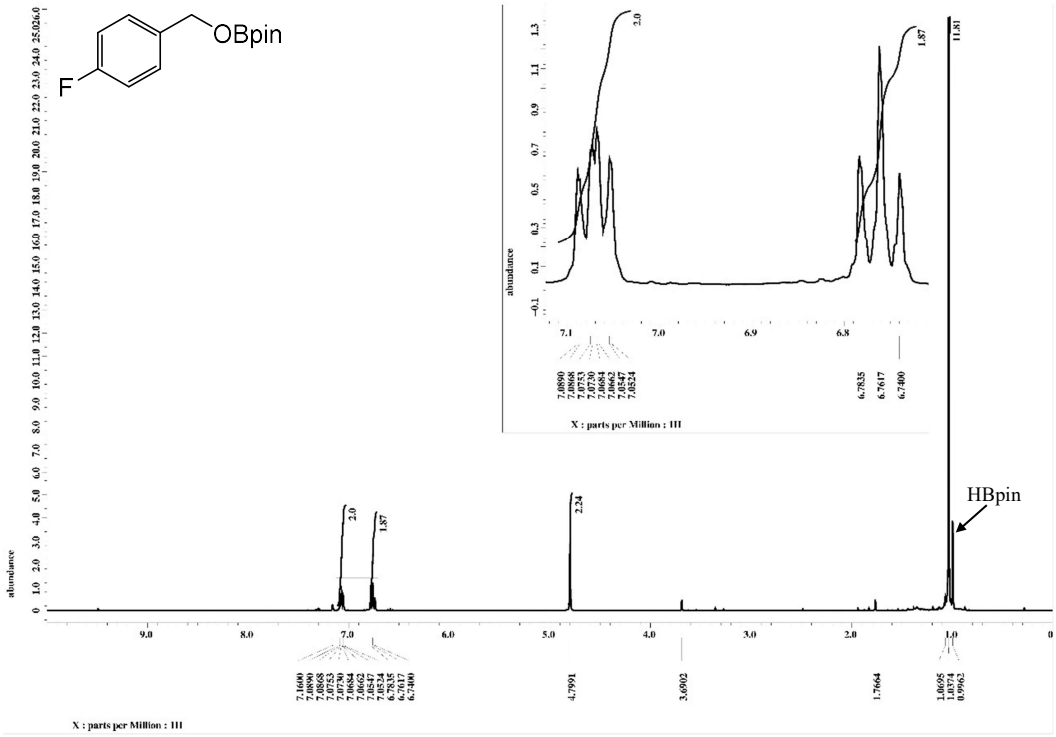

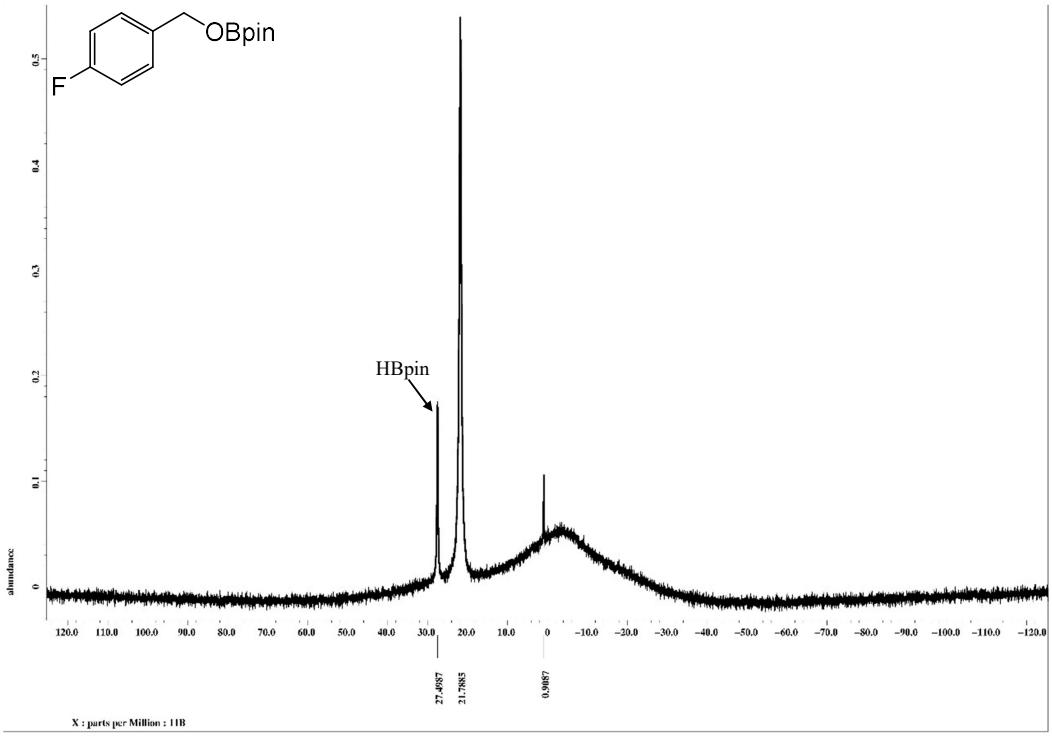

Table S1 Entry 15, ^{1}H, $^{11}B\{^{1}H\}$ NMR Spectra of crude product

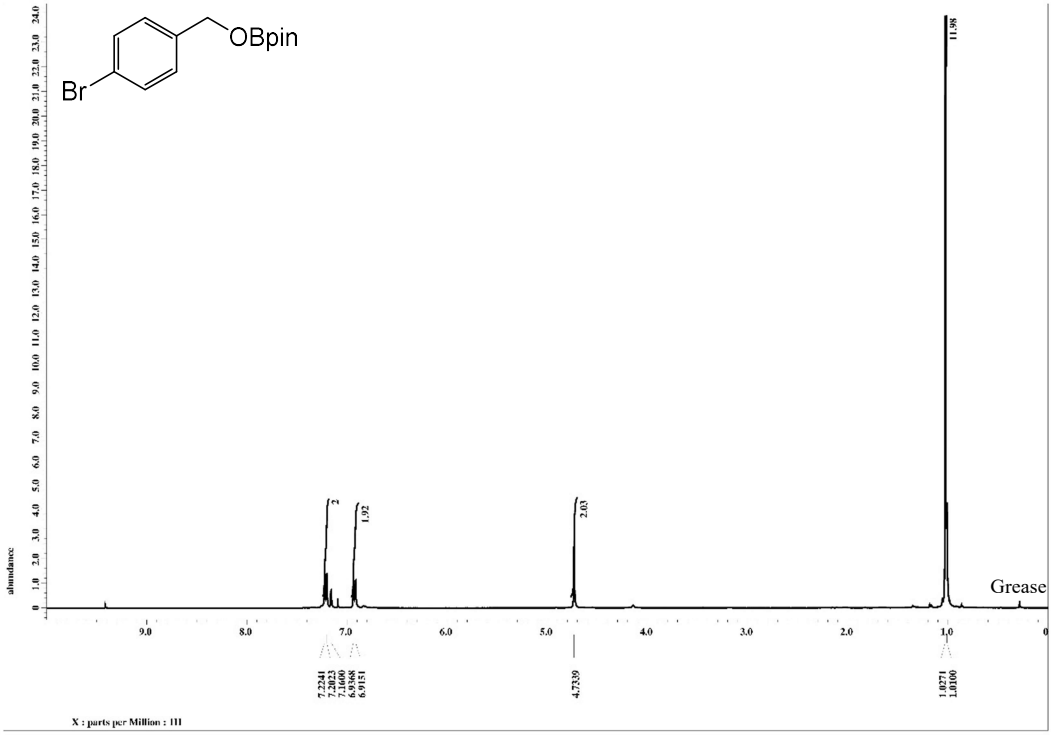

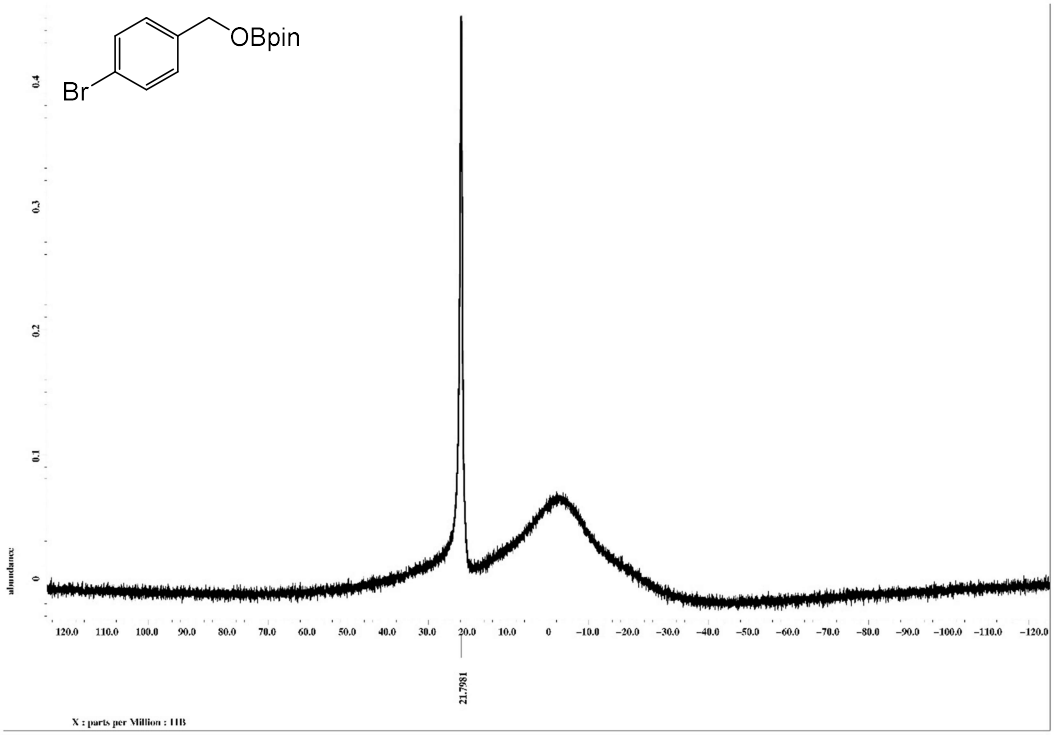

Table S1 Entry 16, ^{1}H, $^{11}B\{^{1}H\}$ NMR Spectra of crude product

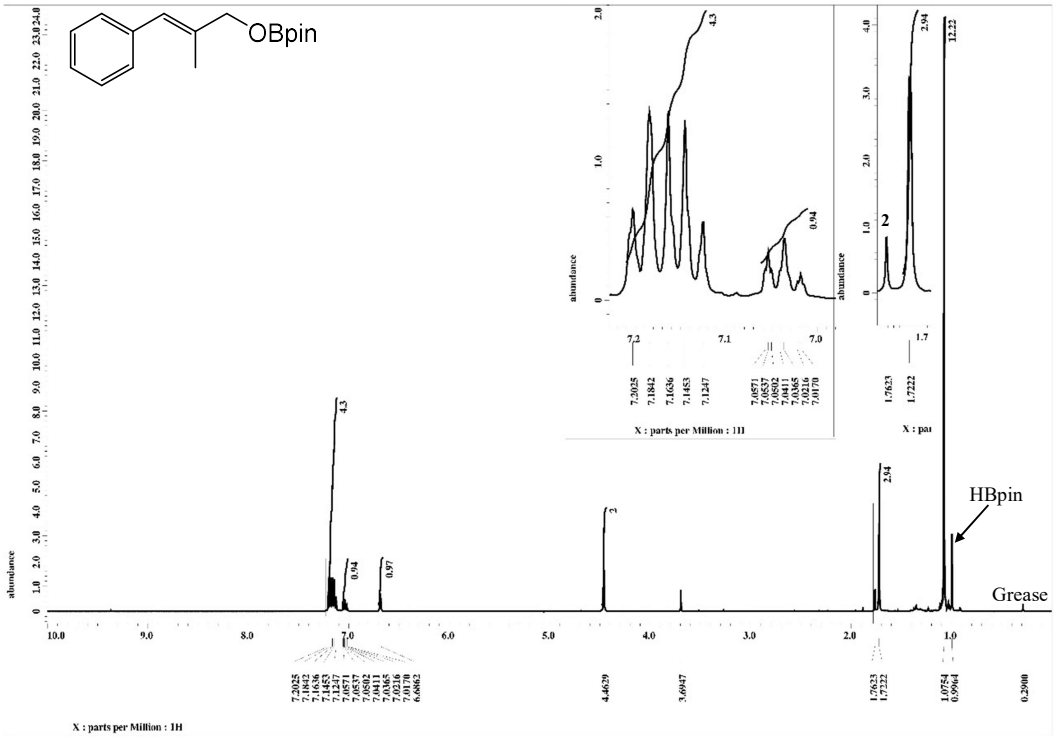

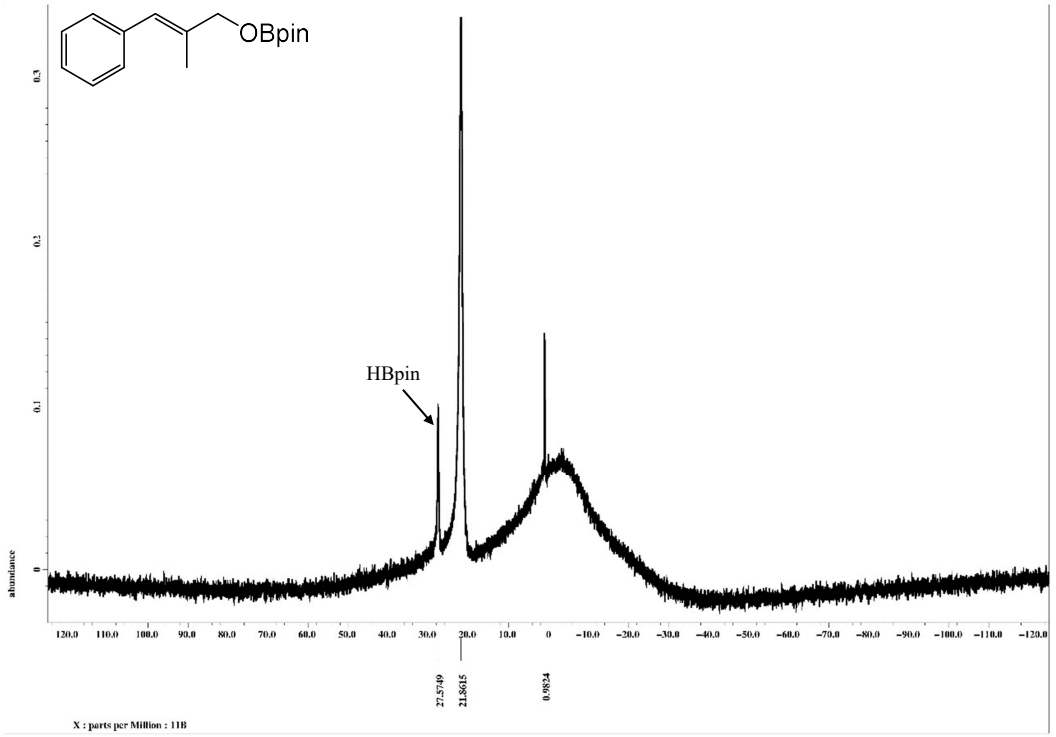

Table S1 Entry 17, ^{1}H, $^{11}B\{^{1}H\}$ NMR Spectra of crude product

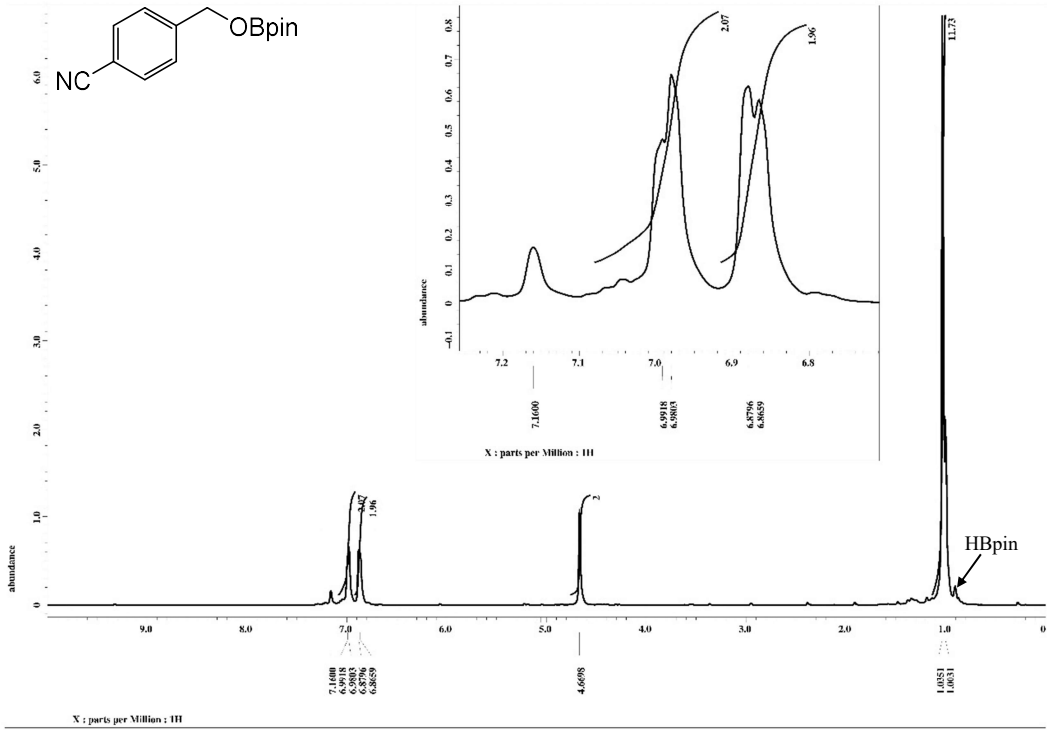

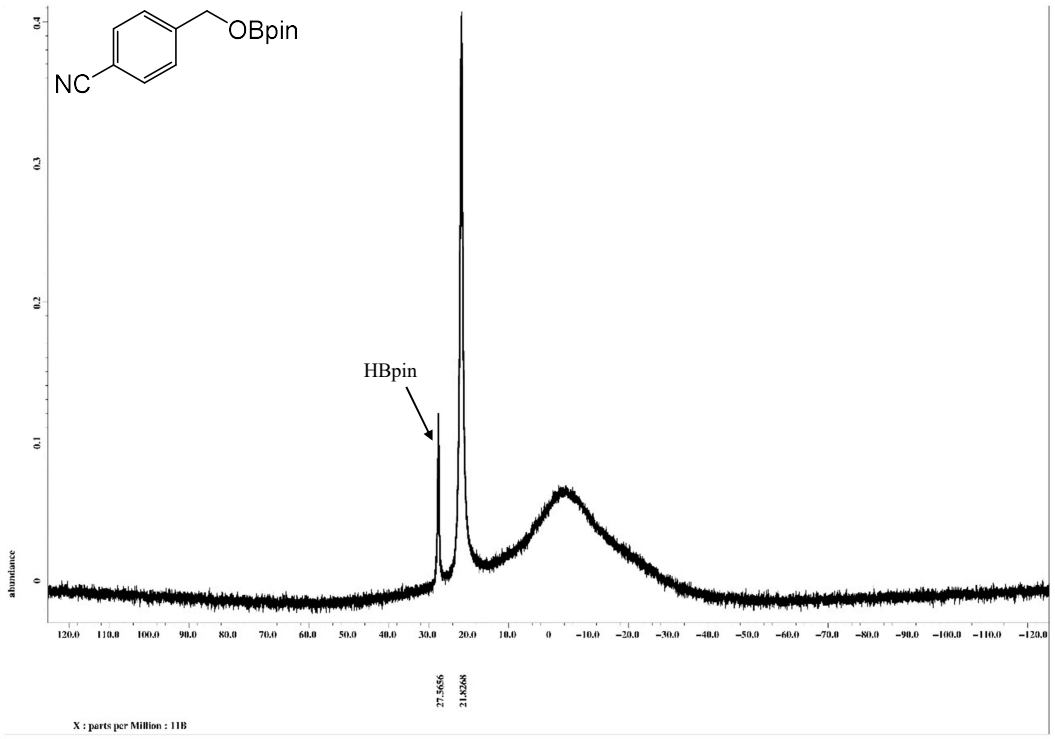

Table S1 Entry 18, ^{1}H, $^{11}B\{^{1}H\}$ NMR Spectra of crude product

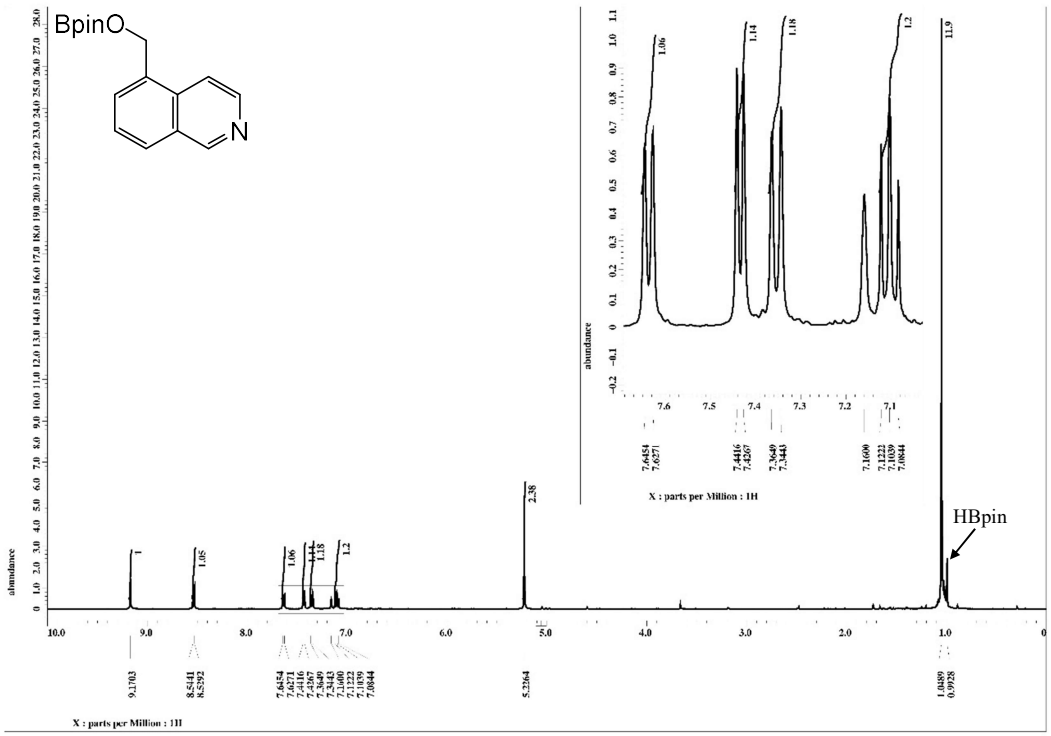

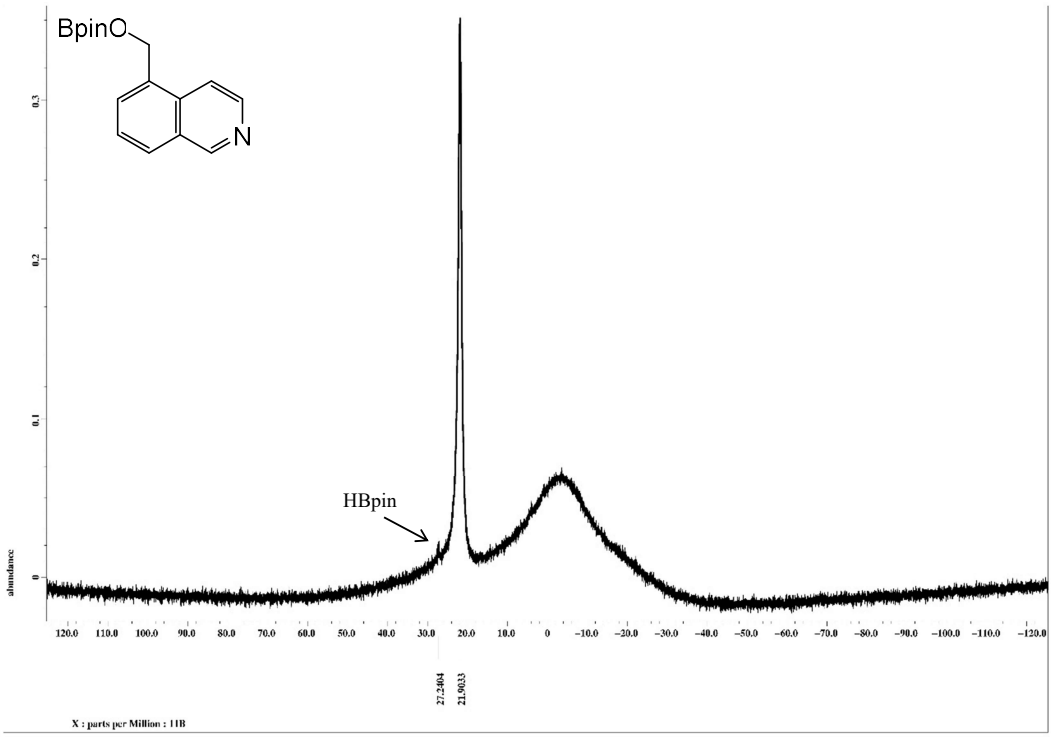

Table S1 Entry 19, ^{1}H, $^{11}B\{^{1}H\}$ NMR Spectra of crude product

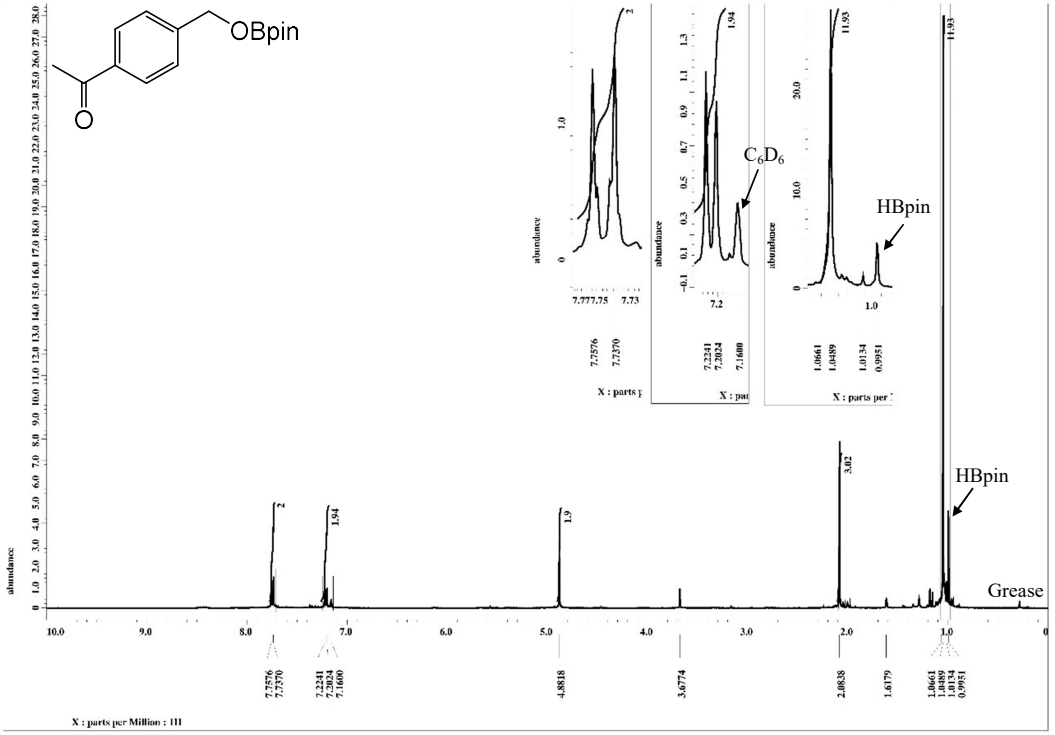

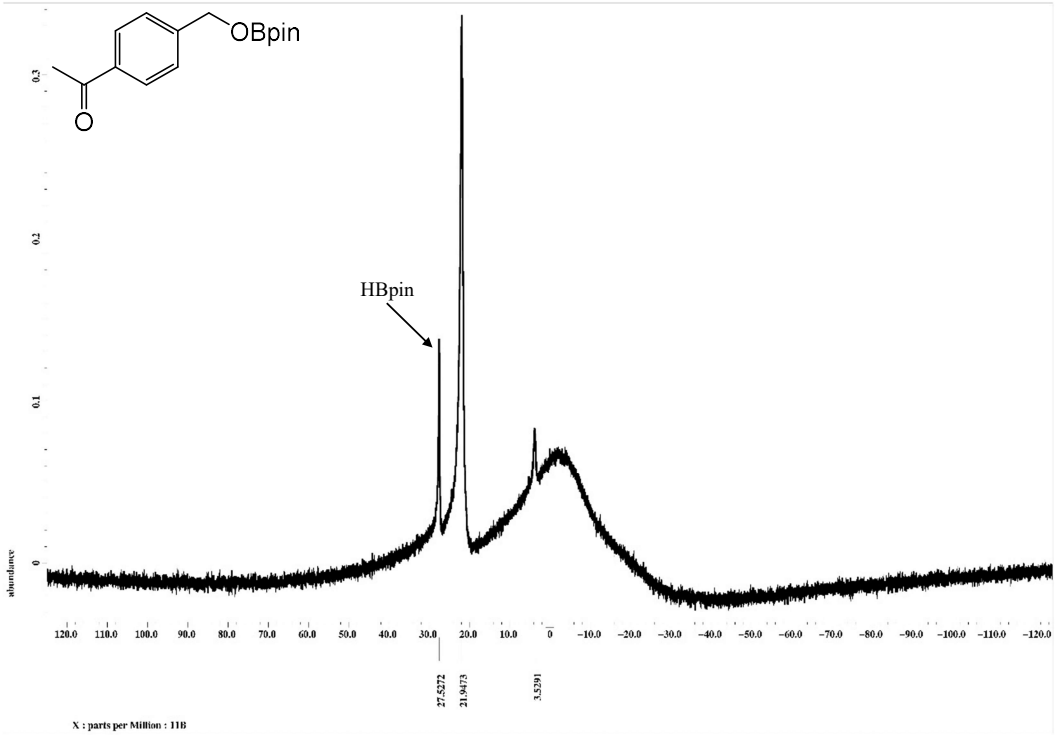

Table S2 Entry 1, ^{1}H, $^{11}B\{^{1}H\}$ NMR Spectra of crude product

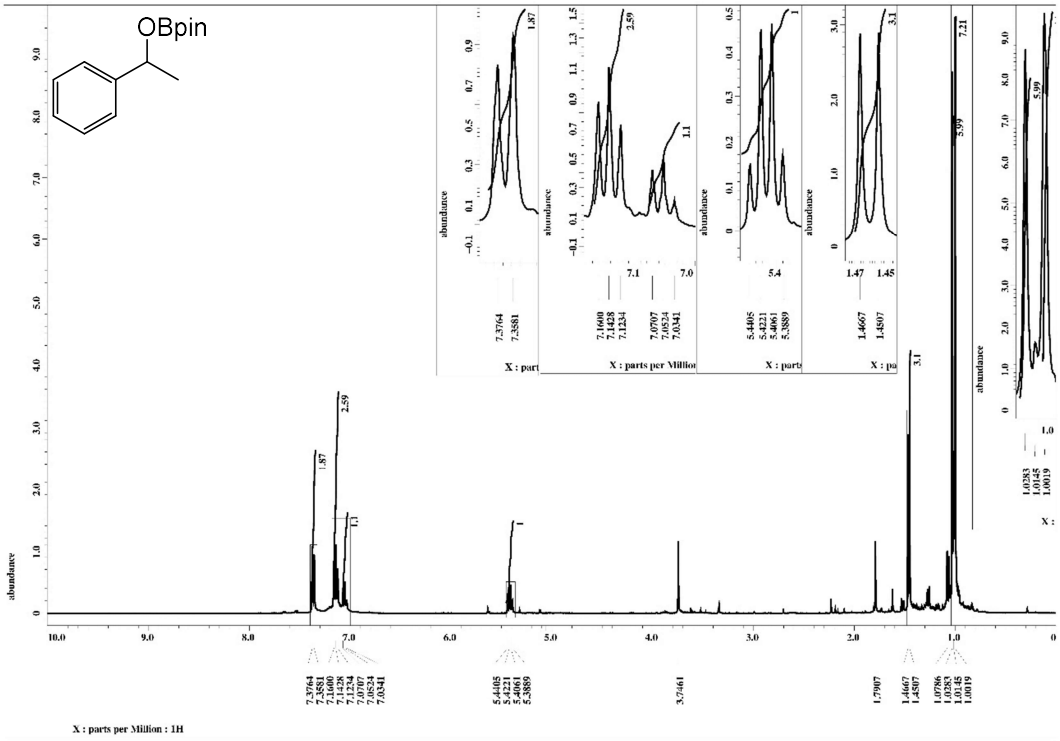

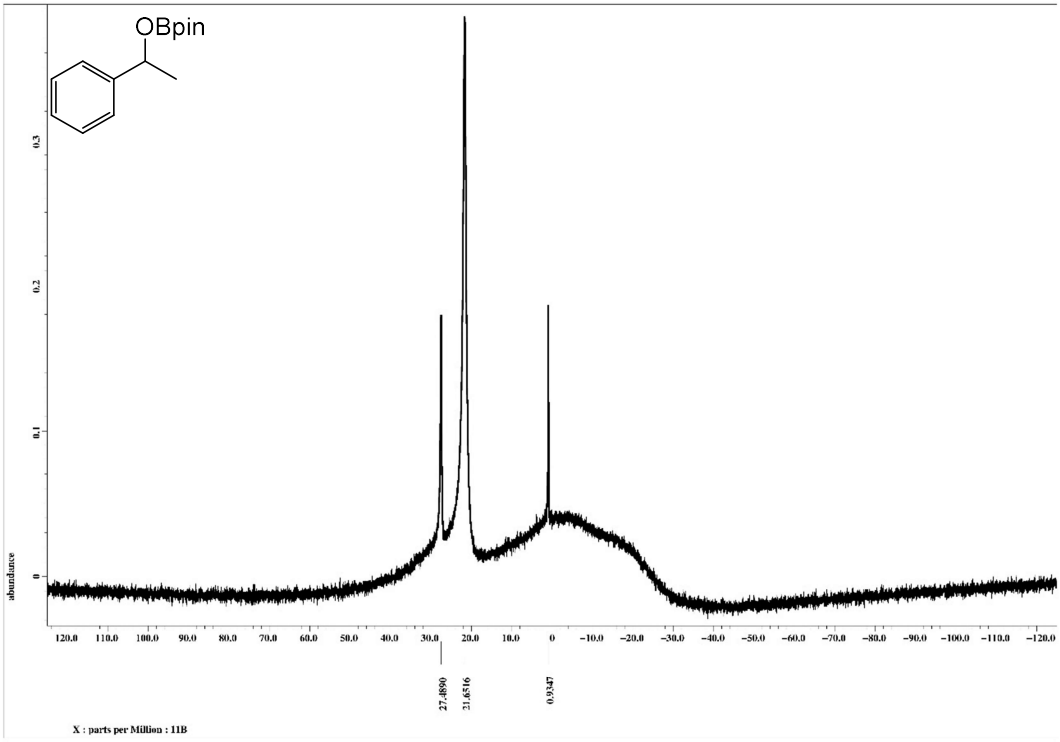

Table S2 Entry 1, ^{1}H, $^{11}B\{^{1}H\}$ NMR Spectra of crude product

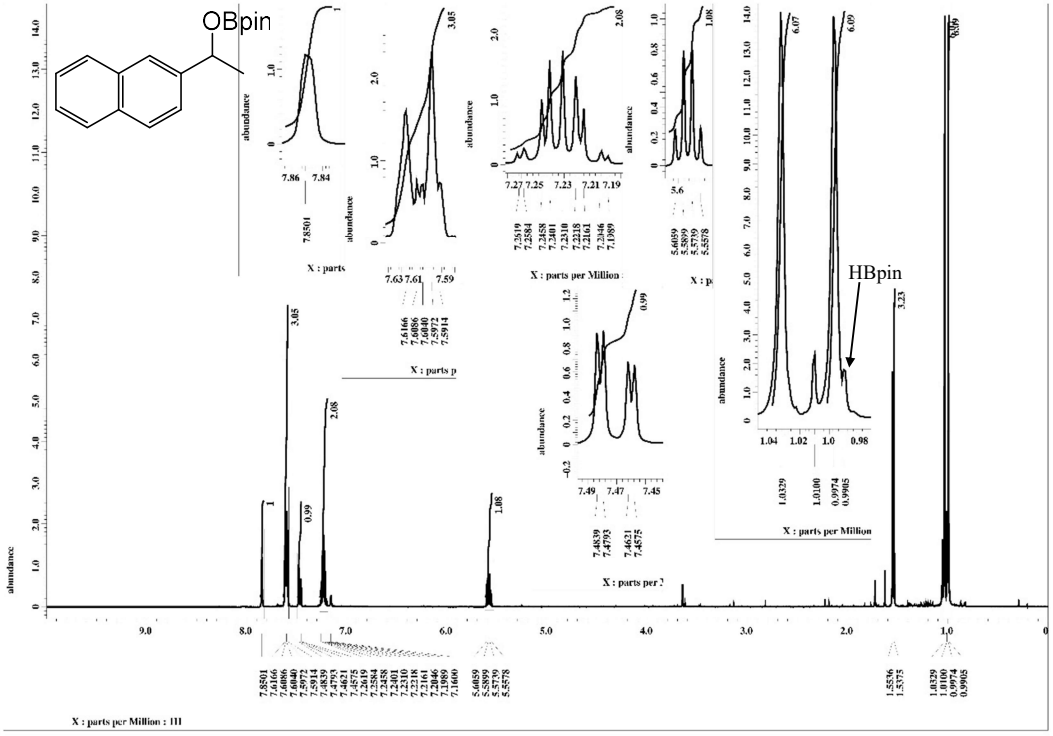

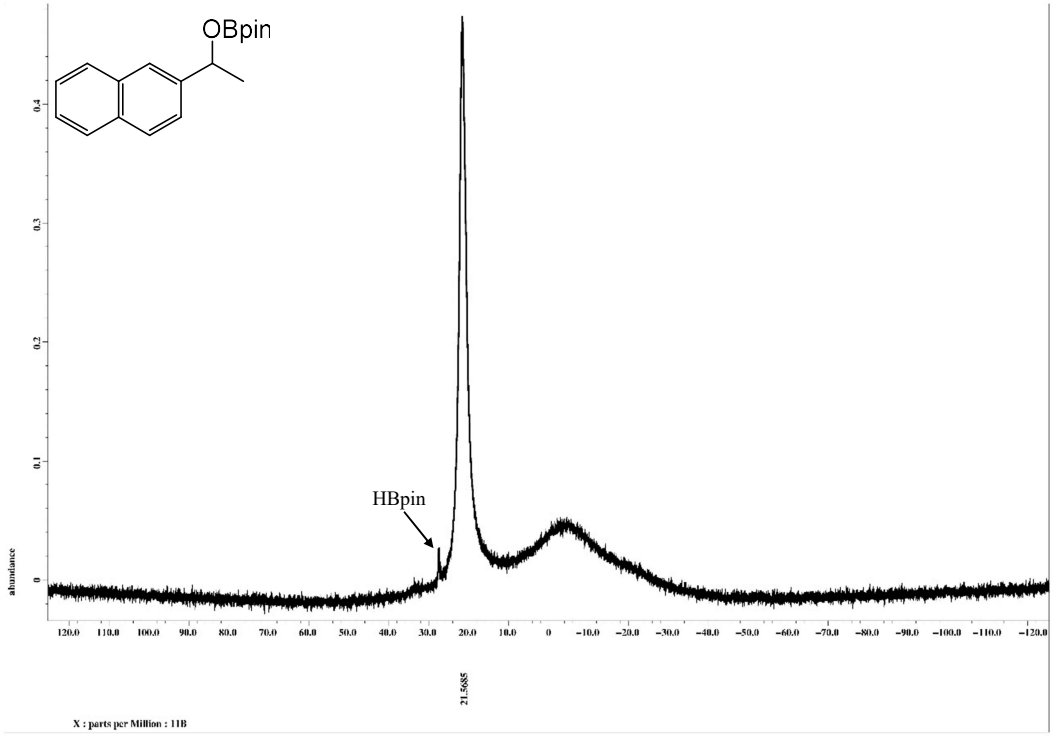

Table S2 Entry 2, ^{1}H, $^{11}B\{^{1}H\}$ NMR Spectra of crude product

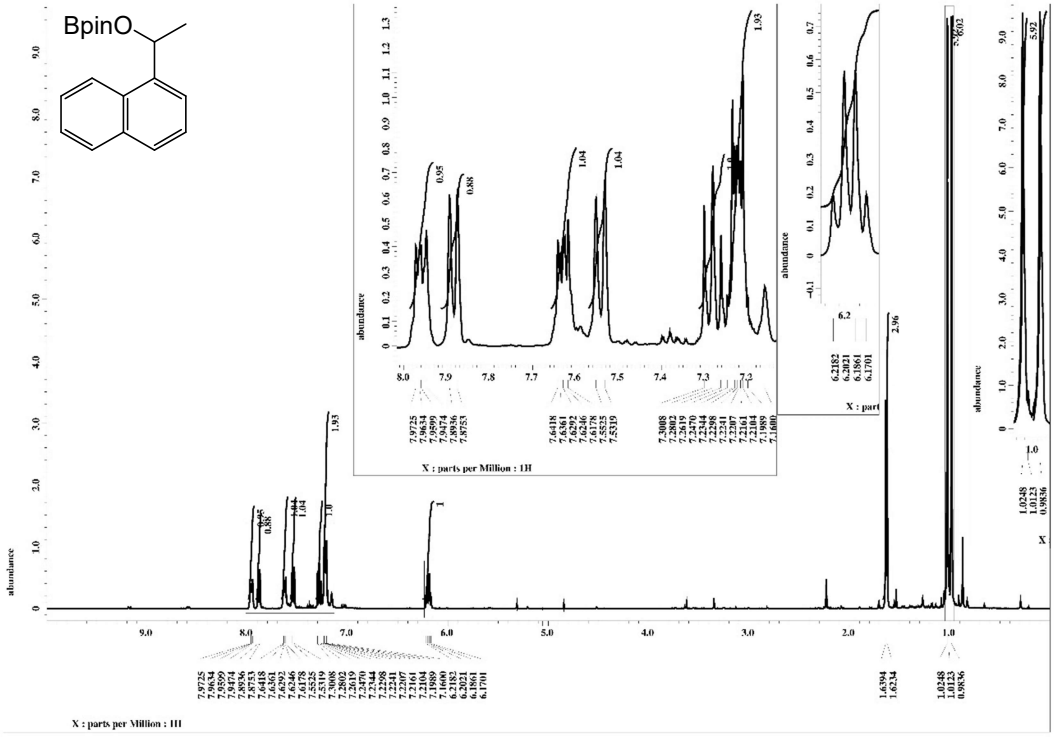

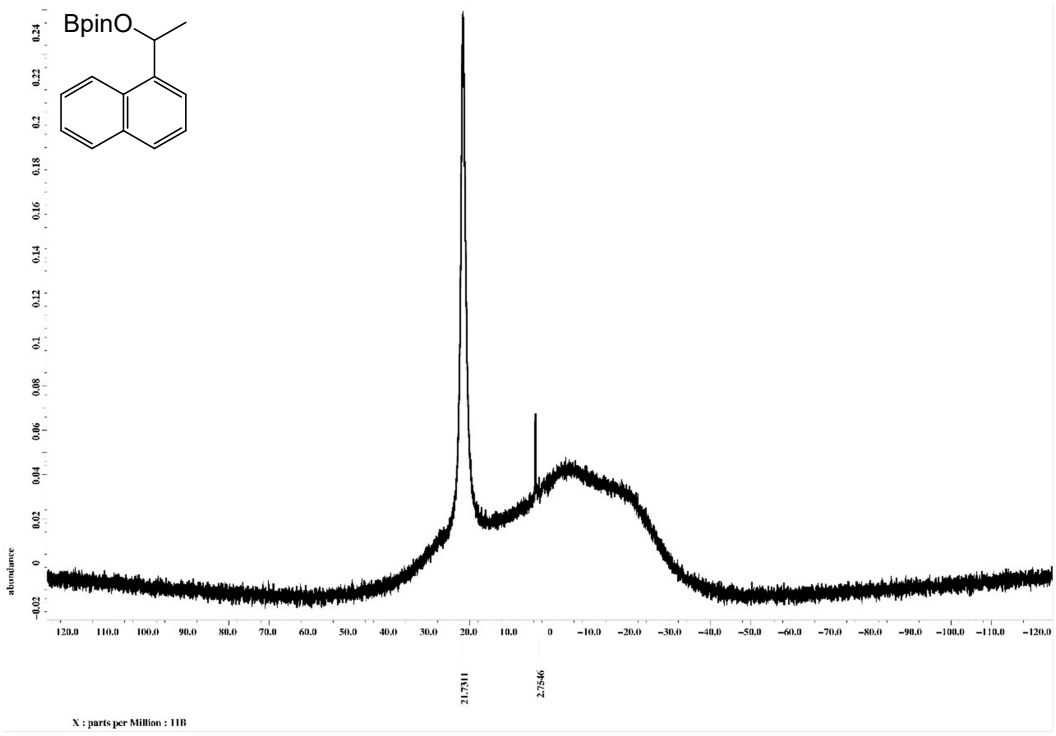

Table S2 Entry 4, ^{1}H, $^{11}B\{^{1}H\}$ NMR Spectra of crude product

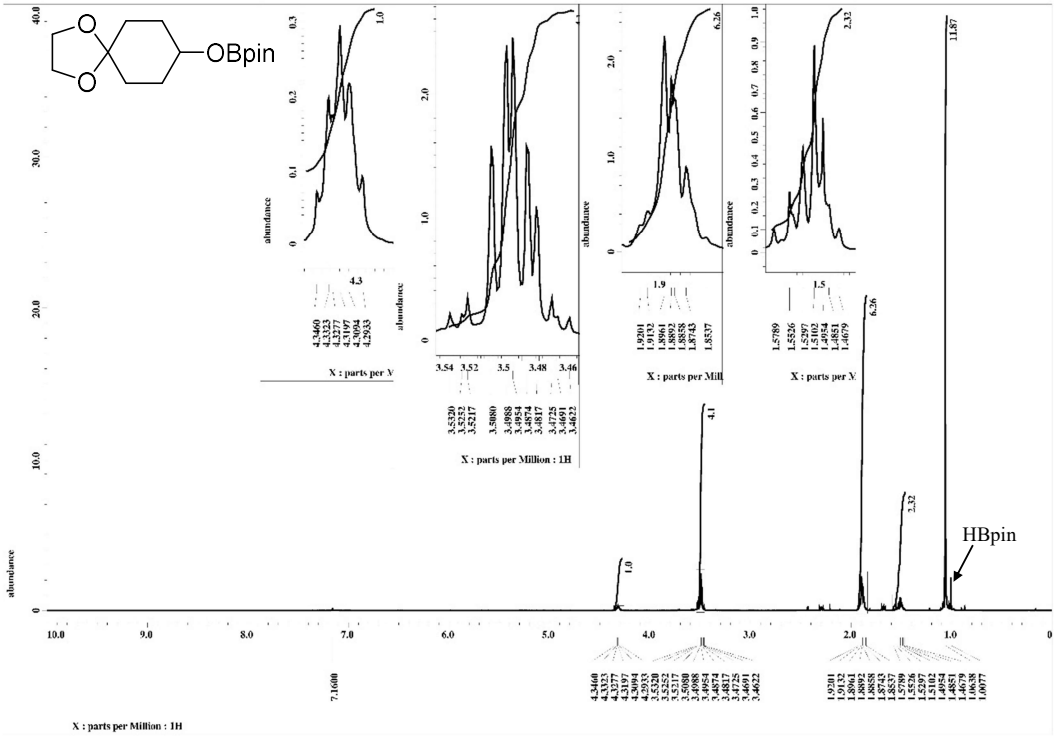

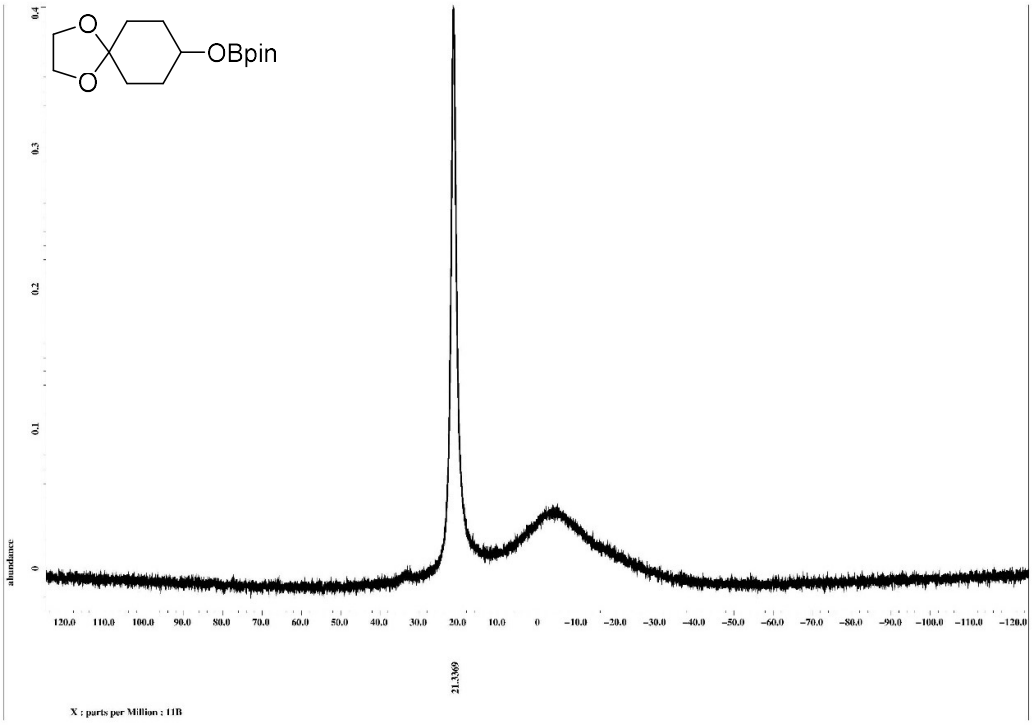

Table S2 Entry 5, ^{1}H, $^{11}B\{^{1}H\}$ NMR Spectra of crude product

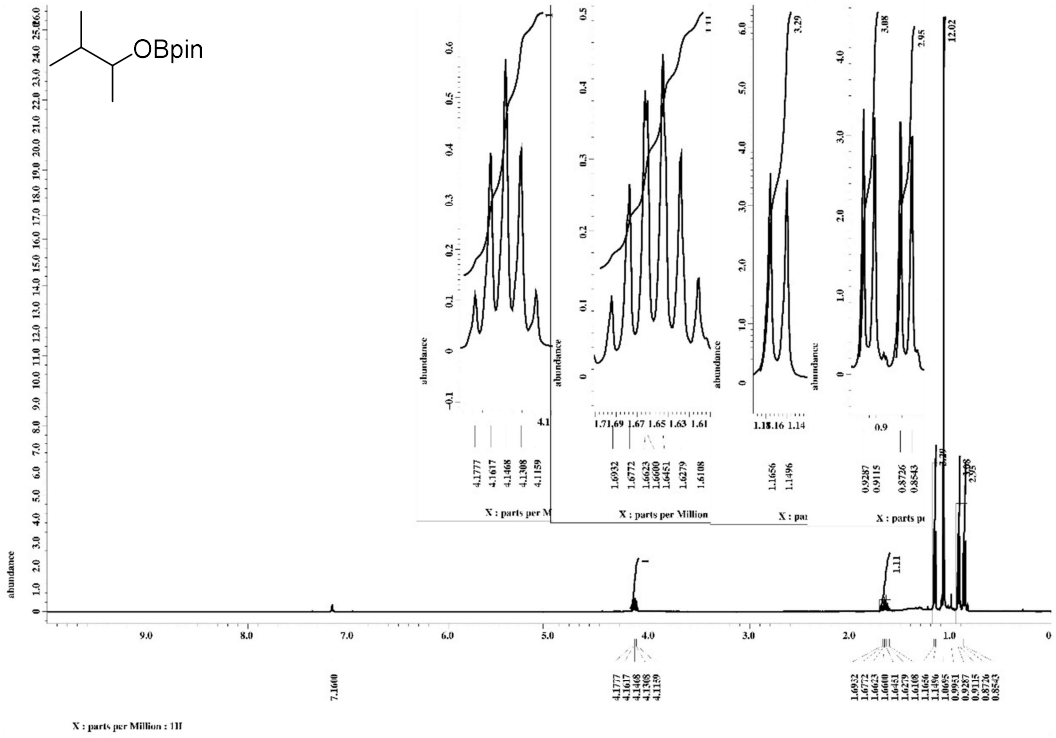

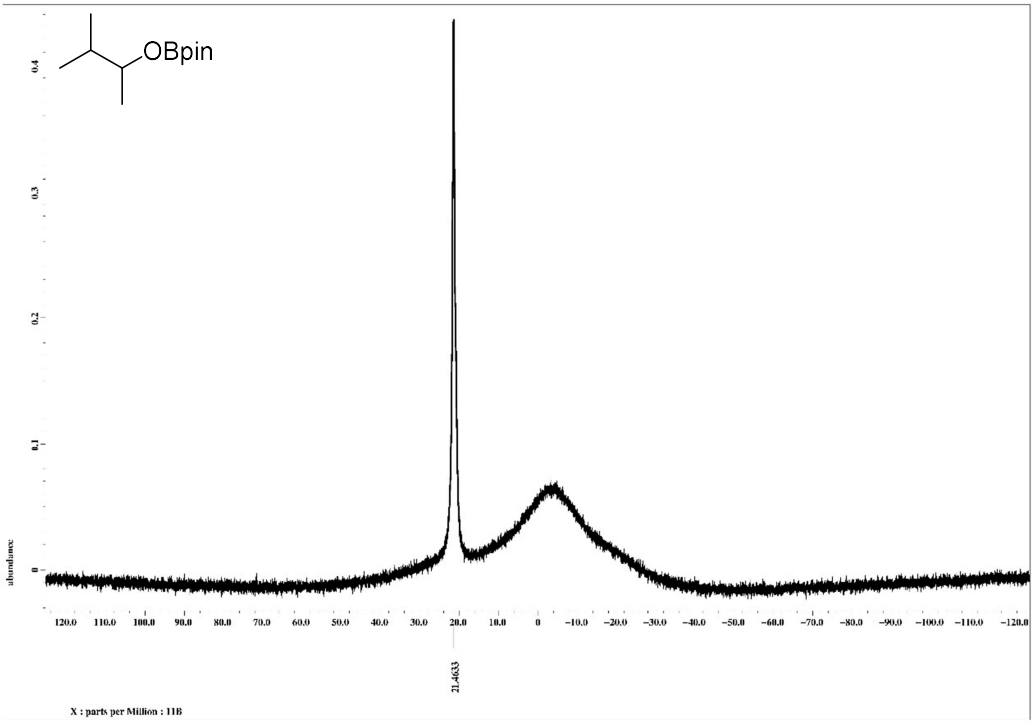

Table S2 Entry 6, ^{1}H, $^{11}B\{^{1}H\}$ NMR Spectra of crude product

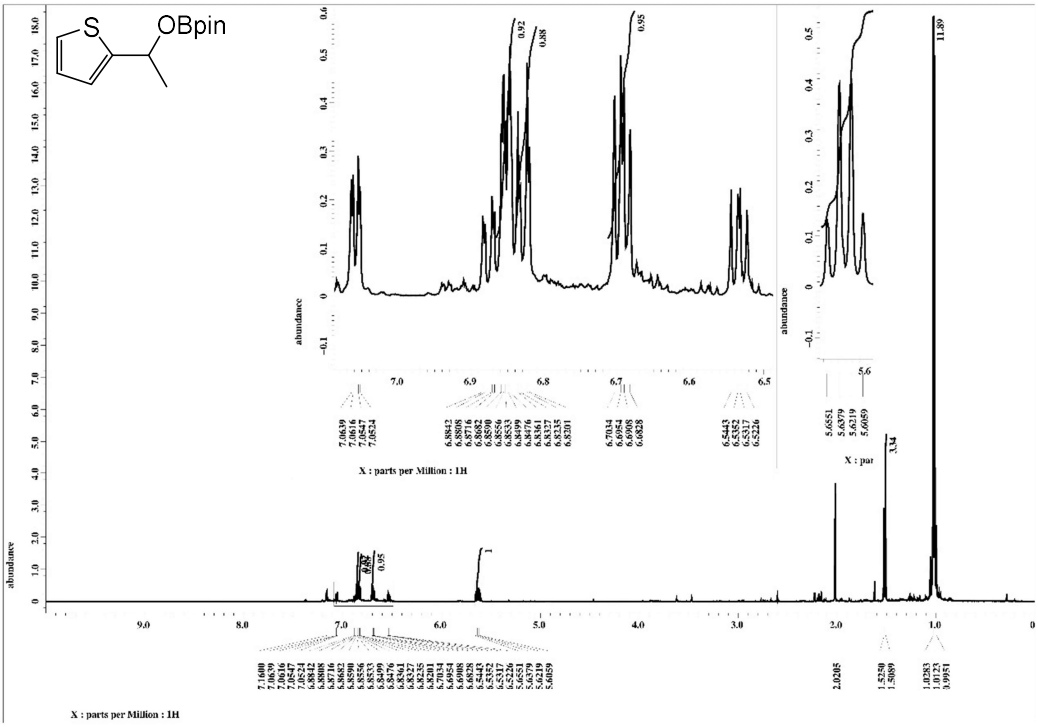

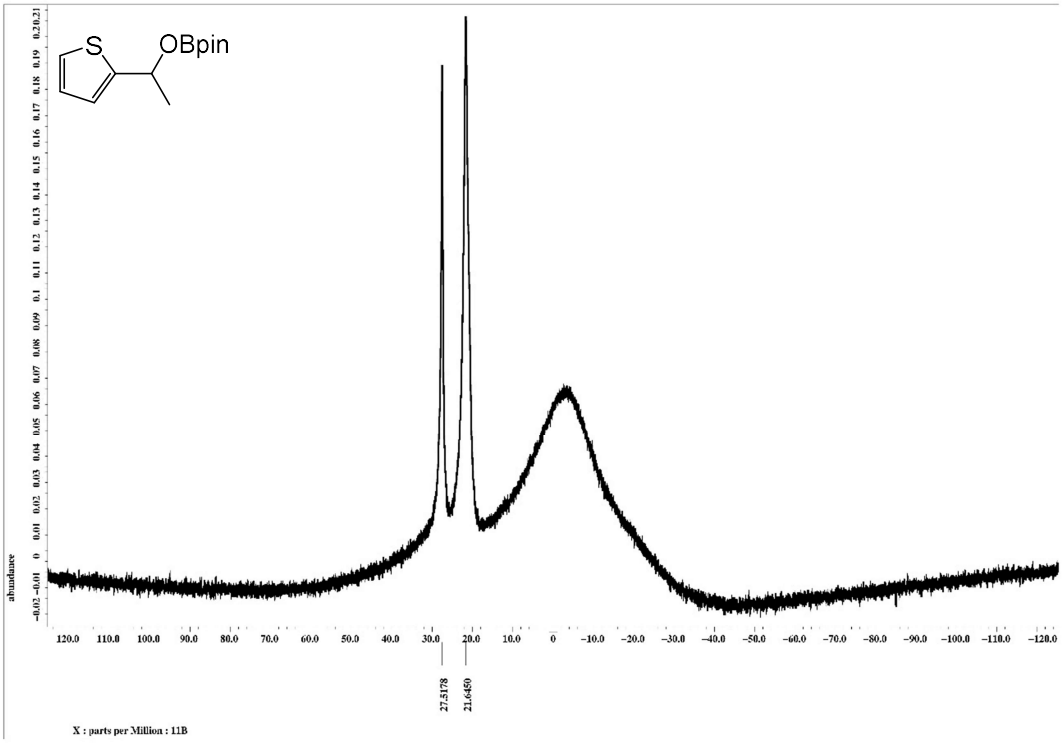

Table S2 Entry 7, ^{1}H, $^{11}B\{^{1}H\}$ NMR Spectra of crude product

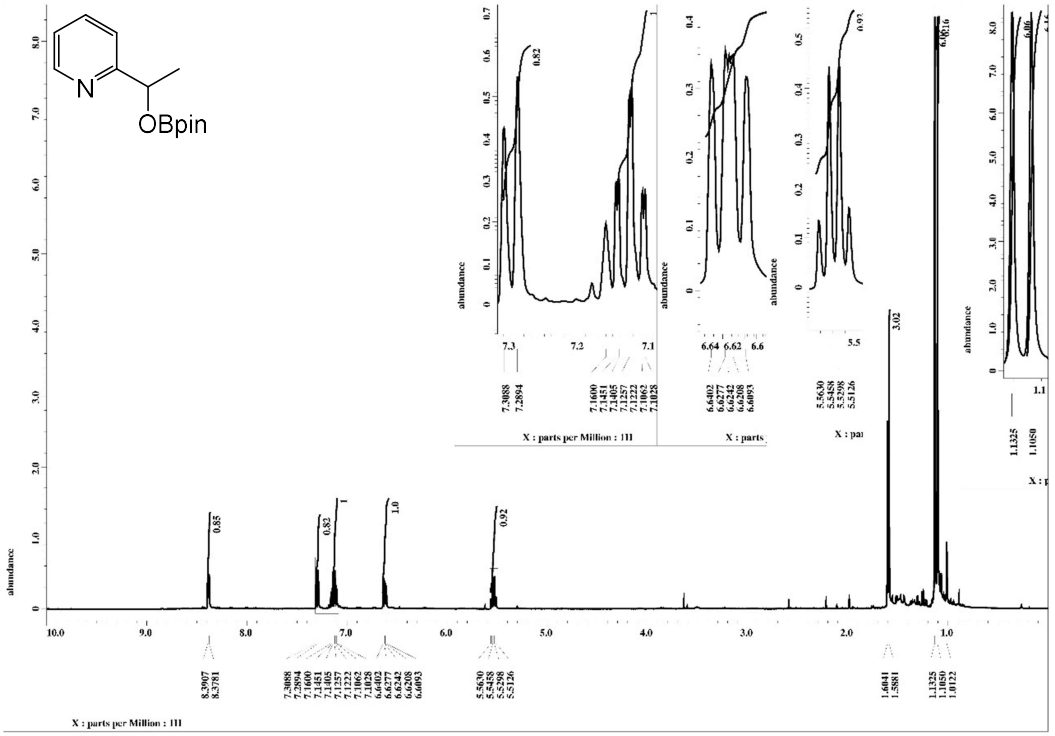

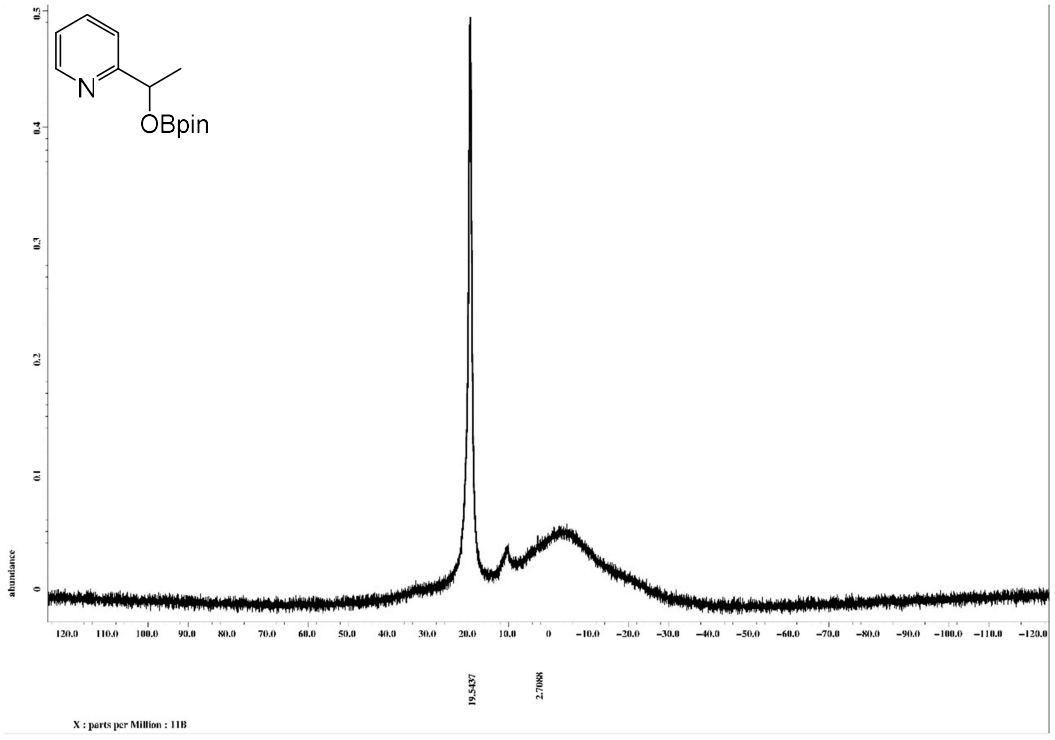

Table S2 Entry 8, ^{1}H, $^{11}B\{^{1}H\}$ NMR Spectra of crude product

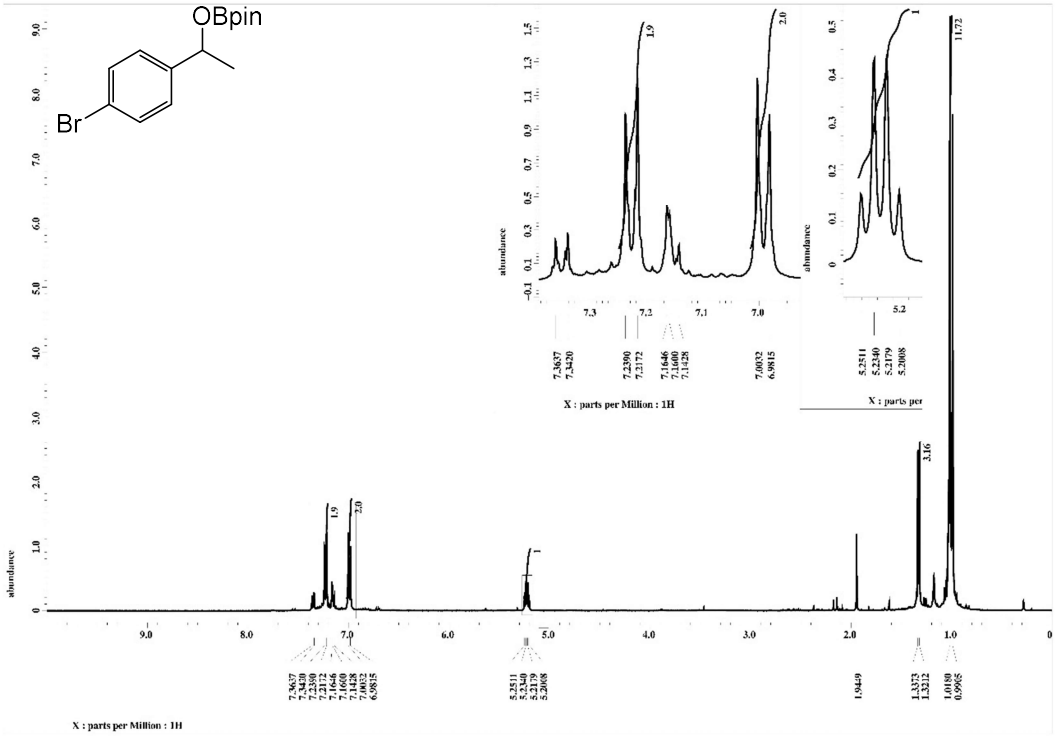

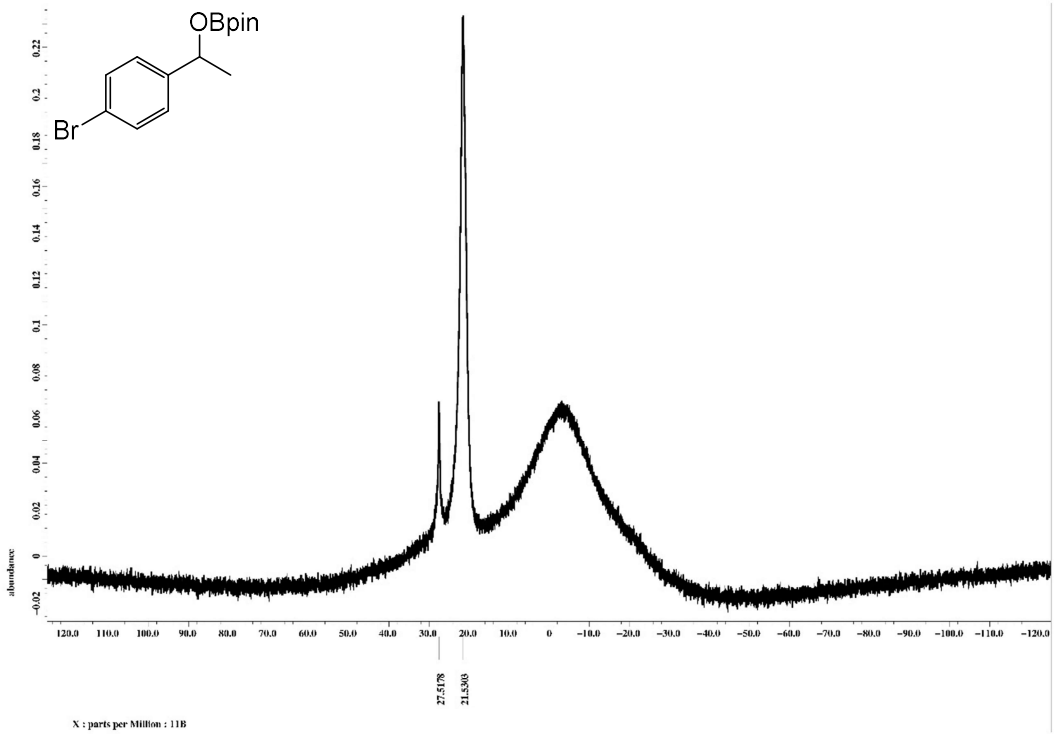

Table S2 Entry 9, ^{1}H, $^{11}B\{^{1}H\}$ NMR Spectra of crude product

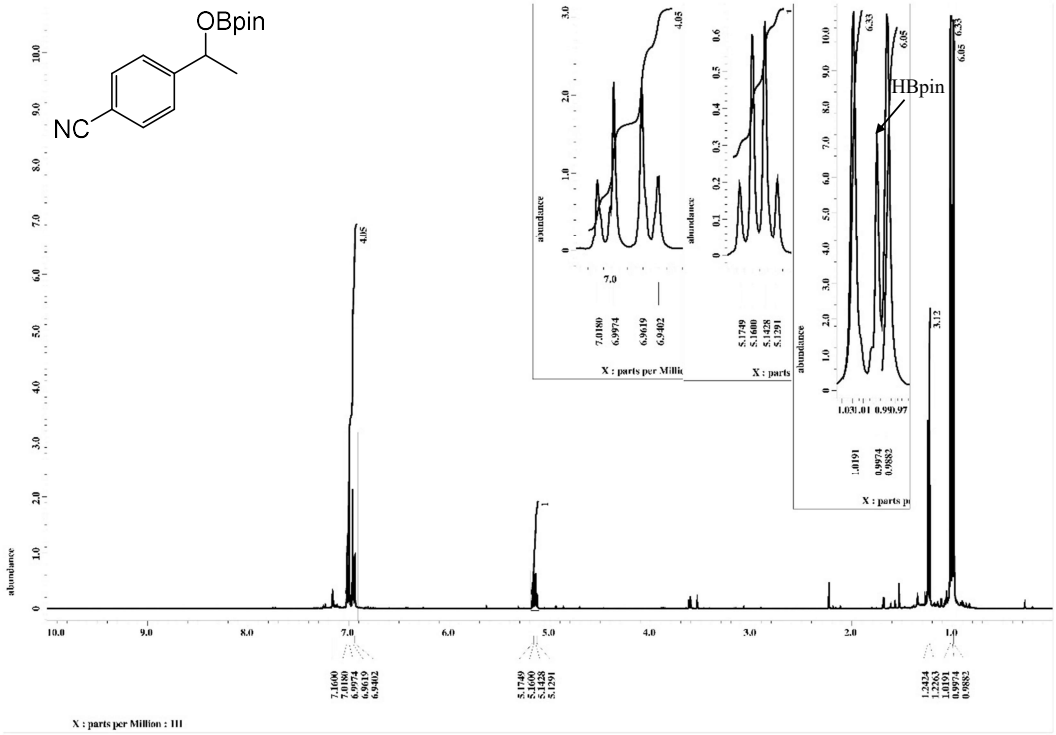

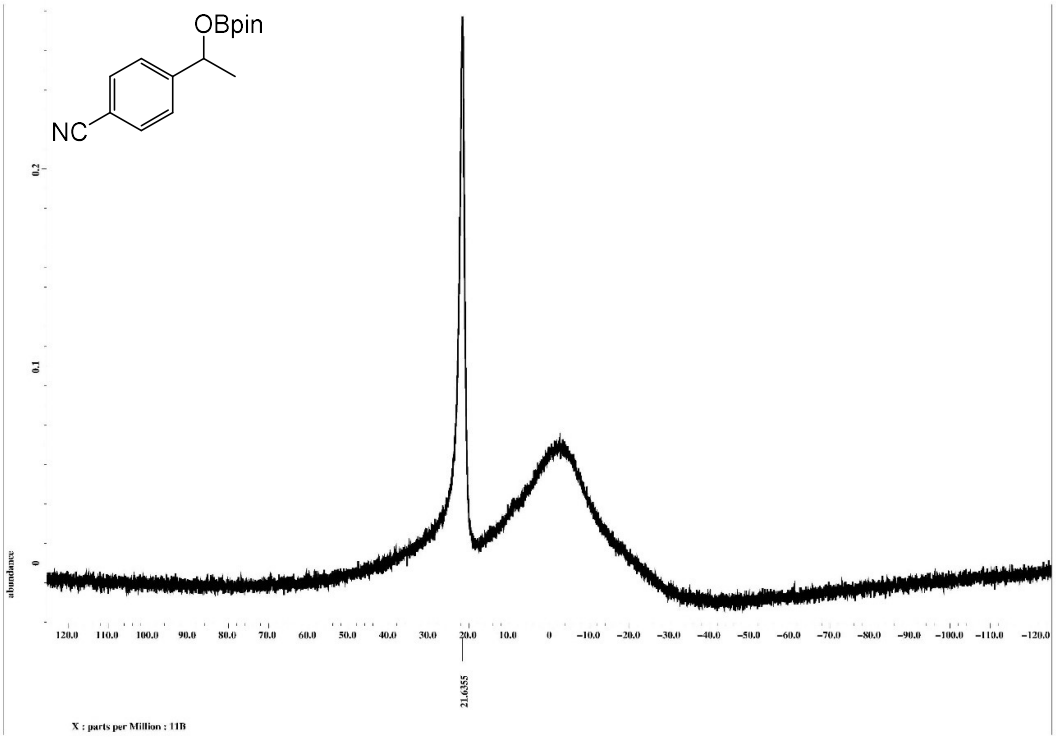

Table S3 Entry 1, ^{1}H, $^{11}B\{^{1}H\}$ NMR Spectra of crude product

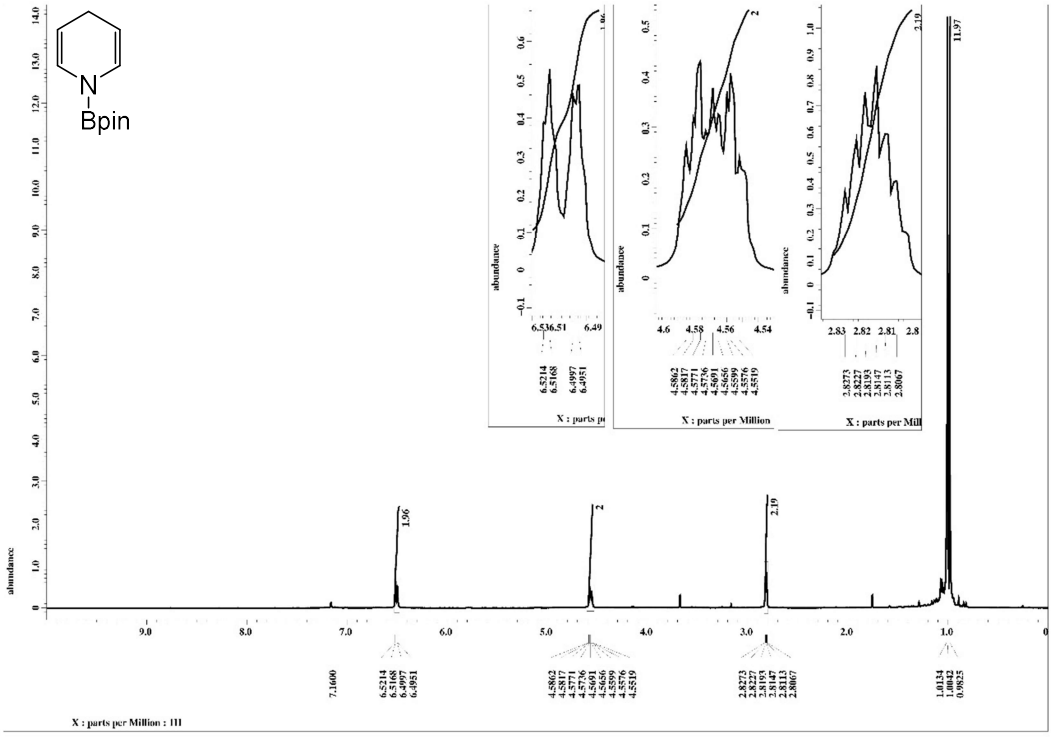

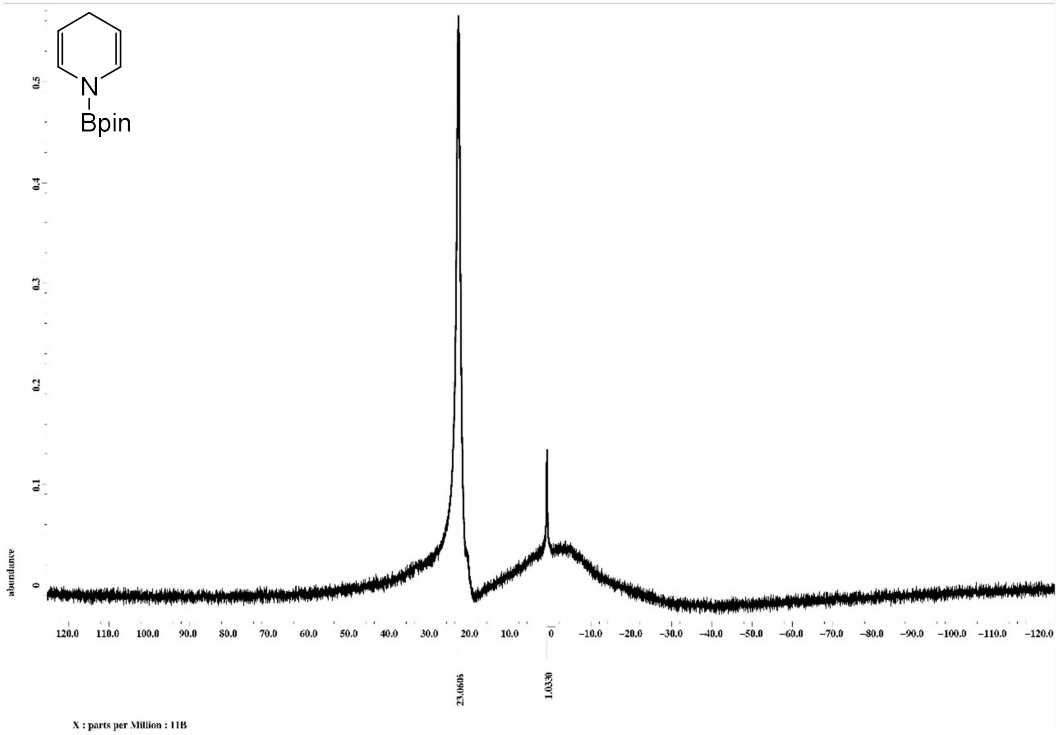

Table S3 Entry 2, ^{1}H, $^{11}B\{^{1}H\}$ NMR Spectra of crude product

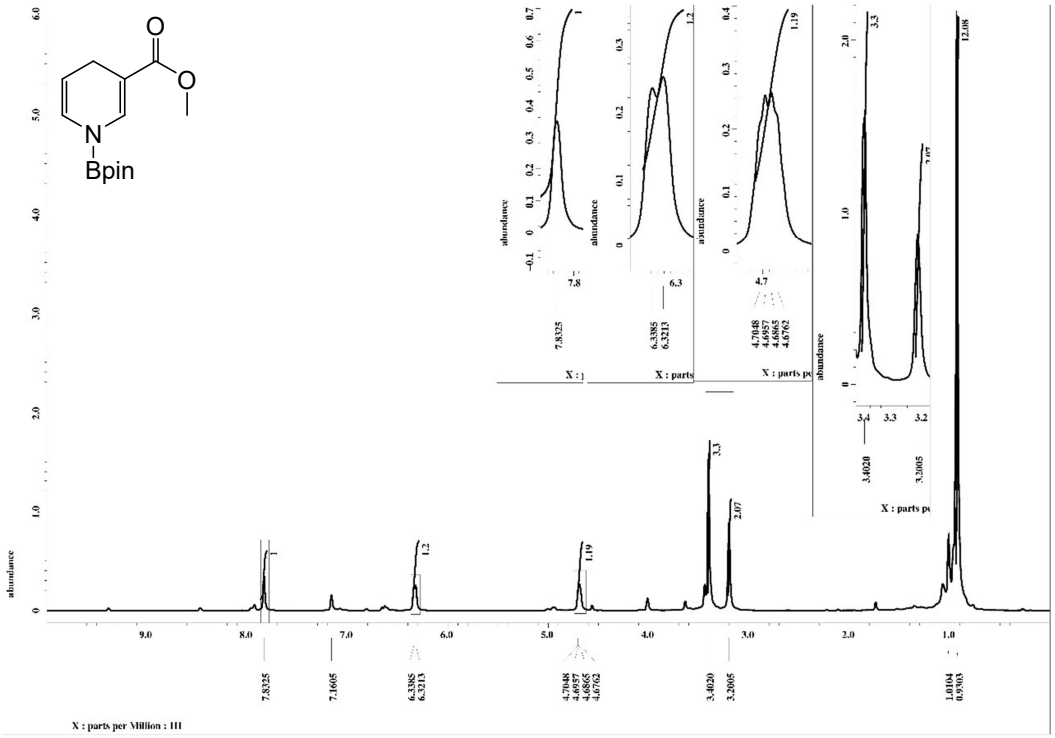

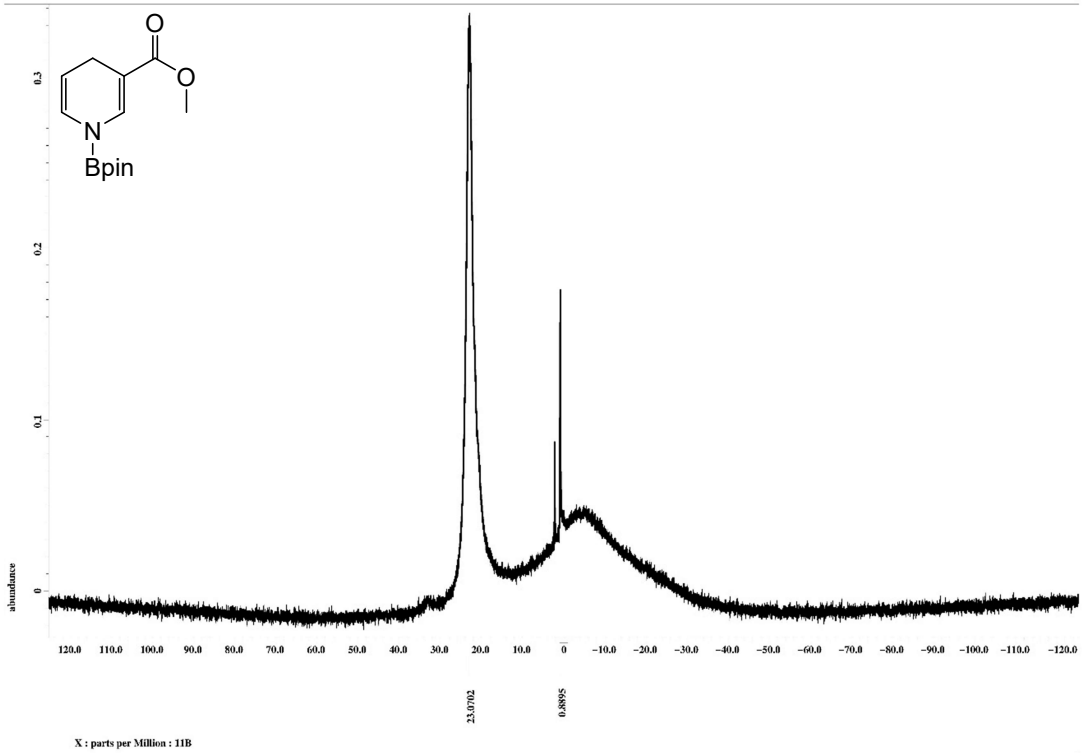

Table S3 Entry 3, ^{1}H, $^{11}B\{^{1}H\}$ NMR Spectra of crude product

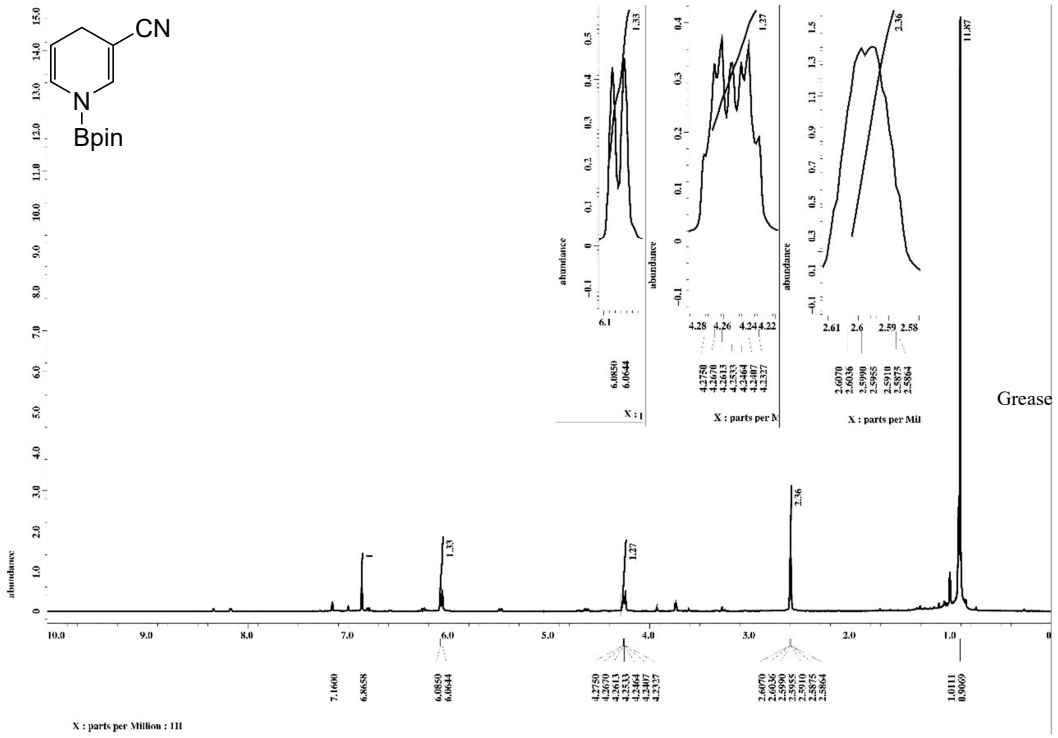

Table S3 Entry 4, ^{1}H, $^{11}B\{^{1}H\}$ NMR Spectra of crude product

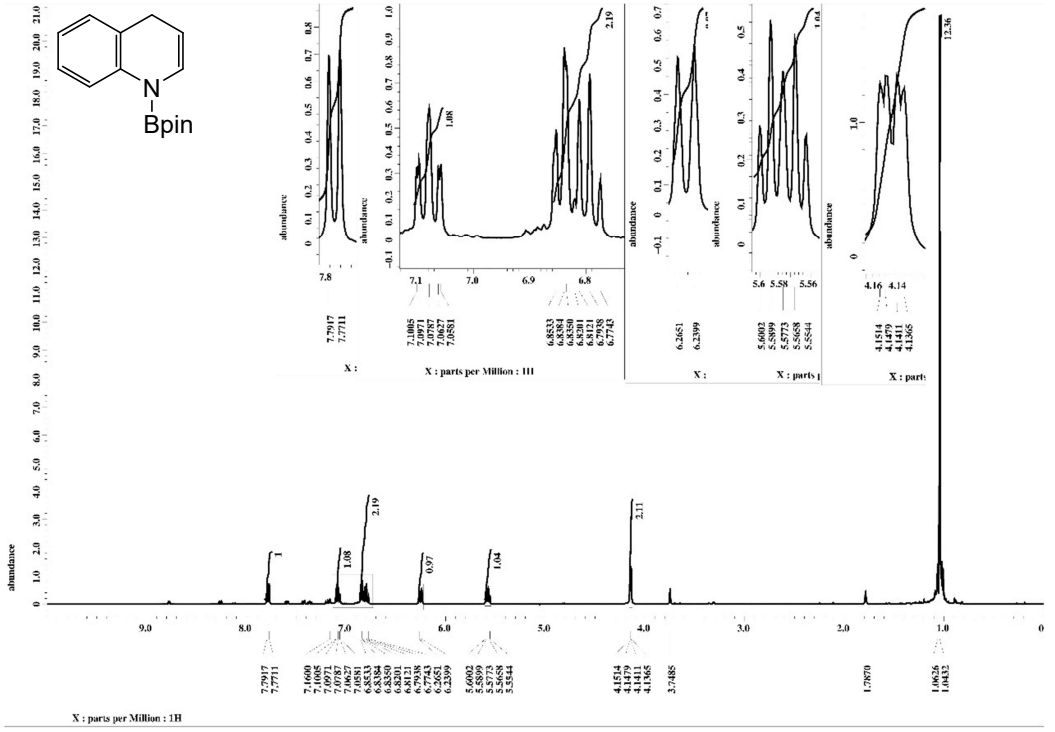

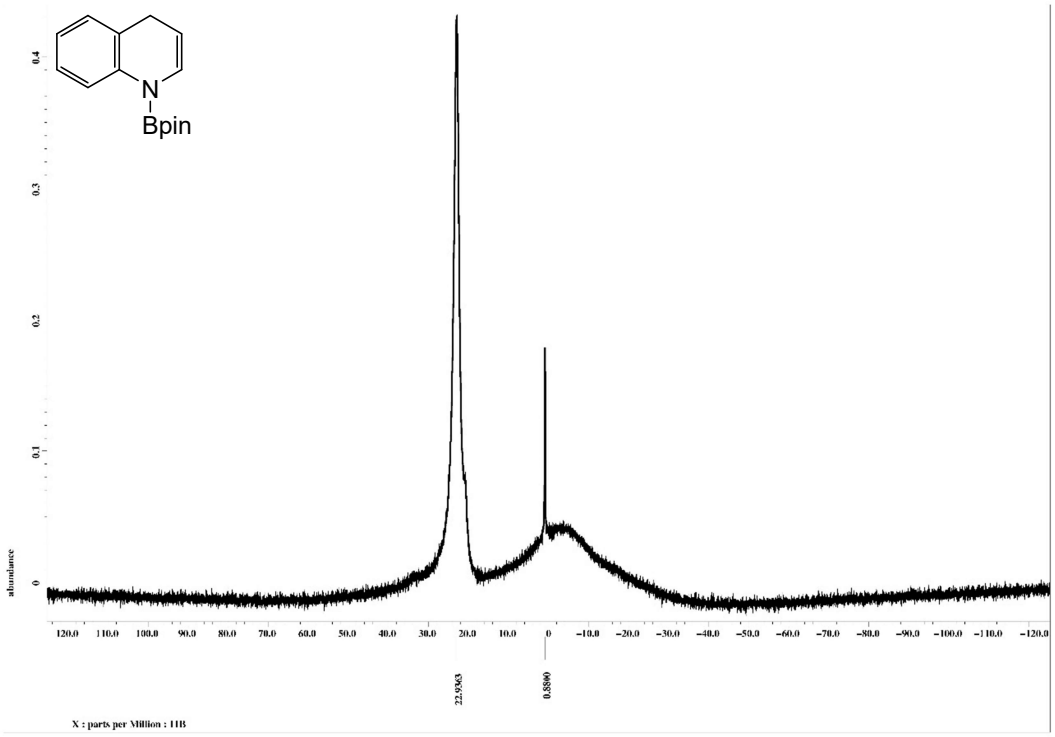

Table S3 Entry 5, ^{1}H, $^{11}B\{^{1}H\}$ NMR Spectra of crude product